LIGAND-INDUCED CLEAVAGE OF DINITROGEN BY A HAFNIUM METALLOCENE COMPLEX

A Thesis

Presented to the Faculty of the Graduate School

of Cornell University

In Partial Fulfillment of the Requirements for the Degree of

Master of Science

by

Scott Peter Semproni

January 2011

ABSTRACT

Side-on bound dinitrogen complexes of zirconium and hafnium, $[(\eta^5\text{-}C_5Me_3H_2)_2M]_2(\eta^2, \eta^2\text{-}N_2)$ (M = Zr, Hf), have been prepared by alkali metal reduction of the corresponding diiodide precursors. UV-Visible spectroscopy and X-ray diffraction studies established a higher degree of N_2 activation in these complexes than those of the type $[(\eta^5\text{-}C_5Me_4H)_2M]_2(\eta^2, \eta^2\text{-}N_2)$ (M = Zr, Hf), likely due to increased metal-nitrogen orbital overlap resulting from contracted metal-metal distances. Addition of four atmospheres of dihydrogen afforded the expected hydrido metallocene azenido complexes $[(\eta^5\text{-}C_5Me_3H_2)_2MH]_2N_2H_2$ (M = Zr, Hf). The iodo hafnocene azenido compound $[(\eta^5\text{-}C_5Me_3H_2)_2HfI]_2N_2H_2$ was obtained by treatment of the hydrido hafnocene azenido precursor with methyl iodide. The first example of an bridging hafnium nitride compound, $[(\eta^5\text{-}C_5Me_3H_2)_2Hf(DMAP)](\mu\text{-}N)[(\eta^5\text{-}C_5Me_3H_2)_2Hf(NCO)]$, was isolated upon treatment of $[(\eta^5\text{-}C_5Me_3H_2)_2Hf]_2(\eta^2, \eta^2\text{-}N_2)$ with carbon monoxide gas in the presence of 4-dimethylaminopyridine. The molecule proved to be a source of the hafnium-nitride fragment, which reacted with terminal alkynes via 1,2-addition at elevated temperatures and furnished the μ-imido acetylido complexes $[(\eta^5\text{-}C_5Me_3H_2)_2Hf(CCR)](\mu\text{-}NH)[(\eta^5\text{-}C_5Me_3H_2)_2Hf(NCO)]$ (R = Ph, $SiMe_3$). The hafnium nitride has also been shown to react with an additional molecule of carbon monoxide to yield the μ-isocyanate isocyanato compound $[(\eta^5\text{-}C_5Me_3H_2)_2Hf](\eta^3, \eta^1, \mu\text{-}NCO)[(\eta^5\text{-}C_5Me_3H_2)_2Hf(NCO)]$. The hafnocene-$N_2$ complex also undergoes a unique series of reactions with primary silanes, leading to the production of monosilylated dinitrogen units. Complete N-N bond scission is achieved upon thermoylsis of the mono-silylated compounds, and N-C bond formation can be achieved by upon treatment of the silylated compound with CO. Trapping of the hafnium μ-nitride and N_2 functionalization with silanes are reactions which are unique to the 1,2,4-trimethylcyclopentadienyl

hafnocene-N_2 compound. The origin of this unique reactivity has been attributed to the reduced steric profile of the trisubstituted metallocene, which allows shorter metal-metal contact distances and produces a highly activated, but sterically accessible dinitrogen fragment.

BIOGRAPHICAL SKETCH

Scott Semproni was born in 1987 in Vancouver, BC, Canada, where he grew to appreciate free healthcare and the absence of mail delivery on Saturdays. He graduated from Templeton Mini School in 2004 before attending the University of British Columbia in Vancouver. Serendipitously, in the summer of his third year at UBC, he was introduced to the research group of Professor Peter Legzdins, and began to investigate the properties of monocyclopentadienyl tungsten allyl alkyl nitrosyl complexes. After two and a half years in the Legzdins laboratory, Scott graduated with a B.S. in Chemistry in 2009 and moved to Cornell University to begin his graduate studies under Professor Paul Chirik. He spent the next year and a half loving life at Cornell and researching dinitrogen activation with hafnium metallocene complexes in his 'spare' time. In January of 2011, Scott will move to Princeton University to continue his doctoral studies with Prof. Paul Chirik.

Cookie loves milk!

-Unknown

ACKNOWLEDGEMENTS

This manuscript is dedicated to those who have made its creation possible. I owe a great debt of graditude to Peter Legzdins, who first introduced me to synthetic organometallic chemistry and fostered my love of science. Working in his laboratory gave me the skills and confidence I needed to transition to graduate school. My maturation as a scientist only began in earnest with the beginning of my thesis research. Paul Chirik and Peter Wolczanski have provided an excellent grounding in organometallic chemistry that I hope to continue to build upon during the final portion of my doctoral studies. My colleagues and friends in the Chirik group made my thesis research less of a trial and more of an adventure. Their humor, candor and willingness to teach me have allowed me to mature as a person and as a chemist. In particular, I have to acknowledge Donald Knobloch for his tutelage in the 'black magic' that is producing new metallocene dinitrogen compounds. Portions of this thesis would not exist without the input from various members of the Cornell staff, particularly Ivan Keresztes and Emil Lobkovsky.

Finally, to quote John Donne, no man is an island. Without the constant love and support of my family and friends, both in Ithaca and in Vancouver, this thesis, and my graduate career in general, would not have been possible. I owe a great debt to my parents, Luciano and Patricia, and my brother and sister, Michael and Milena, for their continuing love and support from across the continent. My time at Cornell would not have been nearly as enjoyable without my friends, who provided an excellent outlet for my 'highbrow' humor. And lastly, Angie; without your constant love and support, my time in Ithaca would not have been the same. This one's for you.

TABLE OF CONTENTS

LIST OF FIGURES

LIST OF TABLES

LIST OF ABBREVIATIONS

DMAP = 4-dimethylamino-pyridine

Cp = cyclopentadienyl ($C_5H_5^-$)

Cp* = pentamethylcyclopentadienyl ($C_5Me_5^-$)

1 = [(η^5-$C_5Me_3H_2$)$_2$Hf]

2 = [(η^5-C_5Me_4H)$_2$Hf]

3 = [(η^5-$C_5Me_3H_2$)$_2$Zr]

4 = [(η^5-C_5Me_4H)$_2$Zr]

5 = [(η^5-$C_5Me_3H_2$)$_2$Ti]

NMR = Nuclear magnetic resonance

IR = infra-red

COSY = Correlated spectroscopy

HSQC = Heteronuclear single quantum coherence

HMBC = Heteronuclear multiple bond coherence

Cy = cyclohexyl

^{n}Hex = *n*-hexyl

CHAPTER 1

Synthesis and Reactivity of Bis(1,2,4-Trimethylcyclopentadienyl) Zirconium and Hafnium Dinitrogen Complexes: Trapping of a Transient μ-Nitrido Fragment

Abstract

Side-on bound dinitrogen complexes of zirconium and hafnium, $[(\eta^5\text{-}C_5Me_3H_2)_2M]_2(\eta^2, \eta^2\text{-}N_2)$ (M = Zr, Hf), have been prepared by alkali metal reduction of the corresponding diiodide precursors. UV-Visible spectroscopy and X-ray diffraction studies established a higher degree of N_2 activation in these complexes than those of the type $[(\eta^5\text{-}C_5Me_4H)_2M]_2(\eta^2, \eta^2\text{-}N_2)$ (M = Zr, Hf), likely due to increased metal-nitrogen orbital overlap resulting from contracted metal-metal distances. Addition of 4 atmospheres of dihydrogen afforded the expected hydrido metallocene azenido complexes, $[(\eta^5\text{-}C_5Me_3H_2)_2MH]_2N_2H_2$ (M = Zr, Hf). The iodo hafnocene azenido compound $[(\eta^5\text{-}C_5Me_3H_2)_2HfI]_2N_2H_2$ was obtained by treatment of the hydrido hafnocene azenido precursor with methyl iodide. The first example of an bridging hafnium nitride compound, $[(\eta^5\text{-}C_5Me_3H_2)_2Hf(DMAP)](\mu\text{-}N)[(\eta^5\text{-}C_5Me_3H_2)_2Hf(NCO)]$, was isolated from treatment of $[(\eta^5\text{-}C_5Me_3H_2)_2Hf]_2(\eta^2, \eta^2\text{-}N_2)$ with carbon monoxide gas in the presence of 4-dimethylaminopyridine. The nitride reacted with terminal alkynes via 1,2-addition at elevated temperatures and furnished the μ-imido acetylido complexes $[(\eta^5\text{-}C_5Me_3H_2)_2Hf(CCR)](\mu\text{-}NH)[(\eta^5\text{-}C_5Me_3H_2)_2Hf(NCO)]$ (R = Ph, $SiMe_3$). The hafnium nitride has also been shown to react with an additional molecule of carbon monoxide to yield the μ-isocyanate isocyanato compound $[(\eta^5\text{-}C_5Me_3H_2)_2Hf](\eta^3, \eta^1, \mu\text{-}NCO)[(\eta^5\text{-}C_5Me_3H_2)_2Hf(NCO)]$. Incorporation of ^{13}CO gas into the μ-isocyanate fragment occurred when the compound was left to stand under 1 atmosphere of isotopically labeled carbon monoxide, demonstrating reversible insertion/de-insertion of CO into the hafnium nitride functionality.

Introduction

The conversion of atmospheric dinitrogen and hydrogen to ammonia via the Haber-Bosch process is of enormous importance to modern society. By some estimates, 50% of the world's population is supported by fertilizer derived from Haber-Bosch ammonia.[1] However, the high temperatures and pressures at which the reaction is performed on an industrial scale means that approximately 1% of the world's energy supply is devoted to fueling the Haber-Bosch process, often with energy derived from non-renewable resources.[2] Consequently, enormous effort has been expended in recent years attempting to find homogenous transition metal systems which can assemble nitrogen-element bonds directly from atmospheric dinitrogen and suitable reagents. Fryzuk first demonstrated N-H bond formation directly from N_2 and H_2 at ambient temperature and pressure through the use of a zirconium complex supported by a macrocyclic 'P_2N_2' type ligand. Addition of H_2 to the nitrogen compound $[(P_2N_2)Zr]_2(\mu_2,\eta^2, \eta^2\text{-}N_2)$ (P_2N_2 = $PhP(CH_2SiMe_2NSiMe_2CH_2)_2PPh$) resulted in one new N-H bond along with concomitant formation of a bridging zirconium hydride.[3] Our laboratory has reported the complete hydrogenation of dinitrogen to ammonia using a zirconocene dinitrogen compound, $[(C_5Me_4H)_2Zr]_2(\eta^2, \eta^2\text{-}N_2)$, which contains a strongly activated N_2 ligand **(Figure 1.1)**.[4]

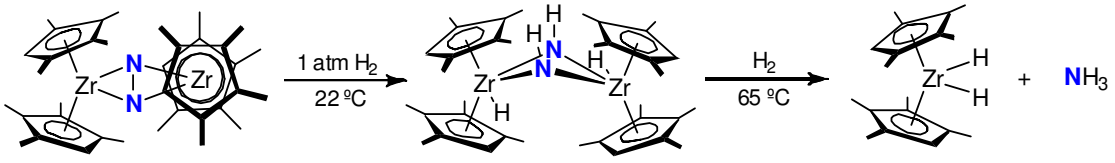

Figure 1.1 Hydrogenation of N_2 to ammonia using $[(C_5Me_4H)_2Zr]_2(\eta^2, \eta^2\text{-}N_2)$

Recent work both by our laboratory[5] and that of Sita[6] has shown that strongly activated group 4 dinitrogen compounds can access unique N-C bond forming reactions under

mild conditions. Thus, addition of 1 atmosphere of carbon monoxide to the *ansa*-hafnocene $[Me_2Si(\eta^5\text{-}C_5Me_4H)(\eta^5\text{-}C_5H_3\text{-}3\text{-}tBu)Hf]_2(\eta^2, \eta^2\text{-}N_2)$ (N-N bond distance = 1.457(5) Å) afforded the hafnium 'oxamidide' product $[Me_2Si(\eta^5\text{-}C_5Me_4H)(\eta^5\text{-}C_5H_3\text{-}3\text{-}tBu)Hf]_2(N_2C_2O_2)$ arising from N-N bond scission with concomitant C-C bond formation **(Figure 1.2)**.

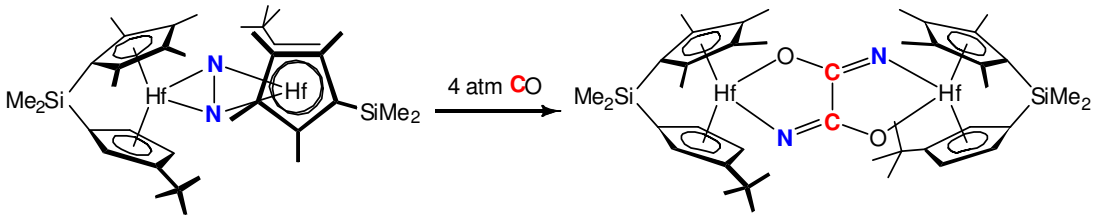

Figure 1.2 Cleavage of dinitrogen by carbon monoxide

In a fundamentally different approach to dinitrogen functionalization, Sita has shown that treatment of the monocyclopentadienyl amidinate hafnium compound $[(\eta^5\text{-}C_5Me_4H)M(N(iPr)C(Me)N(iPr))]_2$ ($\eta^2, \eta^2\text{-}N_2$) (N-N bond distance = 1.635(5) Å), with ethyl bromide led to N-C bond formation **(Figure 1.3)**.

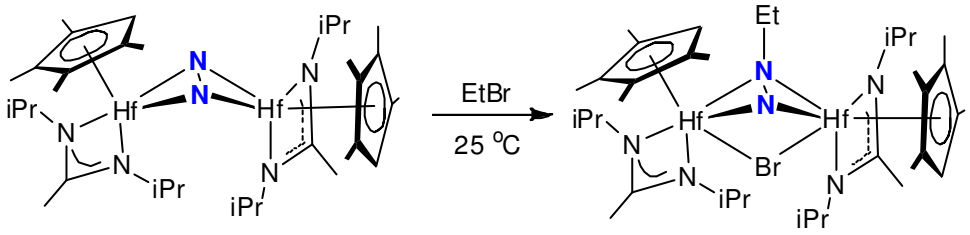

Figure 1.3 Electrophilic addition of ethyl bromide to a strongly activated dinitrogen compound prepared by Sita.[6]

Notably, the N-N bond was not cleaved in this process, and only one nitrogen atom was functionalized. This represents a rare example in Group 4 chemistry of N-C bond formation derived from the treatment of dinitrogen with strong electrophiles.[7]

These reactions highlight the unique dinitrogen functionalization chemistry that is available by modification of ancillary ligand environments. Furthermore, these results also demonstrate the importance of strong N_2 activation in both allowing ligand functionalization and preventing deleterious side reactions. In this chapter, the synthesis and characterization of two new metallocene dinitrogen complexes with high degrees of N_2 activation will be discussed. In addition, a unique N_2 functionalization reaction will be presented that underlines the subtle impact of ancillary ligand modification on the reactivity of metallocene dinitrogen compounds.

Results and Discussion

Synthesis and Reactivity of a Strongly Activated Hafnocene Dinitrogen Compound. Previous work in our laboratory has shown that side-on zirconium and hafnium dinitrogen complexes with the tetramethylcyclopentadienyl ligand undergo facile 1,2-addition reactions with dihydrogen, leading to the formation of N-H and M-H bonds.[4,8] In contrast, the permethylated end-on dinitrogen complex, $[(C_5Me_5)_2Zr(N_2)]_2(\eta^1, \eta^1\text{-}N_2)$ prepared by Bercaw,[9] loses N_2 upon addition of dihydrogen. Consequently, in order to discover new routes for the assembly of nitrogen-element bonds from atmospheric dinitrogen, strongly activated metallocene dinitrogen complexes of the less sterically demanding 1,2,4-trimethylcyclopentadienyl ligand were targeted with the goal of accessing N-E bond forming reactions. 1,2,4-trimethylcyclopentadiene was prepared in moderate yield by methylation of 3,4-dimethylcyclopent-2-enone[10] with MeMgBr (**Figure 1.4**). Thermal dehydration of the resulting tertiary allylic alcohol furnished the cyclopentadiene as a light yellow oil.

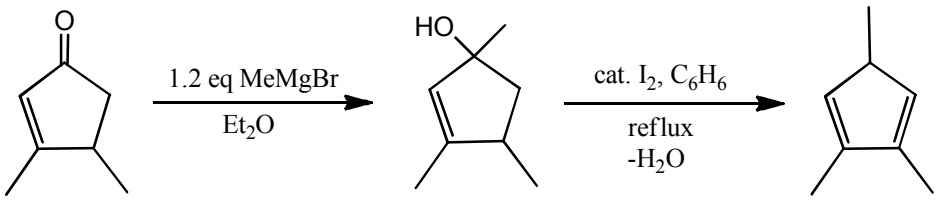

Figure 1.4 Synthesis of 1,2,4-trimethylcyclopentadiene[10]

Deprotonation of the diene with *n*-butyllithium resulted in isolation of Li[C_5-1,2,4-Me_3H_2] as an off-white solid which was subsequently used to prepare (η^5-$C_5Me_3H_2)_2HfI_2$ (**1-I_2**) in a procedure analogous to that of (η^5-$C_5Me_4H)_2HfI_2$.[8] Reduction of **1-I_2** with an excess of sodium amalgam under 1 atmosphere of dinitrogen furnished [(η^5-$C_5Me_3H_2)_2Hf]_2$(η^2, η^2-N_2) (**1-N_2**) as a dark purple solid (**Figure 1.5**).

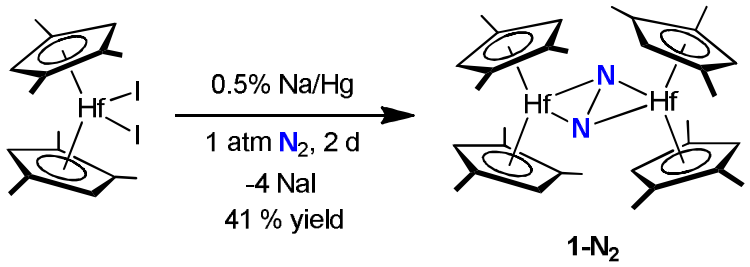

Figure 1.5 Preparation of **1-N_2**

Dark purple benzene-d_6 solutions of **1-N_2** exhibit one sharp Cp hydrogen resonance and two sharp Cp methyl resonances in a 2:1 ratio as judged by ^{1}H NMR spectroscopy. The number of signals is consistent with the D_{2d} solid state structure (*vide infra*) being maintained in solution. The {^{1}H}^{15}N NMR spectrum of **1-N_2** exhibits a singlet at 570.2 ppm, shifted downfield from 590.5 ppm observed for [(η^5-$C_5Me_4H)_2Hf]_2$(η^2, η^2-N_2) (**2-N_2**).[8] All ^{15}N NMR spectra are referenced externally to liquid ammonia at 0 ppm.

X-ray diffraction studies established the side-on hapticity of the dinitrogen ligand with a significantly lengthened nitrogen bond length of 1.457(5) Å, consistent

with an N-N single bond (for comparison, the N-N bond in N_2 is 1.098 Å and that in N_2H_4 is 1.462 Å)[2] (**Figure 1.6**). Selected metrical parameters are presented in **Table 1.1** along with those of **2-N_2**.[8] The wedge dihedral angle of 48.1° in **1-N_2** reduced from 65.0° in **2-N_2**, and **1-N_2** also possesses a shorter metal-metal distance compared to **2-N_2** (3.853 vs 3.913 Å). The less sterically demanding 1,2,4-trimethylcyclopentadienyl ligand allows greater approach of the two metal centers to the side-on dinitrogen fragment and produces greater overlap with nitrogen π* orbitals, likely leading to greater dinitrogen activation. Additionally, the hafnium-nitrogen bond lengths of 2.0590(12) Å in **1-N_2** suggest slightly more metal-imido character compared to **2-N_2.**

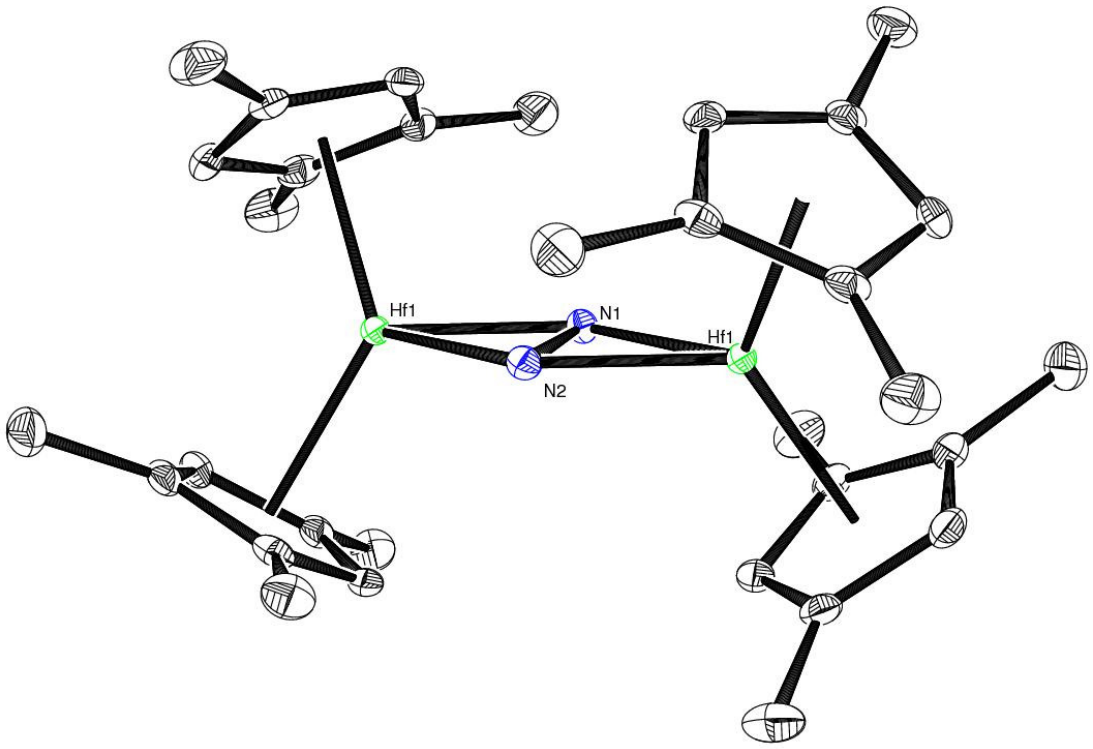

Figure 1.6 ORTEP plot of **1-N_2** at 30% probably ellipsoids. Hydrogen atoms and one fluorobenzene solvent molecule omitted for clarity.

The hafnocene dinitrogen compound was readily hydrogenated by treatment of a toluene solution of **1-N_2** with 4 atmospheres of hydrogen gas and afforded the hydrido hafnocene diazenido complex $[(\eta^5\text{-}C_5Me_3H_2)_2HfH]_2(\eta^2, \eta^2\text{-}N_2H_2)$ **(1-N_2H_4) (Figure 1.7)**.

Table 1.1. Selected Bond Distances (Å) and Angles (°) for **1-N_2, 1-N_2H_4, 2-N_2**[8], and **2-N_2H_4**.[8]

	1-N_2	**2-N_2**	**1-N_2H_4**	**2-N_2H_4**
Hf(1)-N(1)	2.0590(12)	2.072(3)	2.165(3)	2.1755(19)
Hf(1)-N(2)	2.0599(12)	2.089(4)	2.272(3)	2.295(2)
N(1)-N(2)	1.457(5)	1.423(11)	1.462(4)	1.467(4)
Hf(1)-Hf(2)	3.853	3.913	3.932	3.888
Wedge Dihedral[11]	48.1	65.0	54.4	69.7

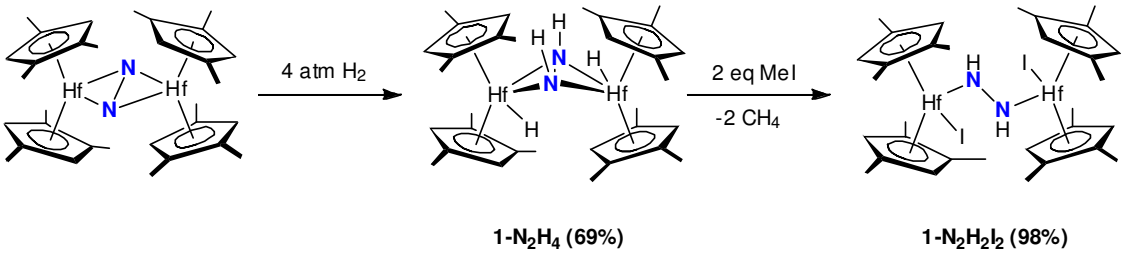

Figure 1.7. Preparation of **1-N_2H_4** and **1-$N_2H_2I_2$**

Crystals of **1-N_2H_4** suitable for X-ray diffraction studies were obtained from slow evaporation of concentrated pentane solutions. The solid state molecule structure of **1-N_2H_4** is presented in **Figure 1.8**, and its metrical parameters are presented in **Table 1.1**. The data were of sufficient quality such that the hydrogen atoms attached to hafnium and nitrogen were located in the Fourier difference map and freely refined. The

metrical parameters are similar to those found for **2-N_2H_4**, with the exception of a smaller wedge dihedral angle.

The ^{1}H NMR spectrum of the isolated white powder in toluene-d_8 at 23 ^{o}C exhibits 4 broad Cp hydrogen resonances and a number of broad peaks spanning 1.37-2.50 ppm for the Cp methyl groups, consistent with a dynamic process on the time scale of the NMR experiment. A sharp resonance at 8.19 ppm is assigned to a Hf-H, while a resonance at 1.21 ppm is assigned as an N-H peak on the basis of deuterium labeling experiments. The location of these resonances is similar to those observed for **2-N_2**.[8] Cooling the solution to -30 ^{o}C resulted in sharpening of the cyclopentadienyl resonances until 6 Cp methyl environments were observed, consistent with a C_2 symmetric molecule (**Figure 1.9**). The location of the Hf-H and N-H resonances remains essentially invariant with temperature. Previously, this dynamic process was tentatively assigned to inversion of the diazenido core.[12]

Treatment of a toluene solution of **1-N_2H_4** with 2 equivalents of methyl iodide at ambient temperature resulted in immediate darkening of the solution from light yellow to dark red with concomitant release of methane gas (**Figure 1.7).** The hafnium diazenido iodide complex $[(\eta^5\text{-}C_5Me_3H_2)_2HfI]_2(\eta^1, \eta^1\text{-}N_2H_2)$ (**1-$N_2H_2I_2$**) was isolated as a dark red powder; its IR spectrum recorded in KBr displays a sharp signal at 3389 cm^{-1} assigned to an N-H stretch and shifted significantly from that of **1-N_2H_4** at 3290 cm^{-1}. The ^{1}H NMR spectrum of **1-$N_2H_2I_2$** in benzene-d_6 displays 3 Cp methyl and 2 Cp hydrogen resonances, consistent with a C_{2v} symmetric molecule. In addition, a sharp singlet at 8.07 ppm is assigned to the N-H protons based on isotopic labeling experiments with D_2 gas. This substantial difference in chemical shift from 1.21 to 8.07 ppm on going from **1-N_2H_4** to **1-$N_2H_2I_2$** was previously attributed to a change in hapticity of the diazenido core from η^2, η^2 to η^1, η^1.[12] Overall, despite the greater

activation of the dinitrogen fragment in **1-N_2**, its reactivity with H_2 and electrophiles mirrors that of other group 4 metallocene compounds.[4,12]

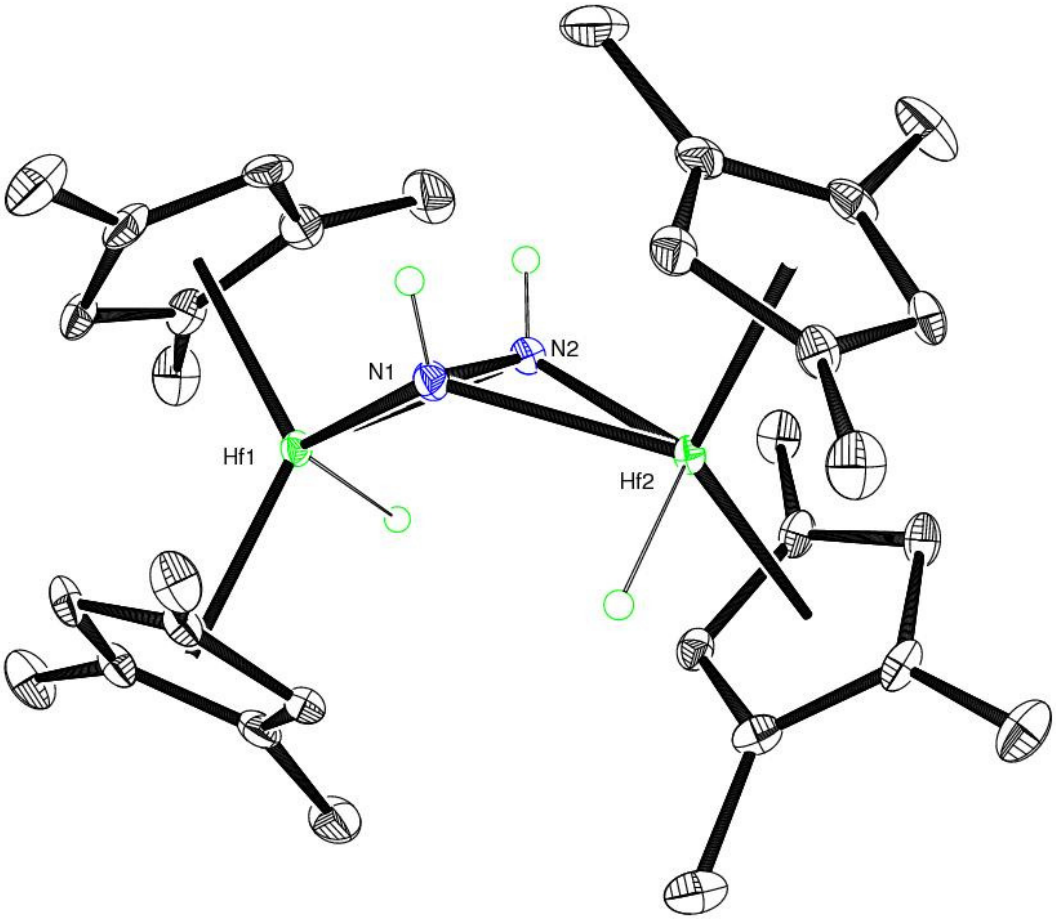

Figure 1.8 ORTEP plot of **1-N_2H_4** at 30% probability ellipsoids. Hydrogen atoms, except for those attached to hafnium and nitrogen, omitted for clarity.

The Synthesis of a Strongly Activated Zirconium Dinitrogen Compound.

The strongly activated dinitrogen ligand in **1-N_2** and the previous isolation of a rare side-on bound titanium dinitrogen compound $[(\eta^5\text{-}C_5Me_3H_2)_2Ti]_2(\eta^2, \eta^2\text{-}N_2)$[13] prompted us to investigate the synthesis of the zirconium congener $[(\eta^5\text{-}C_5Me_3H_2)_2Zr]_2(\eta^2, \eta^2\text{-}N_2)$ (**3-N_2**) in order to probe differences in activation and reactivity of side-on bound

dinitrogen units in a homologous series of Group 4 metallocene complexes. In pursuit of this goal, $(\eta^5\text{-}C_5Me_3H_2)_2ZrCl_2$ (**3-Cl$_2$**) was prepared in the same manner as **1-Cl$_2$** and isolated as a light yellow solid.

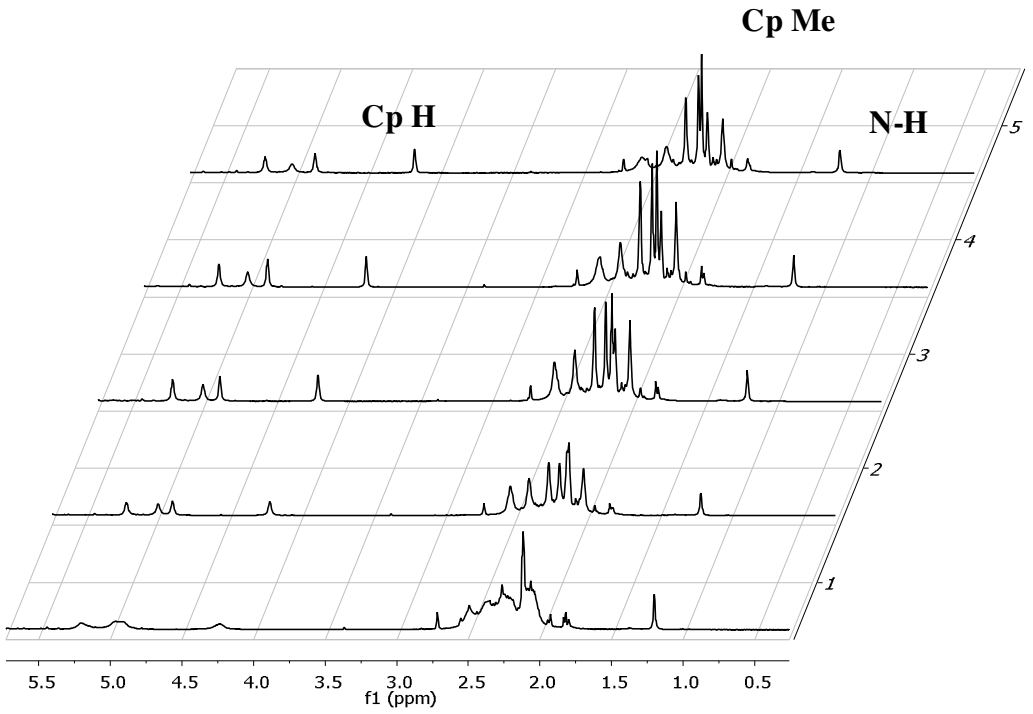

Figure 1.9 Variable temperature ^{1}H NMR spectra of **1-N$_2$H$_4$** in toluene-d_8 (1 = 25 ^{o}C, 2 = 0 ^{o}C, 3 = -10 ^{o}C, 4 = -20 ^{o}C, 5 = -30 ^{o}C)

However, attempts to synthesize the dinitrogen compound via reduction of **3-Cl$_2$** with excess sodium amalgam were unsuccessful and only provided the zirconocene mono chloride dimer, $[(\eta^5\text{-}C_5Me_3H_2)_2ZrCl]_2$.[14,15,16] In an effort to circumvent deleterious mono halide dimer formation, the more easily reduced zirconocene diiodide $(\eta^5\text{-}C_5Me_3H_2)_2ZrI_2$ **(3-I$_2$)** was synthesized by treatment of a solution of **3-Cl$_2$** with trimethylsilyliodide for 1 week or boron triiodide for 3 days (**Figure 1.10**).

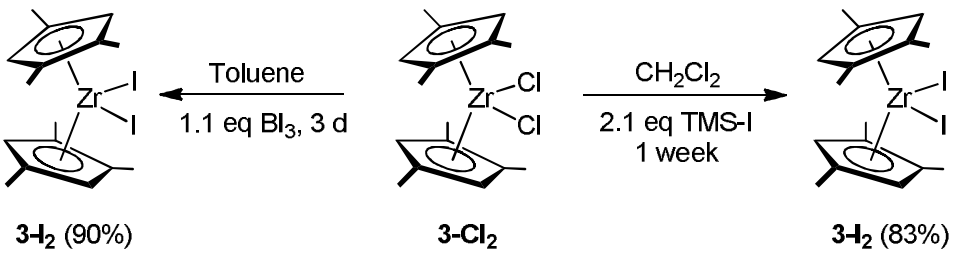

Figure 1.10. Iodination of **3-Cl$_2$**.

Reduction of **3-I$_2$** with 6 equivalents of sodium amalgam in toluene immediately produced a deep purple solution. Over the course of four days, the solution gradually turned light red, and upon work-up furnished **3-N$_2$** as a dark green microcrystalline solid in 41% yield. The ^{1}H NMR spectrum of **3-N$_2$** in benzene-d_6 is similar to that of **1-N$_2$**. Gently heating a benzene-d_6 solution of **3-N$_2$** under 1 atm of $^{15}N_2$ gas for 3 days, followed by $\{^1H\}^{15}N$ NMR analysis reveals a singlet at 608.74 ppm, shifted downfield from 621.1 ppm observed for **4-N$_2$**.[8] This suggests that at elevated temperatures, exchange of coordinated dinitrogen with free nitrogen gas is possible. However, IR analysis of toluene solutions of **3-N$_2$** at room temperature did not reveal any N-N stretching bands, suggesting a side-on hapticity of the dinitrogen fragment under ambient conditions. Additionally, toluene solutions of **3-N$_2$** are dark green at room temperature and remain so at -35 ^{o}C, in contrast to $[(\eta^5\text{-}C_5Me_4H)_2Zr]_2(\eta^2, \eta^2\text{-}N_2)$ (**4-N$_2$**), which is dark green in the solid state but deep purple in solution. This color change likely results from coordination of additional dinitrogen to zirconium, with a concomitant haptotropic shift of the side-on dinitrogen to an end-on binding mode, producing $[(\eta^5\text{-}C_5Me_4H)_2Zr(N_2)]_2(\eta^1, \eta^1\text{-}N_2)$ (**4-(N$_2$)$_3$**) [9,16,17] (**Figure 1.11**). The absence of this effect with **3-N$_2$** suggests a more strongly activated side-on bound dinitrogen fragment which is less prone to undergoing haptropic rearrangement than that of **4-N$_2$**. Similarly, this rearrangement was not observed for the strongly activated *ansa*-

zirconocene dinitrogen compound $[Me_2Si(\eta^5\text{-}C_5Me_4H)(\eta^5\text{-}C_5H_3\text{-}3\text{-}tBu)Zr]_2(\eta^2, \eta^2\text{-}N_2)$, which has an N-N bond length of 1.406(4) Å.[18]

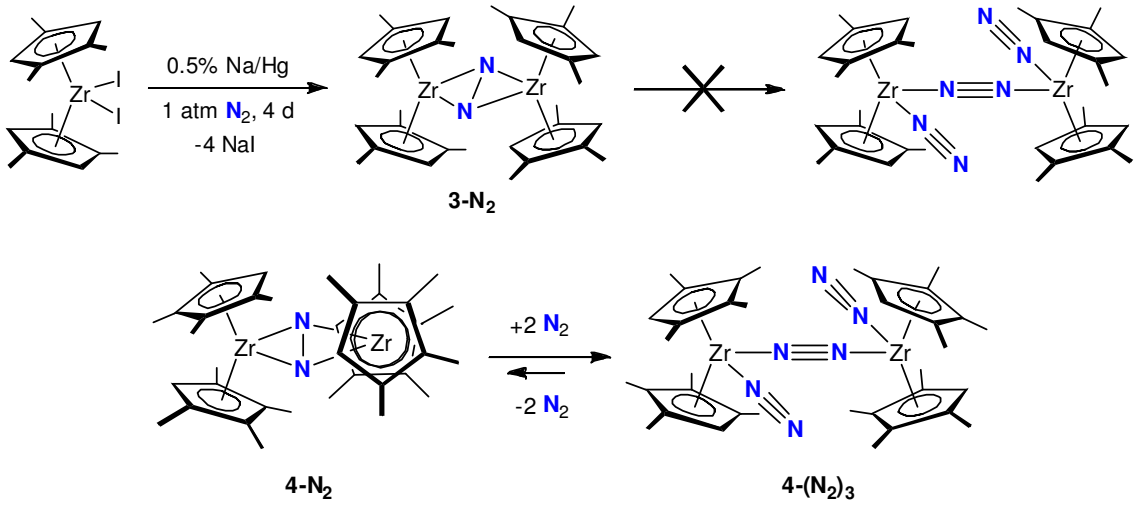

Figure 1.11. Synthesis of **3-N_2** and haptotropic behavior of zirconocene nitrogen compounds.

Unfortunately, X-ray diffraction analysis of single crystals of **3-N_2** have not allowed a meaningful discussion of metrical parameters due to co-crystallization of trace amounts of the zirconocene mono iodide dimer, so the exact degree of dinitrogen activation is unknown.

Hydrogenation of **3-N_2** to $[(\eta^5\text{-}C_5Me_3H_2)_2ZrH]_2(\eta^2, \eta^2\text{-}N_2H_2)$ (**3-N_2H_4**) was accomplished at ambient temperature by stirring a toluene solution under four atmospheres of hydrogen gas for two hours. The resulting white powder exhibited similar spectroscopic features to **1-N_2H_4**. The room temperature ^{1}H NMR in toluene-d_8 features four broad overlapping Cp methyl resonances and three broad Cp hydrogen resonances. Signals attributable to the nitrogen and zirconium bound hydrogens respectively were located at 1.50 and 4.49 ppm by isotopic labeling with D_2 gas.

Cooling of the solution resulted in the observation of six and four well separated Cp methyl and Cp hydrogen resonances, as observed with **1-N_2H_4**.

Electronic Spectra of 1-N_2 and 3-N_2. Having prepared a series of Group 4 metallocene compounds which varied only in metal identity, we were interested in comparing the electronic spectra of **1-N_2**, **3-N_2** and $[(\eta^5\text{-}C_5Me_3H_2)_2Ti]_2(\eta^2, \eta^2\text{-}N_2)$ (**5-N_2**). Pentane solutions of **1-N_2** and **3-N_2** were analyzed and are presented in **Figure 1.12**. Molar absorptivities (ε) and wavelengths of maximum absorbance (λ_{max}) are presented in **Table 1.2.** The most prominent features in the electronic spectra of **1-N_2** are the intense absorption bands at 911 and 848 nm.

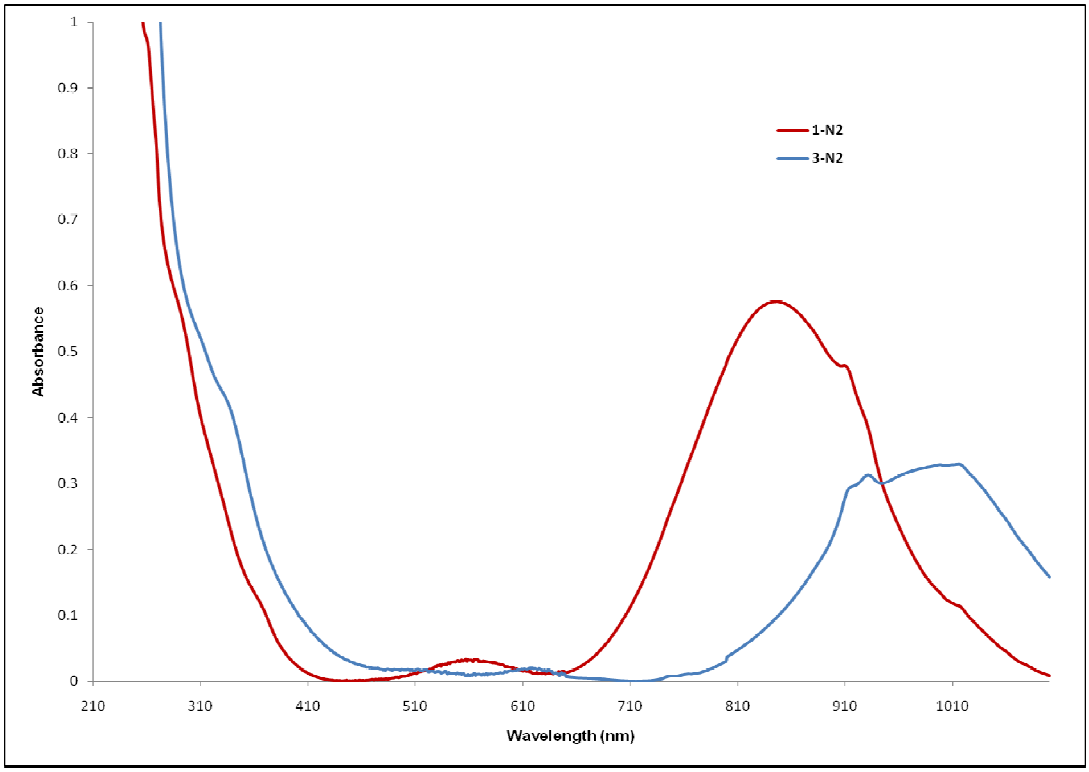

Figure 1.12 Electronic spectra of **1-N_2** and **3-N_2** in pentane solution.

These are assigned as ligand-to-metal charge transfer arising from transition from a HOMO consisting of the hafnium-nitrogen back-bond to an unoccupied orbital

which is almost entirely hafnium $1a_1$ in composition.[8] The related hafnocene **2-N_2** exhibits a similar charge transfer band at 886 nm in heptane with an extinction coefficient of 6536 M^{-1} cm^{-1}.[8] The observed blue shift for **1-N_2** is consistent with the greater activation of the dinitrogen fragment in this compound; the HOMO is pushed lower in energy as a result of greater overlap in the hafnium-nitrogen back-bond. The features in the near-infrared region of the spectrum for **3-N_2** are red-shifted, as expected for a 2nd row transition metal with a higher energy HOMO, and are less intense. Unlike its heavier congeners, the structure of **5-N_2** is best described as consisting of a $[N_2]^{2-}$ ligand bridging two Ti(III) centers.[13]

Table 1.2. Electronic spectral parameters of **1-N_2, 3-N_2** and **5-N_2** in pentane solution

1-N_2		**3-N_2**		**5-N_2**[13]	
λ_{max} (nm)	ε (M^{-1} cm^{-1})	λ_{max} (nm)	ε (M^{-1} cm^{-1})	λ_{max} (nm)	ε (M^{-1} cm^{-1})
560	888	621	176	310	10400
848	16899	914	3260	353	11500
911	12442	1017	4125	571	4700

Consequently, it lacks any salient ligand-to-metal charge transfer bands in the near-infrared region of the spectrum, but possesses two intense absorptions (10400 and 11500 M^{-1} cm^{-1}) at 310 and 353 nm.[13] The near-infrared features of the complexes track the degree of N_2 activation, with bands being blue-shifted as the degree of nitrogen-metal backbonding increases.

Trapping of a Transient μ-Nitrido Fragment. Previous investigations have shown that metallocene dinitrogen compounds react rapidly with CO gas to afford

hafnium and zirconium 'oxamidide' complexes in which the N-N bond has been cleaved and new C-C bonds have been formed.[5,19] In order to access the impact of ancillary ligand environment on an established N-C bond forming reaction, **1-N$_2$** was treated with four atmospheres of CO gas at ambient temperature. Protonation of the resulting complex mixture did confirm the formation of some oxamidide complex (evinced by the appearance of free oxamide in the ^{1}H NMR spectrum recorded in dimethylsulfoxide-d_6), however, the reaction did not cleanly provide an isolable organometallic product. In an effort to stabilize the oxamidide complex upon formation, an excess of 4-dimethylamino-pyridine (DMAP) was added to a toluene-d_8 solution of **1-N$_2$**. The ^{1}H NMR spectrum of the resulting dark green solution showed four significantly broadened Cp hydrogen resonances as well as one broad multiplet in the Cp methyl region. Cooling the solution to -10 ^{o}C resulted in sharpening of the Cp hydrogen resonances and decoalescence of the broad multiplet into 6 distinct Cp methyl signals, consistent with a C_s symmetric structure. No peaks for coordinated DMAP were observed, even at temperatures as low as -60 ^{o}C; however, the reduced symmetry of the compound implies some interaction with DMAP.

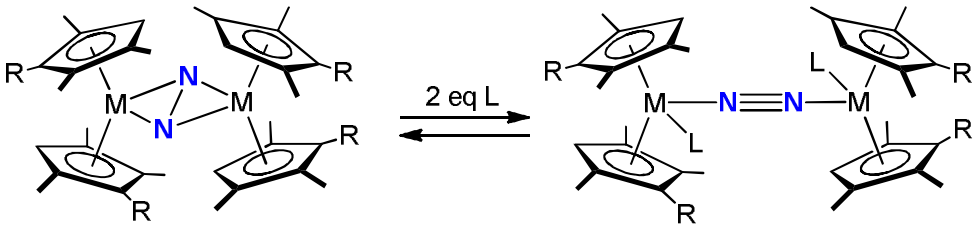

Figure 1.13 Side-on/end-on isomerization of metallocene dinitrogen compounds.

Previous studies performed with **3-N$_2$** and PMe_3 suggest that a side-on/end-on isomerization of dinitrogen is possible,[20] and one possible structure for **1-N$_2$** and DMAP

is presented in **Figure 1.13**. Addition of four atmospheres of CO to an ink-green solution of **1-N_2** and DMAP resulted in an immediate color change to dark red. ^{1}H NMR spectroscopic analysis of the resulting mixture revealed formation of a new C_s symmetric organometallic product **(Figure 1.14)**. In addition to the six Cp methyl and four Cp hydrogen resonances expected for a C_s symmetric product, the ^{1}H NMR spectrum of the product, [(η^5-$C_5Me_3H_2$)$_2$Hf(DMAP)](μ-N)[(η^5-$C_5Me_3H_2$)$_2$Hf(NCO)] **(1-(N)(DMAP)(NCO))**, exhibited two doublets at 6.20 and 8.45 ppm which were consistent with one molecule of coordinated DMAP. A very intense IR band at 2219 cm^{-1} in KBr, which shifted to 2163 cm^{-1} upon isotopic labeling with ^{13}CO, suggested the presence of a terminal isocyanate ligand.

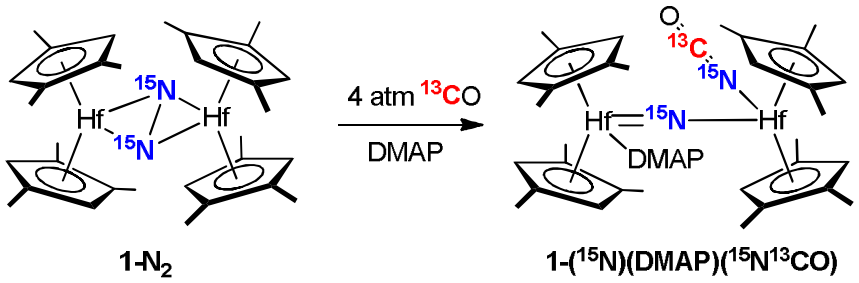

Figure 1.14 Trapping of a hafnium μ-nitrido by 4-N,N-dimethylamino-pyridine.

^{13}C NMR spectroscopic analysis of the doubly labeled compound **1-(^{15}N)(DMAP)(^{15}N^{13}CO)** revealed a doublet centered at 135.2 ppm with a carbon-nitrogen one bond coupling constant of 32.2 Hz, also consistent with a terminal isocyanate ligand.[19] Correspondingly, the benzene-d_6 {^{1}H}^{15}N NMR spectrum revealed a doublet at 88.53 ppm with an identical 32.2 Hz coupling constant. In addition, a singlet was observed at 567.49 ppm which was assigned to the bridging nitrido fragment (**Figure 1.15**).

A bridging nitrido compound of this type has been postulated as an intermediate in the reaction of **2-N_2** with CO gas, and has been trapped as a μ-imido with H_2, acetylenes and by intramolecular C-H activation.[19] However, it was transient and hence not isolable. In contrast, **1-(N)(DMAP)(NCO)** is stable indefinitely in the solid state and in solution. Performing the trapping experiment using either **3-N_2** or [$Me_2Si(\eta^5$-$C_5Me_4H)(\eta^5$-C_5H_3-3-tBu)Hf]$_2(\eta^2, \eta^2$-$N_2)$ was unsuccessful, while attempting to trap the bridging nitrido of **1-N_2** with a less potent nucleophile such as PMe_3 or pyridine only resulted in complex mixtures of products, demonstrating the unique stability of the **1-N_2** and DMAP combination.

Functionalization of a Hafnium μ-Nitrido with Terminal Alkynes and CO. In order to unequivocally confirm the isolation of a hafnium nitride in the absence of a solid-state structure, efforts were made to functionalize the hafnium nitride with various reagents. Based on previous investigations in our laboratory[17, 19] and that of Fryzuk[21], terminal alkynes were targeted as potential reagents. Thus, treatment of a toluene solution of **1-(N)(DMAP)(NCO)** with one equivalent of trimethylsilylacetylene or phenylacetylene at 75 ^oC for 18 hours cleanly afforded a new C_s symmetric product (**Figure 1.16**) resulting from 1,2-addition of the acetylene C-H bond across the Hf-N bond. The elevated temperatures required are likely due to the need to dissociate the coordinated DMAP molecule prior to C-H activation. Infrared spectroscopy on a toluene solution of **1-(NH)(CCSiMe_3)(NCO)** revealed bands at 3575, 2083 and 2038 cm^{-1}, which were assigned to N-H, isocyanate and acetylido stretches respectively.

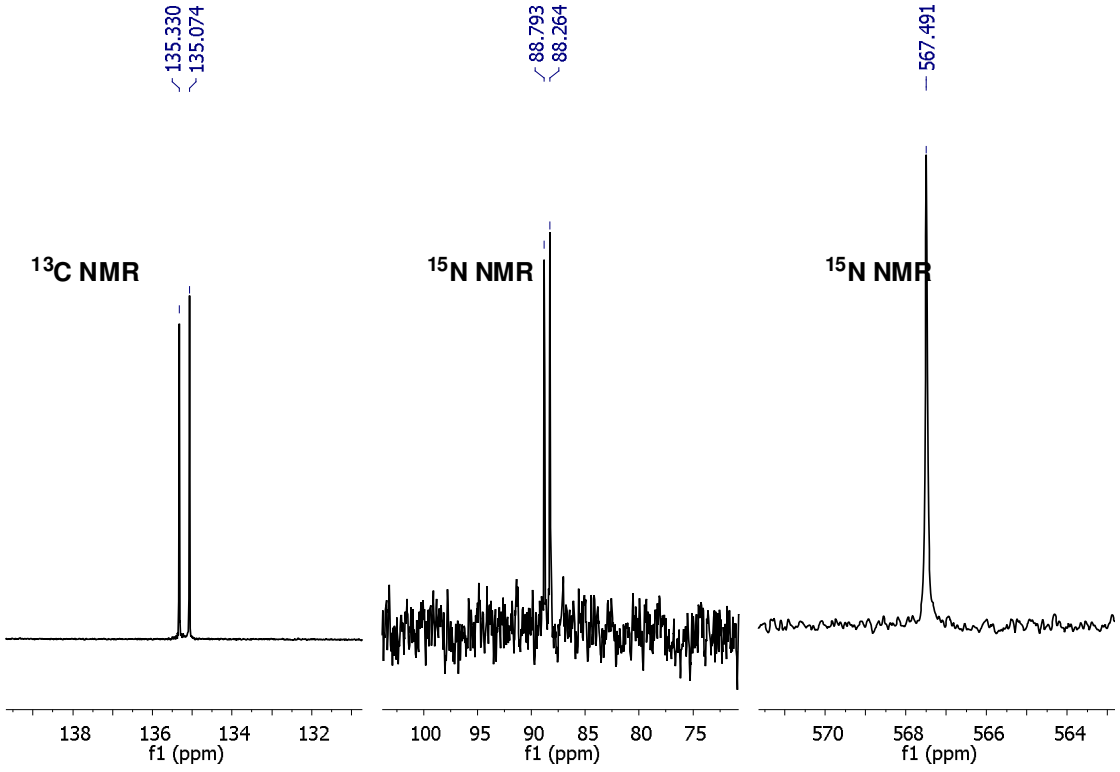

Figure 1.15 Selected regions of the ^{13}C and ^{15}N NMR spectra of **(1-(^{15}N)(DMAP)(^{15}N^{13}CO)).**

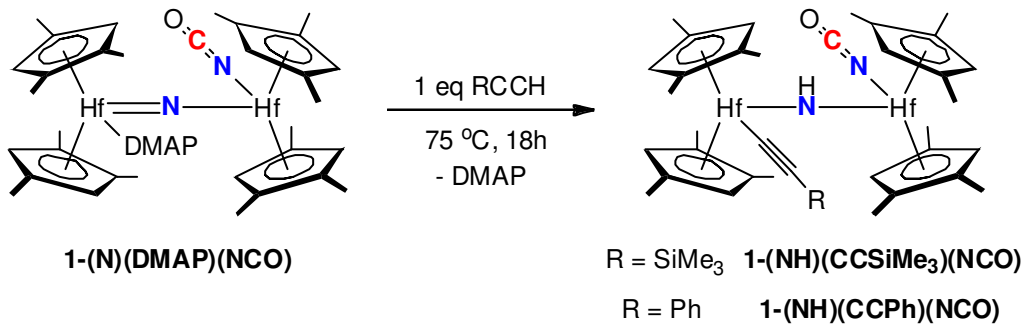

Figure 1.16 Functionalization of a hafnium μ-nitrido with terminal alkynes.

Solution ^{15}N NMR data for the doubly labeled compound **1-(^{15}NH)(CCSiMe$_3$)(^{15}N^{13}CO)** revealed two peaks; one doublet centered at 92.23 ppm with a 32.6 Hz coupling which was assigned to the isocyanate nitrogen, and one singlet

at 283.42 ppm which was assigned to the bridging imido fragment on the basis of an ^{15}N-^{1}H HSQC experiment. The same experiment also revealed the presence of an N-H resonance in the ^{1}H NMR spectrum at 6.79 ppm. These data are similar to those of compound **1-(^{15}NH)(CCPh)(^{15}N^{13}CO)**, and full spectral data for both compounds are reported in **Table 1.3**.

Table 1.3. Spectral data for **1-(^{15}NH)(CCSiMe$_3$)(^{15}N^{13}CO)** and **1-(^{15}NH)(CCPh)(^{15}N^{13}CO)**

	1-(^{15}NH)(CCSiMe$_3$)(^{15}N^{13}CO)	**1-(^{15}NH)(CCPh)(^{15}N^{13}CO)**
N-*H* (ppm)[b]	6.79	7.01
^{15}*N*-H (ppm)[c]	283.42	282.11
^{15}NCO (ppm)[c]	92.23 (J = 32.6)	91.67 (J = 32.6)
N^{13}CO (ppm)[d]	135.73 (J = 32.6)	135.70 (J = 32.6)

[a] Frequences determined by solution IR (toluene). [b] ^{1}H NMR spectra recorded in benzene-d_6 at 23 ^{o}C. [c] ^{15}N NMR spectra recorded in benzene-d_6 at 23 ^{o}C. [d] ^{13}C NMR spectra recorded in benzene-d_6 at 23 ^{o}C.

The data are analogous to that reported for the related *ansa*-hafnocene compound [Me$_2$Si(η^5-C$_5$Me$_4$)(η^5-C$_5$H$_3$-3-tBu)Hf]$_2$(μ-NH)(CCPh)(NCO).[19] These functionalization experiments support the formulation of **1-(N)(DMAP)(NCO)** as a bridging nitrido compound.

In an attempt to determine if the DMAP stabilized nitride was an intermediate on the pathway to form the putative oxamidide product [(η^5-C$_5$Me$_3$H$_2$)$_2$Hf]$_2$(N$_2$C$_2$O$_2$), **1-(N)(DMAP)(NCO)** was treated with four atmospheres of CO at ambient temperature. Spectroscopic analysis of the resulting reaction mixture revealed the formation of a single organometallic product **(Figure 1.17)**. Protonolysis studies yielded only small amounts of ammonium chloride, inconsistent with oxamidide formation, and multinuclear NMR analysis instead identified the new product as the bridging

isocyanato compound [(η^5-$C_5Me_3H_2$)$_2$Hf(η^3, η^1, μ-NCO)(η^5-$C_5Me_3H_2$)$_2$Hf(NCO)] (**1-(μ-NCO)(NCO)**).

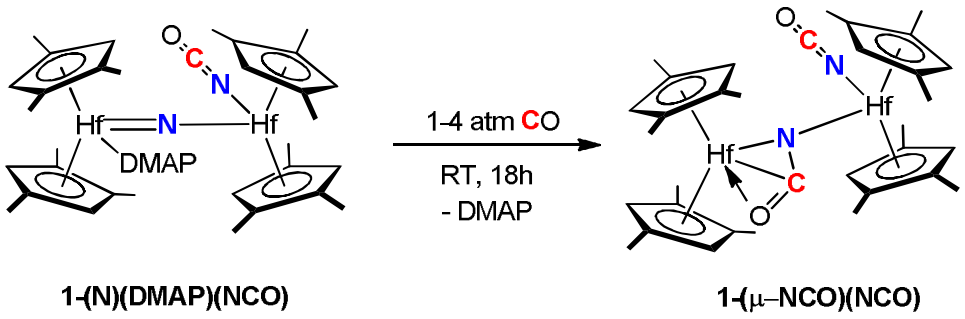

Figure 1.17 Functionalization of hafnium μ-nitrido with additional CO.

Evidence for terminal and bridging isocyanates was provided by ^{13}C NMR spectroscopy, which revealed a peak centered at 135.4 ppm with a $^1J_{CN}$ of 32.8 Hz, indicative of a terminal isocyanate (*vide infra)*, as well as a second doublet at 164.1 ppm with $^1J_{CN}$ of 8.3 Hz. Corresponding peaks were located in the ^{15}N NMR spectrum at 94.15 ($^1J_{CN}$ of 32.8 Hz) and 324.15 ($^1J_{CN}$ of 8.3 Hz) ppm (**Figures 1.19 and 1.20**). The downfield peak was assigned to the μ-isocyanate fragment on the basis of its chemical shift and smaller carbon-nitrogen coupling constant. Solution IR spectroscopy revealed a single intense stretch centered at 2223 cm^{-1}, which shifted to 2163cm^{-1} when ^{13}CO was used.

The reaction likely proceeds by the following mechanism: initial dissociation of DMAP from hafnium, followed by coordination of CO and subsequent insertion into the Hf-nitride bond to form the bridging isocyanate fragment (**Figure 1.18**). The conversion of **A** to **B** is likely irreversible due to the presence of excess CO; however, the insertion of CO into the Hf-nitride bond was determined to be kinetically reversible (*vide infra*). A sample of **1-(μ-NCO)(NCO)** left under an atmosphere of ^{13}CO for 2

days revealed incorporation of labeled carbon solely into the bridging isocyanate position as judged by ^{13}C NMR spectroscopy.

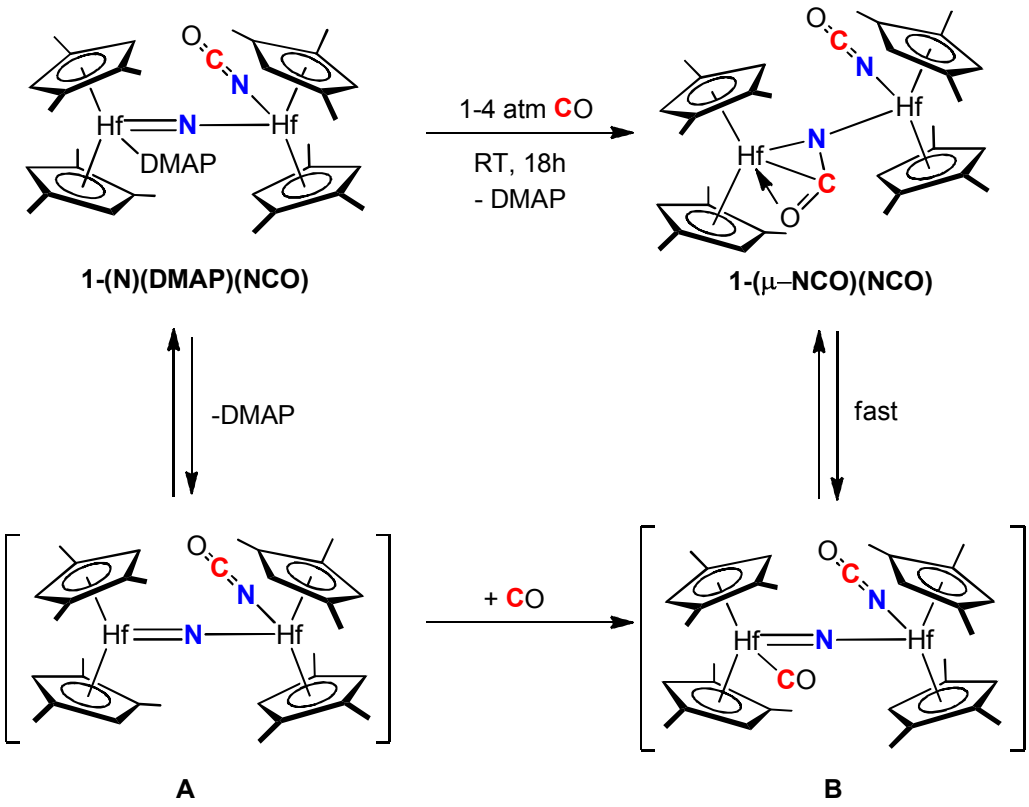

Figure 1.18 Possible mechanism for formation of **1-(μ-NCO)(NCO)**

Concluding Remarks

Two new metallocene dinitrogen compounds bearing the 1,2,4-trimethylcyclopentadienyl ligand have been synthesized and found to contain strongly activated side-on bound dinitrogen fragments. The high degree of N_2 activation likely results from the lower steric demand of the 1,2,4-trimethylcyclopentadienyl ligand, which allows a shorter metal-metal distance and greater overlap between metal *d* and nitrogen π* orbitals. The high degree of N_2 activation in these compounds results in blue-shifted electronic transitions in the near-infrared. This is consistent with a lower

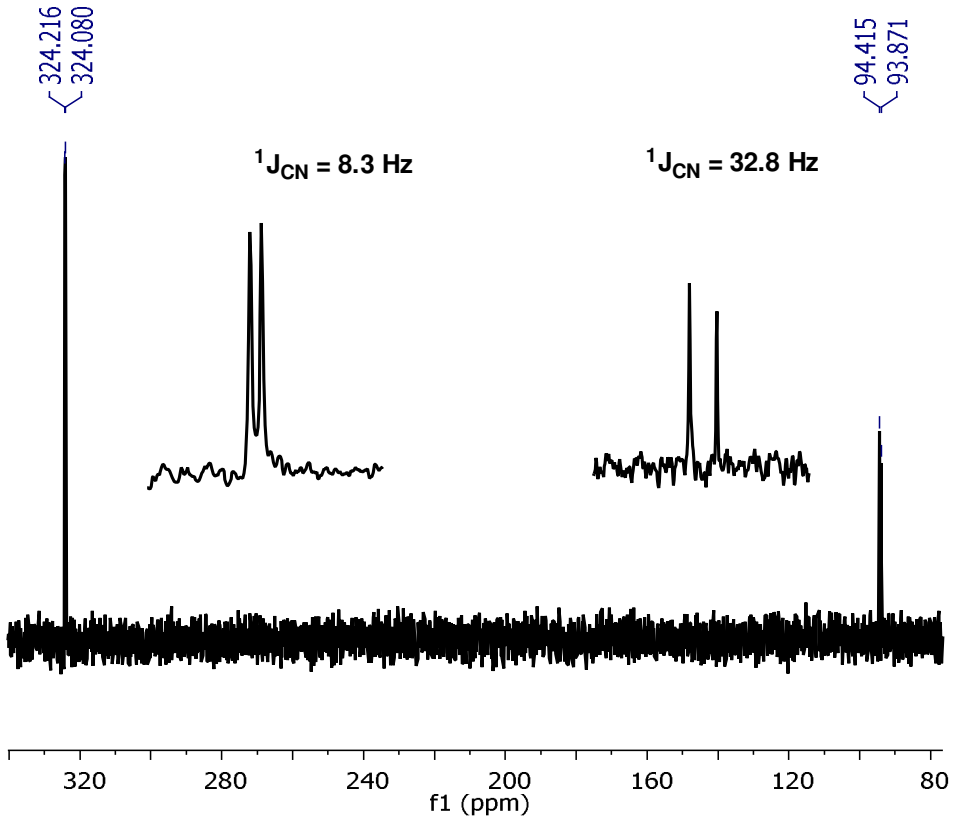

Figure 1.19 ^{15}N NMR spectrum of **1-(μ-NCO)(NCO)** in benzene-d_6.

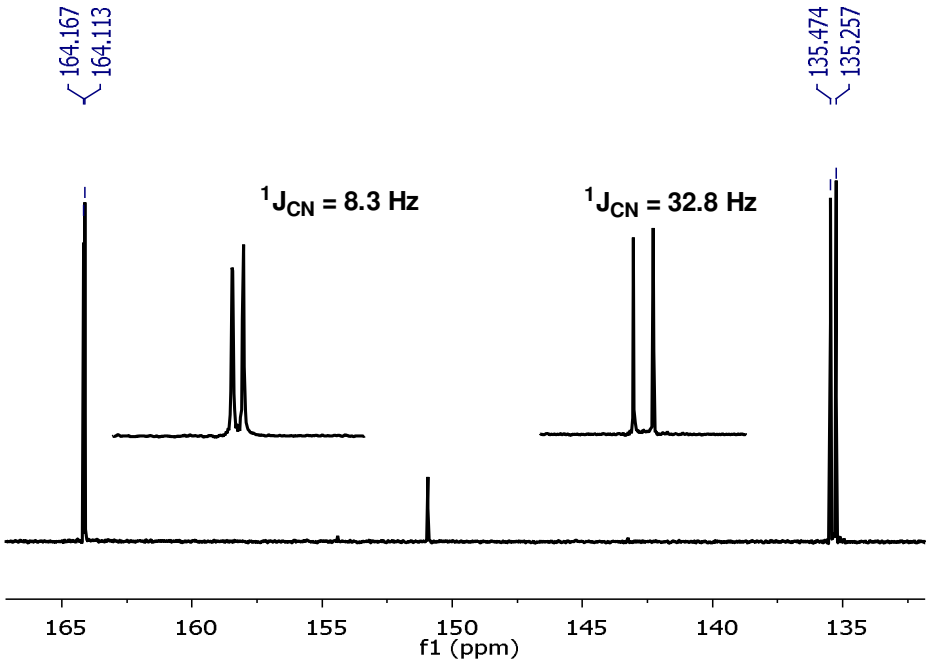

Figure 1.20 ^{13}C NMR spectrum of **1-(μ-NCO)(NCO)** in benzene-d_6.

energy nitrogen π^* LUMO in these complexes compared to those bearing the tetramethylcyclopentadienyl ligand. The reactivity of these new complexes with H_2 occurs analogously to previously established examples, despite their higher degree of N_2 activation. Reaction of the hafnocene dinitrogen compound $[(\eta^5\text{-}C_5Me_3H_2)_2Hf]_2(\eta^2, \eta^2\text{-}N_2)$ with CO in the presence of DMAP has provided the first example of an isolable 'masked' hafnium nitride compound whose chemistry was explored using terminal alkynes and CO. 1,2 addition of terminal alkynes across the hafnium nitride fragment proceeded at elevated temperatures to afford μ-imido acetylido compounds. Reaction of an additional molecule of CO with the hafnium nitride did not afford the expected hafnium 'oxamidide' compound, but rather a μ-isocyanato moiety arising from insertion of CO into the Hf-N linkage. These results highlight the effect of minor changes to the ancillary ligand environment on both dinitrogen activation and functionalization in group 4 metallocene complexes.

Experimental

General Considerations. All air- and moisture-sensitive manipulations were carried out using standard high vacuum line, Schlenk or cannula techniques or in an M. Braun inert atmosphere drybox containing an atmosphere of purified dinitrogen. The drybox was equipped with a cold well designed for freezing samples in liquid nitrogen. Solvents for air- and moisture-sensitive manipulations were dried and deoxygenated using literature procedures. Deuterated solvents for NMR spectroscopy were purchased from Cambridge Isotope Laboratories and were distilled from sodium metal under an atmosphere of argon and stored over 4 Å molecular sieves. Hydrogen and argon gas were purchased from Airgas Incorporated and passed through a column containing manganese oxide supported on vermiculite and 4 Å molecular sieves before admission to the high vacuum line. ^{1}H spectra were recorded on Bruker ARX 300, Varian Mercury

300, Inova 400 and 500 spectrometers operating at 299.763, 299.763, 399.780 and 500.62 MHz, respectively. ^{13}C NMR spectra were obtained on Bruker ARX 300 and Inova 500 spectrometers operating at 75.37 and 100.52 MHz, respectively. All chemical shifts are reported relative to $SiMe_4$ using ^{1}H (residual) chemical shifts of the solvent as a secondary standard. ^{2}H NMR spectra were recorded on a Varian Inova 500 spectrometer operating at 76.851 MHz and the spectra were referenced using an internal benzene-d_6 standard. ^{15}N NMR spectra were recorded on a Varian Inova 500 spectrometer operating at 50.663 MHz and chemical shifts were externally referenced to liquid ammonia. Infrared spectroscopy was conducted on a Thermo-Nicolet Avatar FT-IR spectrometer calibrated with a polystyrene standard.

Single crystals suitable for X-ray diffraction were coated with polyisobutylene oil in a drybox and were quickly transferred to the goniometer head of a Siemens SMART CCD Area detector system or a Bruker X8 APEX2 system equipped with a molybdenum X-ray tube (λ = 0.71073 A). Preliminary data revealed the crystal system. A hemisphere routine was used for data collection and determination of lattice constants. The space group was identified and the data were processed using the Bruker SAINT program and corrected for absorption using SADABS. The structures were solved using direct methods (SHELXS) completed by subsequent Fourier synthesis and refined by full-matrix least-squares procedures. Elemental analyses were performed at Robertson Microlit Laboratories, Inc., in Madison, NJ.

UV-Vis spectra were recorded on a Cary WinUV 5000 spectrophotometer from 200 to 1100 nm with a diode array detector. 3,4-dimethyl-cyclopent-2-enone was prepared according to literature procedures.[10] The metallocene diiodides (η^5-$C_5Me_3H_2)_2HfI_2$ and (η^5-$C_5Me_3H_2)_2ZrI_2$ were prepared in a similar manner to (η^5-$C_5Me_4H)_2HfI_2$.[8] $^{15}N_2$ gas was purchased from Cambridge Isotope Laboratories. All other chemicals were purchased from Aldrich or Acros and used as received.

Synthesis of 1,2,4-trimethylcyclopentadiene. In the glovebox, a 3-neck, 1 L round bottom flask was charged with a large stirbar and MeMgBr (42.5, 0.1275 mol, 3.0 M in diethyl ether). The Grignard was diluted with additional diethyl ether (200 mL) and the flask was fitted with a gas inlet, stopper, and 100 mL pressure equalized dropping funnel. The flask was removed to a Schlenk line the dropping funnel was charged with 3,4-dimethyl-cyclopent-2-enone (12.2 g, 0.111 mol) and diethyl ether (50 mL) against an argon counterflow. With rapid stirring, the solution was cooled to -78 ^{o}C with a dry-ice/acetone bath and the enone was added over the course of 1 h. The mixture was slowly warmed to room temperature before being poured over an ice-cold 25% ammonium chloride solution (500 mL). The ether layer was separated and the aqueous layer extracted with ether (100 mL) before the combined organic layers were washed with water (200 mL) and brine (200 mL) and dried over anhydrous sodium sulphate. The resulting light yellow solution was filtered into a 1 L round bottom flask and ether was removed on the rotovap. The resulting yellow oil was dissolved in benzene (75 mL) and a catalytic amount of iodine was added to the solution. The solution was refluxed overnight with a Dean-Stark trap before the benzene was removed on the rotovap. Vacuum distillation of the crude reaction mixture afforded 1,2,4-trimethylcyclopentadiene as a light yellow liquid (9.5 g, 79%). The lithium salt was prepared by deprotonation with ^{n}BuLi in pentane at -78 ^{o}C followed by filtration.

Preparation of [(η^5-$C_5Me_3H_2$)$_2$Hf]$_2$(η^2, η^2-N_2) (1-N_2). A 100 mL round bottom flask was charged with 28.5 g of 0.5% sodium amalgam and toluene (10 mL). With vigorous stirring of the amalgam, a suspension of (η^5-$C_5Me_3H_2$)$_2$HfI$_2$ (0.500 g, 0.774 mmol) in toluene (10 mL) was added. The resulting reaction mixture was stirred for 2 days at ambient temperature under a dinitrogen atmosphere, turning deep purple after one hour.

Following filtration through Celite, the solvent was removed in vacuo, leaving a dark purple solid which was re-crystallized from pentane at -35 °C to afford 0.255 g of [(η^5-$C_5Me_3H_2$)$_2$Hf]$_2$(η^2, η^2-N_2) as an analytically pure solid (41%). X-ray quality crystals were deposited as purple blocks from a concentrated fluorobenzene solution layered with pentane. Anal Calcd for $C_{32}H_{44}N_2Hf_2$: C, 47.23; H, 5.45; N, 3.44. Found: C, 47.05; H, 5.47; N, 3.19. ^{1}H NMR (benzene- d_6, 23 °C): δ 2.06 (s, 24H, $C_5\mathit{Me}_3H_2$), 2.08 (s, 12H, $C_5\mathit{Me}_3H_2$), 5.44 (s, 4H, $C_5Me_3\mathit{H}_2$). {^{1}H}^{13}C NMR (benzene-d_6, 23 °C): δ 13.0, 14.6 ($C_5\mathit{Me}_3H_2$), 109.6, 116.1 ($\mathit{C}_5Me_3H_2$); One $\mathit{C}_5Me_3H_2$ signal not located. {^{1}H}^{15}N NMR (benzene-d_6, 23 °C): δ 570.20 (Hf-N_2-Hf). UV-Vis (pentane): 560 (888 M^{-1} cm^{-1}), 848 (16 899 M^{-1} cm^{-1}), 911 (12 442 M^{-1} cm^{-1}).

Preparation of [(η^5-$C_5Me_3H_2$)$_2$HfH]$_2$$N_2H_2$ (1-N_2H_4). A thick walled glass reaction vessel was charged with a stirbar, [(η^5-$C_5Me_3H_2$)$_2$Hf]$_2$(η^2, η^2-N_2) (74 mg, 0.09 mmol) and toluene (10 mL). On a high vacuum line, the vessel was frozen, evacuated, and H_2 gas (4 atm) was admitted to the vessel. The reaction mixture was stirred for 3 hours, changing from deep purple to light yellow. The volatiles were removed in vacuo and the residue was re-crystallized from pentane at -35 °C to yield 50 mg of [(η^5-$C_5Me_3H_2$)$_2$HfH]$_2$$N_2H_2$ as a white powder (69 %). Anal. Calcd for $C_{32}H_{48}Hf_2N_2$: C. 47.00; H, 5.92; N, 3.43. Found: C, 47.03; H, 6.00; N, 3.32. ^{1}H NMR (benzene-d_6, 23 °C): δ 1.21 (s, 2H, NH), 1.97-2.49 (br m, 36H, $C_5\mathit{Me}_3H_2$), 4.24 (br s, 2H, $C_5Me_3\mathit{H}_2$), 4.92 (br s, 2H, $C_5Me_3\mathit{H}_2$), 5.00 (br s, 2H, $C_5Me_3\mathit{H}_2$), 5.20 (br s, 2H, $C_5Me_3\mathit{H}_2$), 8.19 (s, 2H, Hf-H). ^{1}H NMR (toluene-d_8, -30 °C): δ 1.17 (s, 2H, NH), 1.95 (br s, 6H, $C_5\mathit{Me}_3H_2$), 2.10 (br s, 6H, $C_5\mathit{Me}_3H_2$), 2.12 (br s, 6H, $C_5\mathit{Me}_3H_2$), 2.21 (br s, 6H, $C_5\mathit{Me}_3H_2$), 2.34 (br s, 6H, $C_5\mathit{Me}_3H_2$), 2.51 (br s, 6H, $C_5\mathit{Me}_3H_2$), 4.10 (s, 2H, $C_5Me_3\mathit{H}_2$), 4.80 (s, 2H, $C_5Me_3\mathit{H}_2$), 4.97 (s, 2H, $C_5Me_3\mathit{H}_2$), 5.18 (s, 2H, $C_5Me_3\mathit{H}_2$), 8.05 (s, 2H, Hf-H). {^{1}H}^{13}C NMR (toluene-d_8, -30 °C): δ 13.3, 14.4, 14.5, 14.8, 15.6 ($C_5\mathit{Me}_3H_2$), 105.1, 105.7,

109.1, 114.5, 115.1, 116.5, 116.9, 131.9, 132.6, 133.2; One $C_5Me_3H_2$ signal not located. IR (toluene): ν_{NH} = 3290 cm^{-1}.

Preparation of $[(\eta^5\text{-}C_5Me_3H_2)_2HfI]_2N_2H_2$ (1-$N_2H_2I_2$). A thick-walled glass vessel was charged with a stirbar, $[(\eta^5\text{-}C_5Me_3H_2)_2HfH]_2N_2H_2$ (132 mg, 0.16 mmol) and toluene (5 mL). On a high vacuum line, methyl iodide (0.64 mmol) was added via calibrated gas bulb (100.1 mL, 119.3 Torr), and the reaction was stirred at room temperature for two hours. The solvent was removed in vacuo from the resulting deep red solution, and the remaining residue was washed with pentane (10 mL) and dried to afford 170 mg of $[(\eta^5\text{-}C_5Me_3H_2)_2HfINH]_2$ as an orange powder (98%). Anal. Calcd for $C_{32}H_{46}Hf_2I_2N_2$: C. 35.94; H, 4.34; N, 2.62. Found: C, 36.19; H, 4.67; N, 2.38. ^{1}H NMR (benzene-d_6, 23 ^{o}C): δ 1.91 (s, 12H, $C_5Me_3H_2$), 2.08 (s, 12H, $C_5Me_3H_2$), 2.40 (s, 12H, $C_5Me_3H_2$), 5.51 (d, $^4J_{HH}$ = 2.1, 4H, $C_5Me_3H_2$), 5.68 (d, $^4J_{HH}$ = 2.1, 4H, $C_5Me_3H_2$), 8.07 (s, 2H, N*H*). $\{^1H\}^{13}C$ NMR (benzene-d_6, 23 ^{o}C): δ 14.1, 16.2, 16.8 ($C_5Me_3H_2$), 113.2, 113.3, 116.2, 117.7, 123.1 ($C_5Me_3H_2$). IR (KBr): ν_{NH} = 3389 cm^{-1}.

Preparation of $[(\eta^5\text{-}C_5Me_3H_2)_2Zr]_2(\eta^2, \eta^2\text{-}N_2)$ (3-N_2). A 100 mL round bottom flask was charged with 8.4 g of 0.5% sodium amalgam and toluene (10 mL). With vigorous stirring of the amalgam, a suspension of $(\eta^5\text{-}C_5Me_3H_2)_2ZrI_2$ (0.250 g, 0.447 mmol) in toluene (10 mL) was added. The resulting reaction mixture was stirred for 4 days at ambient temperature under a dinitrogen atmosphere, turning deep purple after one hour and red-brown after 3 days. Following filtration through Celite, the solvent was removed in vacuo, leaving a dark green solid which was re-crystallized from pentane at -35 ^{o}C to afford 114 mg of $[(\eta^5\text{-}C_5Me_3H_2)_2Zr]_2(\eta^2, \eta^2\text{-}N_2)$ as an analytically pure green solid (41%). Crystals were deposited as green prisms following slow evaporation of a benzene solution stored at 23 ^{o}C for 3 d. Anal Calcd for $C_{32}H_{44}N_2Zr_2$: C, 60.13; H, 6.94;

N, 4.38. Found: C, 60.12; H, 6.87; N, 3.99. ^{1}H NMR (benzene- d_6, 23 ^{o}C): δ 2.02 (s, 24H, $C_5Me_3H_2$), 2.07 (s, 12H, $C_5Me_3H_2$), 5.32 (s, 4H, $C_5Me_3H_2$). {^{1}H}^{13}C NMR (benzene-d_6, 23 ^{o}C): δ 13.2, 15.1 ($C_5Me_3H_2$), 110.1, 117.7 ($C_5Me_3H_2$); One $C_5Me_3H_2$ signal not located. {^{1}H}^{15}N NMR (benzene-d_6, 23 ^{o}C): δ 608.74 (Zr-N_2-Zr). UV-Vis (pentane): 621 (176 M^{-1} cm^{-1}), 914 (3260 M^{-1} cm^{-1}), 1017 (4125 M^{-1} cm^{-1}).

Preparation of [(η^5-$C_5Me_3H_2$)$_2$ZrH]$_2$$N_2H_2$ (3-N_2H_4). A thick walled glass reaction vessel was charged with a stirbar, [(η^5-$C_5Me_3H_2$)$_2$Zr]$_2$(η^2, η^2-N_2) (75 mg, 0.118 mmol) and toluene (10 mL). On a high vacuum line, the vessel was frozen, evacuated, and H_2 gas (4 atm) was admitted to the vessel. The reaction mixture was stirred for 3 hours, changing from dark green to light yellow. The volatiles were removed in vacuo and the residue was washed with cold pentane (2 x 5 mL) to yield 45 mg of [(η^5-$C_5Me_3H_2$)$_2$ZrH]$_2$$N_2H_2$ as a white powder (60 %). ^{1}H NMR (benzene-d_6, 23 ^{o}C): δ 1.50 (s, 2H, N*H*), 2.02 (br s, 18H, $C_5Me_3H_2$), 2.12 (br s, 3H, $C_5Me_3H_2$), 2.26 (br s, 6H, $C_5Me_3H_2$), 2.36 (br s, 9H, $C_5Me_3H_2$), 4.24 (br s, 2H, $C_5Me_3H_2$), 4.49 (s, 2H, Zr-*H*), 4.88 (br s, 2H, $C_5Me_3H_2$), 5.07 (br m, 4H, $C_5Me_3H_2$). ^{1}H NMR (toluene-d_8, -30 ^{o}C): δ 1.41 (s, 2H, N*H*), 1.94 (s, 6H, $C_5Me_3H_2$), 1.97 (s, 6H, $C_5Me_3H_2$), 2.08 (s, 6H, $C_5Me_3H_2$), 2.15 (s, 6H, $C_5Me_3H_2$), 2.24 (s, 6H, $C_5Me_3H_2$), 2.43 (s, 6H, $C_5Me_3H_2$), 4.22 (s, 2H, $C_5Me_3H_2$), 4.38 (s, 2H, Zr-*H*), 4.91 (s, 2H, $C_5Me_3H_2$), 5.04 (s, 2H, $C_5Me_3H_2$), 5.18 (s, 2H, $C_5Me_3H_2$). {^{1}H}^{13}C NMR (toluene-d_8, -20 ^{o}C): δ 13.6, 14.3, 14.6, 14.6, 15.0 ($C_5Me_3H_2$), 106.3, 106.8, 107.2, 108.9, 111.0, 114.8, 114.9, 115.3, 117.6, 120.0 ($C_5Me_3H_2$). One $C_5Me_3H_2$ signal not located. IR (toluene): ν_{NH} = 3235 cm^{-1}.

Initial product of [(η^5-$C_5Me_3H_2$)$_2$Hf]$_2$(η^2, η^2-N_2) and 4-dimethylamino-pyridine. A J. Young NMR tube was charged with [(η^5-$C_5Me_3H_2$)$_2$Hf]$_2$(η^2, η^2-N_2) (17 mg, 0.021 mmol) and 4-dimethylamino-pyridine (5 mg, 0.041) and dissolved in toluene-d_8 (0.75

mL) to afford a dark inky-green solution. The ^{1}H NMR spectrum was immediately recorded at -10 ^{o}C.

^{1}H NMR (toluene- d_8, 20 ^{o}C): δ 2.11-2.40 (br m, 36H, $C_5Me_3H_2$), 5.02 (br s, 2H, $C_5Me_3H_2$), 5.39 (br s, 2H, $C_5Me_3H_2$), 5.56 (br s, 2H, $C_5Me_3H_2$). ^{1}H NMR (toluene- d_8, -10 ^{o}C): δ 1.78 (s, 6H, $C_5Me_3H_2$), 2.06 (s, 6H, $C_5Me_3H_2$), 2.13 (s, 6H, $C_5Me_3H_2$), 2.36 (s, 6H, $C_5Me_3H_2$), 2.41 (s, 6H, $C_5Me_3H_2$), 2.49 (s, 6H, $C_5Me_3H_2$), 5.01 (br s, 2H, $C_5Me_3H_2$), 5.36 (br s, 2H, $C_5Me_3H_2$), 5.57 (br s, 2H, $C_5Me_3H_2$), 5.61 (br s, 2H, $C_5Me_3H_2$).

Preparation of [(η^5-C$_5$Me$_3$H$_2$)$_2$Hf(DMAP)](μ-N)[(η^5-C$_5$Me$_3$H$_2$)$_2$Hf(NCO)] (1-(N)(DMAP)(NCO)) A thick-walled glass vessel was charged with [(η^5-$C_5Me_3H_2)_2Hf]_2$(η^2, η^2-N_2) (75 mg, 0.092 mmol) and 4-dimethylamino-pyridine (23 mg, 0.184 mmol). Toluene (10 mL) was added and the solution immediately turned an inky blue-green. On a high vacuum line, the vessel was frozen, evacuated, and CO gas (4 atm) was admitted to the vessel. The vessel was thawed and shaken vigorously for 1 minute, whereupon a color change to light red was observed. The solvent was removed in vacuo and the red oil was extracted with toluene (15 mL), concentrated under vacuum, layered with pentane and stored at -35 ^{o}C overnight. [(η^5-$C_5Me_3H_2)_2$Hf(DMAP)](μ-N)[(η^5-$C_5Me_3H_2)_2$Hf(NCO)] deposited as an off-white solid (46 mg, 52 %).^{1}H NMR (benzene- d_6, 23 ^{o}C): δ 1.86 (s, 6H, $C_5Me_3H_2$), 1.88 (s, 6H, $C_5Me_3H_2$), 2.04 (s, 6H, $C_5Me_3H_2$), 2.06 (s, 6H, $C_5Me_3H_2$), 2.43 (s, 12H, $C_5Me_3H_2$ and NMe_2 overlapped), 2.54 (s, 6H, $C_5Me_3H_2$), 5.49 (d, $^4J_{HH}$ = 2.3, 2H, $C_5Me_3H_2$), 5.86 (d, $^4J_{HH}$ = 2.3, 2H, $C_5Me_3H_2$), 6.20 (d, $^3J_{HH}$ = 6.5, 2H, DMAP *m*-ArH), 6.36 (d, $^4J_{HH}$ = 2.3, 2H, $C_5Me_3H_2$), 6.39 (d, $^4J_{HH}$ = 2.3, 2H, $C_5Me_3H_2$), 8.46 (d, $^3J_{HH}$ = 6.5, 2H, DMAP *o*-ArH). {^{1}H}^{13}C NMR (benzene-d_6, 23 ^{o}C): δ 13.5, 13.6, 13.7, 14.6, 16.2, 16.3 ($C_5Me_3H_2$), 38.5 (NMe_2), 107.2 (Ar *C*), 106.5, 110.9, 113.3, 113.5, 114.3, 114.6, 115.8, 116.9, 117.4, 120.0, 120.7 ($C_5Me_3H_2$), 135.2 (d, $^1J_{CN}$ = 32.2, N*C*O), 150.9 (Ar *C*), 154.3

(Ar *C*). $\{^1H\}^{15}N$ NMR (benzene-d_6, 23 °C): δ 88.53 (d, $^1J_{CN}$ = 32.2, *N*CO), 567.49 (s, Hf=*N*). IR (C_6D_6): ν_{NCO} = 2219 cm^{-1}.

Preparation of [(η⁵-$C_5Me_3H_2$)$_2$Hf](η³, η¹, μ-NCO)[(η⁵-$C_5Me_3H_2$)$_2$Hf(NCO)] (1-(μ-NCO)(NCO)). A thick-walled glass vessel was charged with a stirbar, [(η⁵-$C_5Me_3H_2$)$_2$Hf]$_2$(η², η²-N_2) (49 mg, 0.060 mmol) and 4-dimethylamino-pyridine (8 mg, 0.066 mmol). Toluene (10 mL) was added and the solution immediately turned an inky blue-green. On a high vacuum line, the vessel was frozen, evacuated, and CO gas (4 atm) was admitted. The vessel was thawed and shaken vigorously for 1 minute, whereupon a color change to light red was observed. The solution was stirred at room temperature for 18h, changing to a dark brown color. The solvent was removed in vacuo and the brown oil was extracted with toluene (10 mL), concentrated, and stored at -35 °C overnight to induce deposition of [(η⁵-$C_5Me_3H_2$)$_2$Hf(CO)](η³, η¹, μ-NCO)[(η⁵-$C_5Me_3H_2$)$_2$Hf(NCO)] as a white powder (30 mg, 58 %). ^1H NMR (benzene-d_6, 23 °C): δ 1.73 (s, 6H, $C_5Me_3H_2$), 1.92 (s, 6H, $C_5Me_3H_2$), 2.14 (s, 6H, $C_5Me_3H_2$), 2.17 (s, 6H, $C_5Me_3H_2$), 2.18 (s, 6H, $C_5Me_3H_2$), 2.53 (s, 6H, $C_5Me_3H_2$), 5.07 (d, $^4J_{HH}$ = 2.3, 2H, $C_5Me_3H_2$), 5.24 (d, $^4J_{HH}$ = 2.3, 2H, $C_5Me_3H_2$), 5.72 (d, $^4J_{HH}$ = 2.3, 2H, $C_5Me_3H_2$), 5.99 (d, $^4J_{HH}$ = 2.3, 2H, $C_5Me_3H_2$). $\{^1H\}^{13}C$ NMR (benzene-d_6, 23 °C): δ 12.9, 13.3, 13.8, 14.9, 15.3, 15.4 ($C_5Me_3H_2$), 112.8, 113.3, 114.9, 115.3, 117.6, 118.8, 118.9, 119.4, 124.6, 126.0 ($C_5Me_3H_2$), 135.4 (d, $^1J_{CN}$ = 32.8, N*C*O), 164.1 (d, $^1J_{CN}$ = 8.3, CN*C*O). $\{^1H\}^{15}N$ NMR (benzene-d_6, 23 °C): δ 94.15 (d, $^1J_{CN}$ = 32.8, *N*CO), 324.15 (d, $^1J_{CN}$ = 8.3, C*N*CO). IR(C_6D_6): ν_{NH} = 3575 cm^{-1}, ν_{NCO} = 2221 cm^{-1}, $\nu_{^{15}N^{13}CO}$ = 2135 cm^{-1} ν_{CC} = 2038 cm^{-1}.

Preparation of [(η^5-$C_5Me_3H_2$)$_2$Hf(CCPh)](μ-NH)[(η^5-$C_5Me_3H_2$)$_2$Hf(NCO)] (1-(NH)(CCPh)(NCO)). A J. Young tube was charged with [(η^5-$C_5Me_3H_2$)$_2$Hf]$_2$(η^2, η^2-N_2) (16 mg, 0.020 mmol), 4-dimethylamino pyridine (3.6 mg, 0.030 mmol) and benzene-d_6 (0.75 mL). The inky green solution was taken to a high vacuum line, degassed, and CO gas (4 atm) was added. An immediate color change to dark red was observed. The resulting solution was degassed, brought into the glovebox, and phenylacetylene (4.33 μL, 0.040 mmol) was added via microsyringe. The solution was heated to 70 ^{o}C for 18 h. The resulting light orange solution was analyzed by NMR and IR spectroscopy. ^{1}H NMR (benzene- d_6, 23 ^{o}C): δ 1.78 (s, 6H, $C_5Me_3H_2$), 1.95 (s, 6H, $C_5Me_3H_2$), 2.12 (s, 6H, $C_5Me_3H_2$), 2.21 (s, 6H, $C_5Me_3H_2$), 2.24 (s, 6H, $C_5Me_3H_2$), 2.50 (s, 6H, $C_5Me_3H_2$), 5.05 (d, 2H, $^4J_{HH}$ = 2.5, $C_5Me_3H_2$), 5.15 (d, 2H, $^4J_{HH}$ = 2.5, $C_5Me_3H_2$), 5.82 (d, 2H, $^4J_{HH}$ = 2.5, $C_5Me_3H_2$), 6.04 (d, 2H, $^4J_{HH}$ = 2.5, $C_5Me_3H_2$), 6.99 (d, 1H, $^3J_{HH}$ = 7.2, Ar C*H*), 7.01 (br s. overlapped, 1H, μ-N*H*), 7.09 (t, 2H, $^3J_{HH}$ = 7.2, Ar C*H*), 7.60 (d, 2H, $^3J_{HH}$ = 7.0, Ar C*H*). {^{1}H}^{13}C NMR (benzene-d_6, 23 ^{o}C): δ 13.1, 13.9, 14.0, 15.2, 15.3, 15.4 ($C_5Me_3H_2$), 110.7, 111.7, 115.1, 116.0, 116.3, 117.4, 117.9, 118.5, 121.0, 123.5, 125.1, 127.0, 127.8, 129.0, 131.4, 132.7 ($C_5Me_3H_2$ or Ar-*C* or alkene *C*), 135.7 (d, $^1J_{CN}$ = 32.6, N*C*O). {^{1}H}^{15}N NMR (benzene-d_6, 23 ^{o}C): δ 91.67 (d, $^1J_{CN}$ = 32.6, *N*CO), 282.11 (s, μ-*N*H). IR (C_6D_6): ν_{NH} = 3575 cm^{-1}, ν_{15NH} = 3475 cm^{-1}, ν_{NCO} = 2221 cm^{-1}, $\nu_{15N13CO}$ = 2135 cm^{-1} ν_{CC} = 2085 cm^{-1}.

Preparation of [(η^5-$C_5Me_3H_2$)$_2$Hf(CCTMS)](μ-NH)[(η^5-$C_5Me_3H_2$)$_2$Hf(NCO)] (1-(NH)(CCSiMe$_3$)(NCO)). This compound was prepared in a similar manner to that above using [(η^5-$C_5Me_3H_2$)$_2$Hf]$_2$(η^2, η^2-N_2) (15 mg, 0.018 mmol) and trimethylsilylacetylene (5.3 μL, 0.036 mmol). ^{1}H NMR (benzene- d_6, 23 ^{o}C): δ 0.29 (s, 9H, Si*Me*$_3$), 1.78 (s, 6H, $C_5Me_3H_2$), 1.91 (s, 6H, $C_5Me_3H_2$), 2.15 (s, 6H, $C_5Me_3H_2$), 2.20 (s, 6H, $C_5Me_3H_2$), 2.22 (s, 6H, $C_5Me_3H_2$), 2.46 (s, 6H, $C_5Me_3H_2$), 5.01 (br s, 2H,

$C_5Me_3H_2$), 5.18 (br s, 2H, $C_5Me_3H_2$), 5.77 (br s, 2H, $C_5Me_3H_2$), 6.01 (br s, 2H, $C_5Me_3H_2$), 6.79 (s overlapped, $^1J_{NH}$ = 46.4, 1H, μ-N*H*) . {^{1}H}^{13}C NMR (benzene-d_6, 23 ^{o}C): δ 1.05 (Si*Me*$_3$), 13.1, 14.0, 14.0, 15.3, 15.5, 15.6 (C_5*Me*$_3$H$_2$), 110.7, 110.7, 111.7, 115.0, 115.9, 116.4, 117.2, 118.0, 118.7, 123.1, 125.2, (*C*$_5$Me$_3$H$_2$ or NCO or Alkyne C), 125.6 (Alkyne *C*), 135.73 (d, $^1J_{CN}$ = 32.6, N*C*O). {^{1}H}^{15}N NMR (benzene-d_6, 23 ^{o}C): δ 92.23 (d, $^1J_{CN}$ = 32.6, *N*CO), 283.42 (s, $^1J_{NH}$ = 46.4, μ-*N*H). IR(C_6D_6): ν_{NH} = 3575 cm^{-1}, ν_{NCO} = 2083 cm^{-1}, ν_{CC} = 2038, 1994 cm^{-1}.

REFERENCES

[1] Smil, V. *Enriching the Earth: Fritz Haber, Carl Bosch, and the Transformation of World Food Production*; MIT Press: Cambridge, MA, 2001.

[2] (a) Schlogl, R. *Angew. Chem. Int. Ed.* **2003**, *42*, 2004 (b) Fryzuk, M. D.; Johnson, S. A. *Coord. Chem. Rev*. **2000**, *200*, 379.

[3] Fryzuk, M.D.; Love, J.B.; Rettig, S.J.; Young, V.G. *Science* **1997**, *276*, 1445.

[4] Pool, J. A.; Lobkovsky, E.; Chirik, P.J. *Nature* **2004,** *427*, 527.

[5] Knobloch, D.J.; Lobkovsky, E.; Chirik, P.J. *Nature Chemistry* **2010**, *2*, 30.

[6] Hirotsu, M.; Fontaine, P.P.; Zavalij, P.Y.; Sita, L.R. *J. Am. Chem. Soc.* **2007**, *129*, 12690.

[7] Knobloch, D.J.; Benito-Garagorri, D.; Bernskoetter, W.H.; Keresztes, I.; Lobkovsky, E.; Toomey, H.; Chirik, P.J. *J. Am. Chem. Soc.* **2009**, *131*, 14903.

[8] Bernskoetter, W. H.; Olmos, A.V.; Lobkovsky, E.; Chirik, P.J. *Organometallics* **2006**, *25*, 1021.

[9] Manriquez, J.M.; Bercaw, J.E. *J. Am. Chem. Soc.* **1974**, *96*, 6229.

[10] Schwartz, K.D.; White, J.D.; *Organic Syntheses* **2006**, *83*, 420.

[11] The wedge dihedral angle is defined as the angle between the planes formed by the metal center and the attached cyclopentadienyl centroids.

[12] Bernskoetter, W.H.; Pool, J.A.; Lobkovsky, E.; Chirik, P.J. *J. Am. Chem. Soc.* **2005**, *127*, 7901.

[13] Hanna, T.E.; Bernskoetter, W.H.; Bouwkamp, M.W.; Lobkovsky, E.; Chirik, P.J. *Organometallics* **2007**, *26*, 2431.

[14]Cuenca, T.; Royo, P. *J. Organomet. Chem.* **1985**, *293*, 61.

[15] Pool, J. A.; Chirik, P. J. *Can. J. Chem.* **2005**, *83*, 286.

[16] Pool, J. A.; Bernskoetter, W. H.; Chirik, P. J. *J. Am. Chem. Soc.* **2004**, *126*, 14326.

[17] Bernskoetter, W.H.; Lobkovsky, E.; Chirik, P.J. *J. Am. Chem. Soc.* **2005**, *127,* 14051.

[18] Hanna, T.E.; Keresztes, I.; Lobkovsky, E.; Chirik, P.J. *Inorg. Chem.* **2007**, *46*, 675.

[19] Knobloch, D.J.; Lobkovsky, E.; Chirik, P.J. *J. Am. Chem. Soc.* **2010**, *132*, 10553.

[20] Bernskoetter, W.H.; Olmos, A.V.; Pool, J.A.; Lobkovsky, E.; Chirik, P.J. *J. Am. Chem. Soc.* **2006**, *128*, 10696.

[21] Morello, L.; Love, J. B.; Patrick, B. O.; Fryzuk, M. D. *J. Am. Chem. Soc.* **2004**, *126*, 9480

CHAPTER TWO

Functionalization and Cleavage of Dinitrogen by Primary Silanes

Abstract

Addition of primary silanes to a hafnocene complex bearing a strongly activated dinitrogen ligand, $[(\eta^5\text{-}C_5Me_3H_2)_2Hf]_2(\eta^2, \eta^2\text{-}N_2)$, afforded mono-silylated compounds of the type $[(\eta^5\text{-}C_5Me_3H_2)_2Hf](\mu\text{-}H)(\eta^1, \eta^2\text{-}N\text{-}NSiH_2R)$ (R = Cy, ^{n}Hex). Multinuclear and 2-D NMR spectroscopic experiments established the structure of these compounds as consisting of a bridging hydride fragment along with a side-on/end-on dinitrogen unit. The compounds were obtained as a mixture of two isomers which differed by the orientation of one cyclopentadienyl ring; at 23 ^oC, exchange between the two isomers proceeded on the order of 2 s^{-1}. Thermolysis of the mono-silylated compounds led to complete dinitrogen cleavage by 1,2-addition of another Si-H bond, affording the four-membered metallacycle dimer, $[(\eta^5\text{-}C_5Me_3H_2)_2Hf]_2(H)(\mu\text{-}[NH(SiHCy)N])$. This compound represents the first example of silane induced dinitrogen cleavage in group 4 transition metal dinitrogen chemistry. The metallacycle proved to be amenable to further nitrogen functionalization; hydrogenolysis at elevated temperatures furnished the silyl diamide compound, $[(\eta^5\text{-}C_5Me_3H_2)_2Hf]_2(H)_2(\mu\text{-}[NH\text{-}Si(H)(Cy)\text{-}NH])$, in which each nitrogen atom has undergone N-Si and N-H bond formation. Treatment of the mono-silylated compound with carbon monoxide produced $[(\eta^5\text{-}C_5Me_3H_2)_2Hf]_2(\mu\text{-}[N\text{-}N(SiH_2Cy)\text{-}C(H)O])$, in which the formyl group produced by insertion of the hafnium hydride into carbon monoxide has been transferred to the unfunctionalized nitrogen, providing a new route to the formation of N-C bonds. The reaction of the mono-silylated compound with cyclohexylnitrile furnished, $[(\eta^5\text{-}C_5Me_3H_2)_2Hf]_2(\mu\text{-}[N{=}C(H)(Cy)])(\eta^2, \eta^1\text{-}N\text{-}NSiH_2Cy)$, a hafnium dimer with a side-on/end-on dinitrogen unit and a bridging aldimine functionality. No N-C bond formation was observed, but

the presence of significant hafnium-imido character in one of the metal-nitrogen bonds suggested that additional functionalization was possible.

Introduction

Interest in metal complexes bearing dinitrogen ligands has been widespread since the isolation of the first metal-dinitrogen compound in 1965 by Senoff.[1] While hundreds of metal-dinitrogen complexes are now known, very few of them exhibit any productive functionalization chemistry at the N_2 ligand.[2] The high energy costs associated with the Haber-Bosch process make the production of ammonia and other nitrogenous organic compounds directly from atmospheric dinitrogen an attractive synthetic target.[3] In recent years, several metal systems supported by various ligand frameworks have shown the ability to effect the functionalization and full cleavage of dinitrogen.[2] The most exciting of these systems avoid the use of harsh electrophiles to functionalize dinitrogen and instead employ relatively non-polar reagents such as silanes, dihydrogen, and terminal alkynes.[4] Terminal alkynes have been shown to participate in both N-C and N-H bond formation based on the supporting ligand set. Fryzuk and coworkers have demonstrated that cycloaddition of *p*-tolylacetylene to a side-on zirconium dinitrogen compound bearing a macrocyclic P_2N_2 ligand affords a new N-C bond (**Figure 2.1**).[5] Our group has demonstrated N-H bond formation via reaction of a side-on bound zirconocene complex with terminal acetylenes (**Figure 2.2**).[6] The nature of the supporting ligand clearly has a significant effect on the resulting functionalization chemistry. Fryzuk has reported double silylation and cleavage of dinitrogen with silanes for a ditantalum complex (**Figure 2.3**),[7] while mono-silylation of coordinated dinitrogen was reported by Sita[8] for a series of monocyclopentadienyl aminidate hafnium and zirconium complexes (**Figure 2.4**). To date, no reactivity with silanes has been reported for metallocene dinitrogen complexes of the Group 4 metals.

In this chapter, the first example of addition of silanes to a strongly activated hafnocene dinitrogen complex will be discussed, and further functionalization of the dinitrogen core, including complete cleavage of N_2, will be presented.

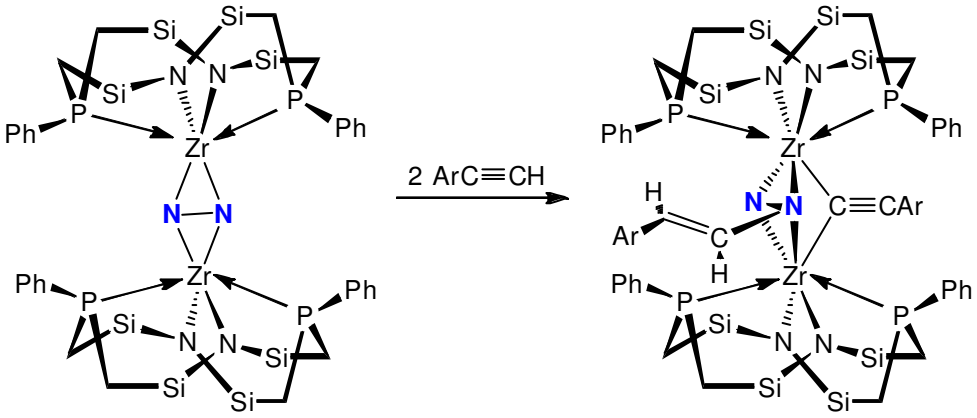

Figure 2.1 Cycloaddition of p-tolylacetylene to a zirconium dinitrogen compound. [5]

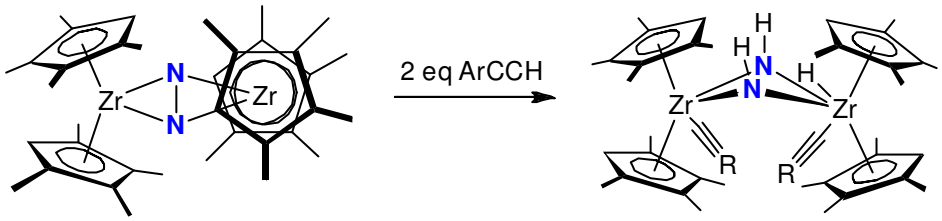

Figure 2.2 Acetylene addition to a zirconocene nitrogen compound. [6]

Results and Discussion

Dinitrogen Cleavage by Primary Silanes. As presented in Chapter 1, the hafnocene $[(\eta^5\text{-}C_5Me_3H_2)_2Hf]_2(\eta^2, \eta^2\text{-}N_2)$ (**1-N₂**) contains a highly activated side-on N_2 ligand with an N-N bond length of 1.457(5) Å. The reduced steric demand of the 1,2,4-trimethylcyclopentadienyl ligand likely allows greater overlap between the hafnium *d* and nitrogen π* orbitals, resulting in greater N_2 activation while still permitting access to the metal centers and the dinitrogen fragment. This led to the first report of an

isolable hafnium μ-nitride, whose chemistry was explored in the previous chapter. This unique combination of steric and electronic factors prompted us to investigate the reactivity of **1-N_2** towards silanes, whose ability to functionalize dinitrogen has been well documented by the groups of Fryzuk[7] **(Figure 2.3)** and Sita[8] **(Figure 2.4).**

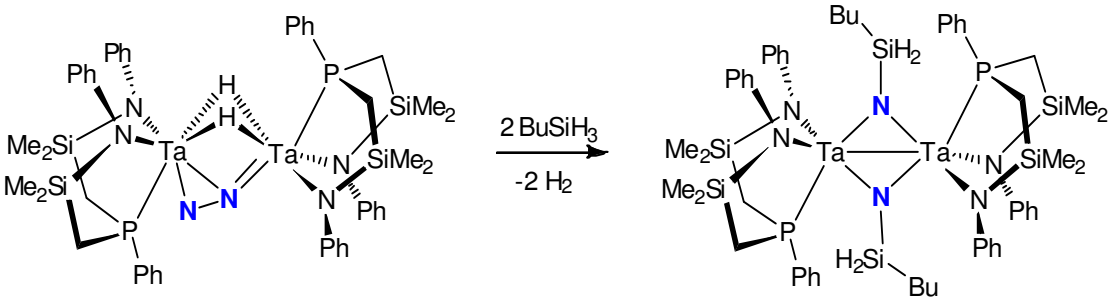

Figure 2.3 Dinitrogen functionalization and cleavage by silanes in a side-on/end-on tantalum complex.[7]

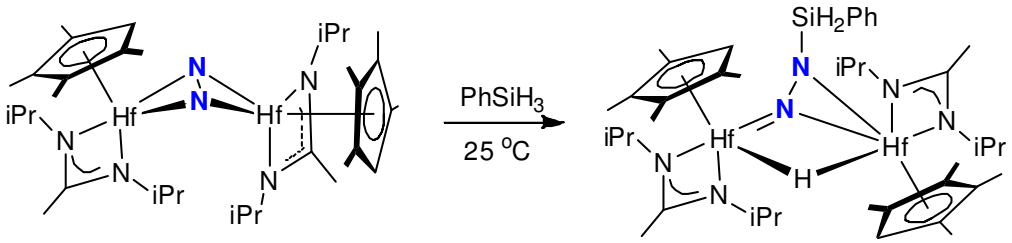

Figure 2.4 Silane addition to dinitrogen in a cyclopentadienyl aminidate hafnium complex.[8]

The addition of one equivalent of cyclohexylsilane to a toluene solution of **1-N_2** produced an immediate color change from deep purple to reddish-brown. ^{1}H NMR spectroscopic analysis in benzene-d_6 revealed the clean formation of two products in an approximately 1:1 ratio. The less symmetric product, [(η^5-$C_5Me_3H_2$)$_2$Hf](μ-H)(η^1, η^2-N-

$NSiH_2Cy$) (**1-CySiH$_3$-*C$_1$***), displayed four inequivalent cyclopentadienyl rings, as expected for a C_1 symmetric dimer. Two diastereotopic Si-H resonances integrating to a single proton each were located at 4.64 and 5.11 ppm. In addition, a singlet at 4.96 ppm integrating to a single proton was assigned as a hafnium hydride, as ^{1}H-^{13}C, ^{1}H-^{15}N and ^{1}H-^{29}Si HSQC experiments indicated it was not attached to any heteroatom. The hafnium hydride displayed coupling to hydrogens on three of the four inequivalent cyclopentadienyl rings in a ^{1}H-^{1}H COSY experiment, suggesting that it was bridging the two metal centers. Further evidence for this assignment was provided by the pronounced upfield chemical shift of the hydride; terminal hafnium hydrides typically encountered in our laboratory are observed downfield,[9] while examples of bridging hydrides provided by Sita are observed at 5.70 and 6.21 ppm.[8,10] The proton-decoupled ^{29}Si NMR spectrum revealed a doublet at -28.67 ppm with a $^{1}J_{SiN}$ of 10.3 Hz, while the ^{15}N NMR spectrum contained two signals; a doublet at 320.97 ppm ($^{1}J_{NN}$ = 13.3) assigned to the unsubstituted nitrogen and a signal at 183.23 ppm[11] consistent with a silylated nitrogen **(Figure 2.5)**. The presence of nitrogen-nitrogen coupling in the ^{15}N NMR spectrum indicated that N-N bond scission had not occurred upon silane addition. Based on the spectroscopic data, **1-CySiH$_3$-*C$_1$*** was tentatively assigned as a dimer with a bridging hafnium hydride and a silylated side-on/end-on dinitrogen unit **(Figure 2.6)**. Similar products have been observed by Sita in cyclopentadienyl/aminidate systems (*vide supra*).[8] The second product, [(η^5-$C_5Me_3H_2$)$_2$Hf](μ-H)(η^2, η^2-N-$NSiH_2Cy$) (**1-CySiH$_3$-*C$_s$***), exhibited C_s symmetry, with four Cp hydrogen and six Cp methyl resonances. A singlet integrating to two protons was observed at 4.85 ppm, and was assigned to a SiH_2Cy group on the basis of a ^{1}H-^{29}Si HSQC experiment. Performing the experiment with **1-^{15}N$_2$** split the signal with a $^{2}J_{NH}$ of 6.5 Hz, indicating that silylation of one of the nitrogen atoms had occurred.

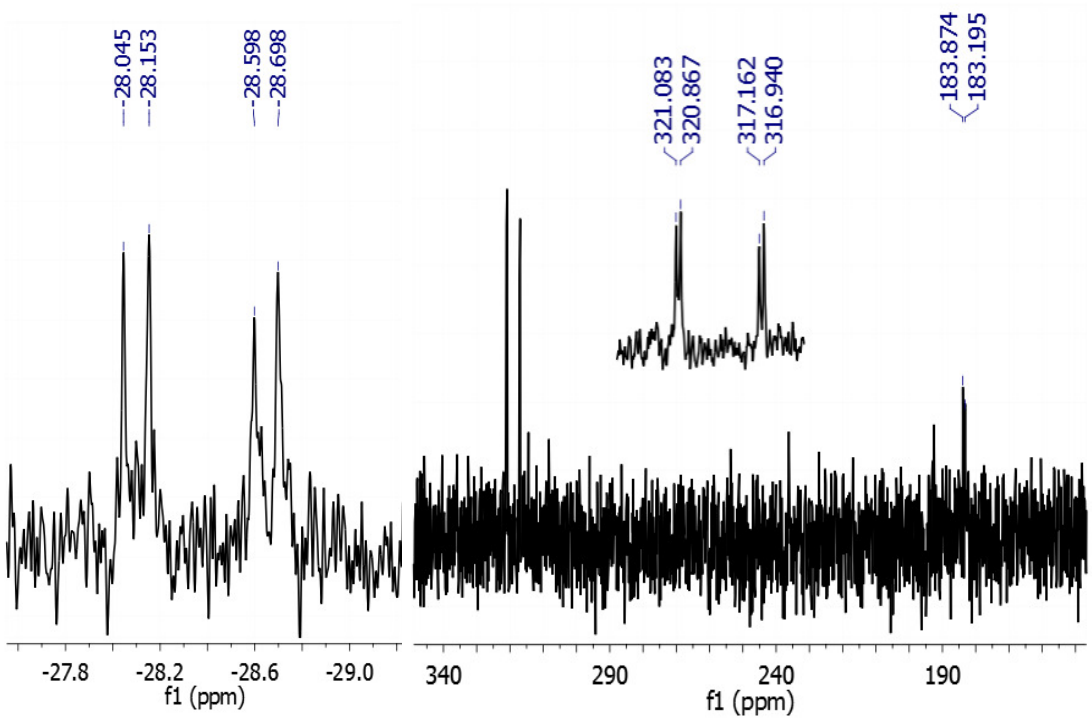

Figure 2.5 ^{29}Si NMR spectrum (left) and ^{15}N NMR spectrum (right) of **1-CySiH$_3$-*C$_s$*** and **1-CySiH$_3$-*C$_1$*** mixture in benzene-*d$_6$*.

In addition, a singlet at 4.77 ppm integrating to a single proton was assigned as a hafnium hydride, as in **1-CySiH$_3$-*C$_1$***. The ^{29}Si and ^{15}N NMR spectra of **1-CySiH$_3$-*C$_s$*** are very similar to those of **1-CySiH$_3$-*C$_1$***. A doublet at -28.1 ppm ($^1J_{SiN}$ = 10.3 Hz) in the ^{29}Si NMR was assigned on the basis of ^{1}H-^{29}Si HSQC experiments, while the ^{15}N NMR again displayed a doublet at 317.05 ppm ($^1J_{NN}$ = 12.9 Hz) and a signal at 183.98 ppm (**Figure 2.5**). The high symmetry of the molecule and its similarity to **1-CySiH$_3$-*C$_1$*** resulted in its assignment as a dimer bearing a mono-silylated side-on/side-on dinitrogen unit and possessing a bridging hafnium hydride (**Figure 2.6**). In an attempt to unambiguously confirm the structure of both molecules, a ^{1}H-^{1}H ROESY experiment was performed. The spectrum revealed chemical exchange between the *C$_1$* and *C$_s$*

structures, indicating that they were in rapid equilibrium. A series of ROESY experiments with different mixing times was performed at 23 °C in an attempt to gain insight on the time-scale of the exchange process.

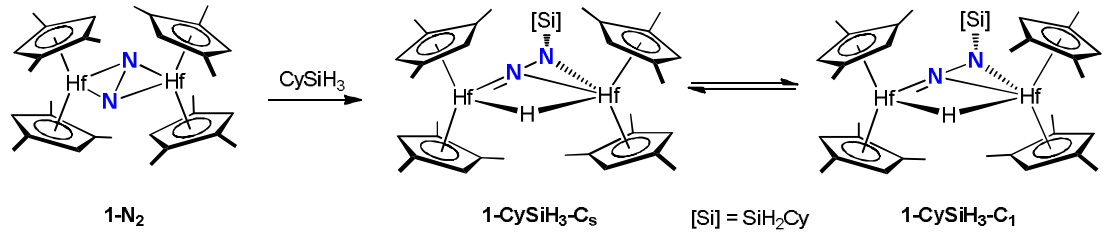

Figure 2.6 Reaction of **1-N_2** with cyclohexylsilane.

Fitting the data with EXSYCalc revealed that the *intra*molecular magnetization exchange rate at 23 °C was approximately 5 s^{-1}, while *inter*molecular magnetization exchange rates[12] between the **1-CySiH_3-*C_1*** and **1-CySiH_3-*C_s*** compounds occurred on the order of 2 s^{-1} at 23 °C. The rapid rate of exchange, in conjunction with the observed 1:1 product ratio, suggests a very small energy difference between the two structures along with a relatively low kinetic barrier. Analysis of ROESY[g] data collected at -70 °C revealed that the C_1 and C_s products differed only in the orientation of one cyclopentadienyl ring (**Figure 2.4**). In the C_s structure, the single methyl groups of the Cp rings have adopted a meso conformation, all directed toward the bridging hydride. A mirror plane runs through the five membered ring formed by the hafnium/hydride/nitrogen core of the molecule. In the C_1 structure, the Cp ring adjacent to the silylated nitrogen has rotated and placed its methyl group anti to the bridging hydride to relieve steric pressure between the ring and the silane. This removes the mirror plane and generates an overall C_1 symmetric structure. Despite the absence of structural confirmation by X-ray diffraction, the reaction of $CySiH_3$ with **1-N_2** represents the first example of dinitrogen functionalization with silanes in Group 4

metallocene chemistry, joining a small number of previous reports for other complexes of the Group 4 and 5 metals.[7,8]

Efforts to perturb the equilibrium between **1-CySiH$_3$-*C$_1$*** and **1-CySiH$_3$-*C$_s$*** by heating the mixture to 65 ^{o}C over the period of 18 h instead resulted in complete conversion of the hafnocene complex to a new C_1 symmetric product **(Figure 2.7**), identified as [(η^5-$C_5Me_3H_2$)$_2$Hf]$_2$(H)(μ-[NH(SiHCy)N]) (**1-SiHCy)** by multinuclear NMR spectroscopy and X-ray diffraction. An intense signal at 3437 cm^{-1} was observed by solution IR spectroscopy in benzene, confirming N-H bond formation. A sharp singlet at 9.76 ppm in the ^{1}H NMR spectrum was diagnostic of a terminal hafnium hydride while a doublet at 4.74 ppm integrating to a single proton corresponded to a SiHCy moiety, as judged by ^{1}H-^{29}Si HSQC spectroscopy. ^{15}N NMR spectroscopy revealed two broad signals at 106.97 and 281.4 ppm, assigned to the *N*H and Hf-*N*-Hf respectively.

Large yellow hexagonal crystals were obtained from a concentrated diethyl ether solution, and a single-crystal X-ray diffraction study was performed **(Figure 2.8)**. The structural data was of sufficient quality such that the hydrogens attached to nitrogen, hafnium, and silicon were located in the Fourier difference map and freely refined.

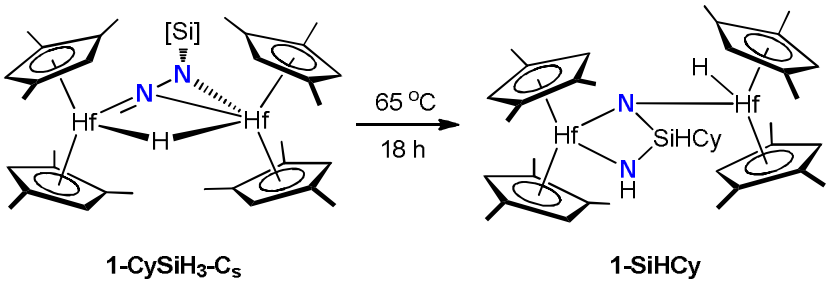

Figure 2.7 Cleavage of N_2 by cyclohexylsilane.

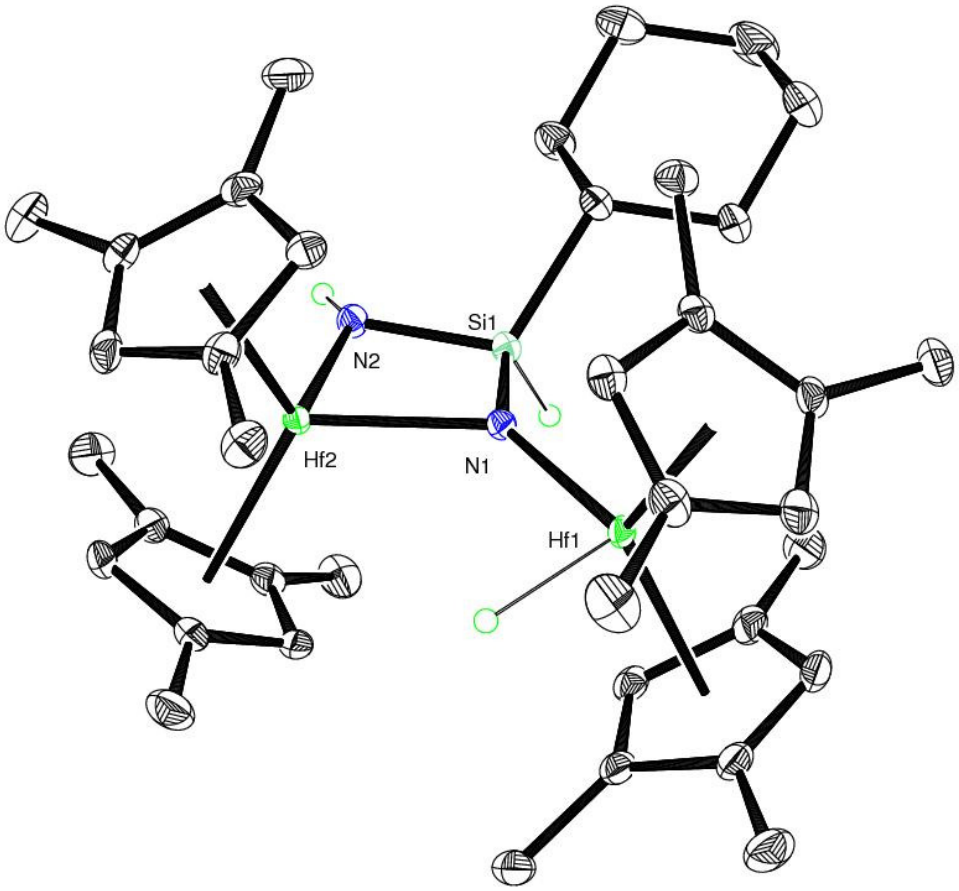

Figure 2.8 ORTEP plot of **1-SiHCy** at 30% probably ellipsoids. Hydrogen atoms, except those attached to hafnium, nitrogen, and silicon are omitted for clarity.

Table 2.1. Selected Bond Distances (Å) and Angles (°) for **1-SiHCy**

Hf(1)-N(1)	2.0415(18)	Hf(1)-N(1)-Hf(2)	128.05(9)
Hf(2)-N(1)	2.1521(18)	N(2)-Si(1)-N(1)	97.88(9)
Hf(2)-N(2)	2.053(2)	N(2)-Hf(2)-N(1)	76.49(7)
Si(1)-N(1)	1.732(2)	Si(1)-N(2)-Hf(2)	94.47(9)
Si(1)-N(2)	1.722(2)	Si(1)-N(1)-Hf(2)	90.77(8)

Selected metrical parameters are presented in **Table 2.1**. The core of the molecule is a four-membered ring consisting of alternating hafnium, nitrogen and silicon atoms and is puckered out of the plane of the metal centers by 5°. The sum of the angles around N(2) is 358.29° while that around N(1) is 358.36°, indicating some sp^2 character. The planarity around the nitrogen atoms may be explained in part by the presence of multiple-bond character between the Hf(1)-N(1) and Hf(2)-N(2) (*vide infra*).

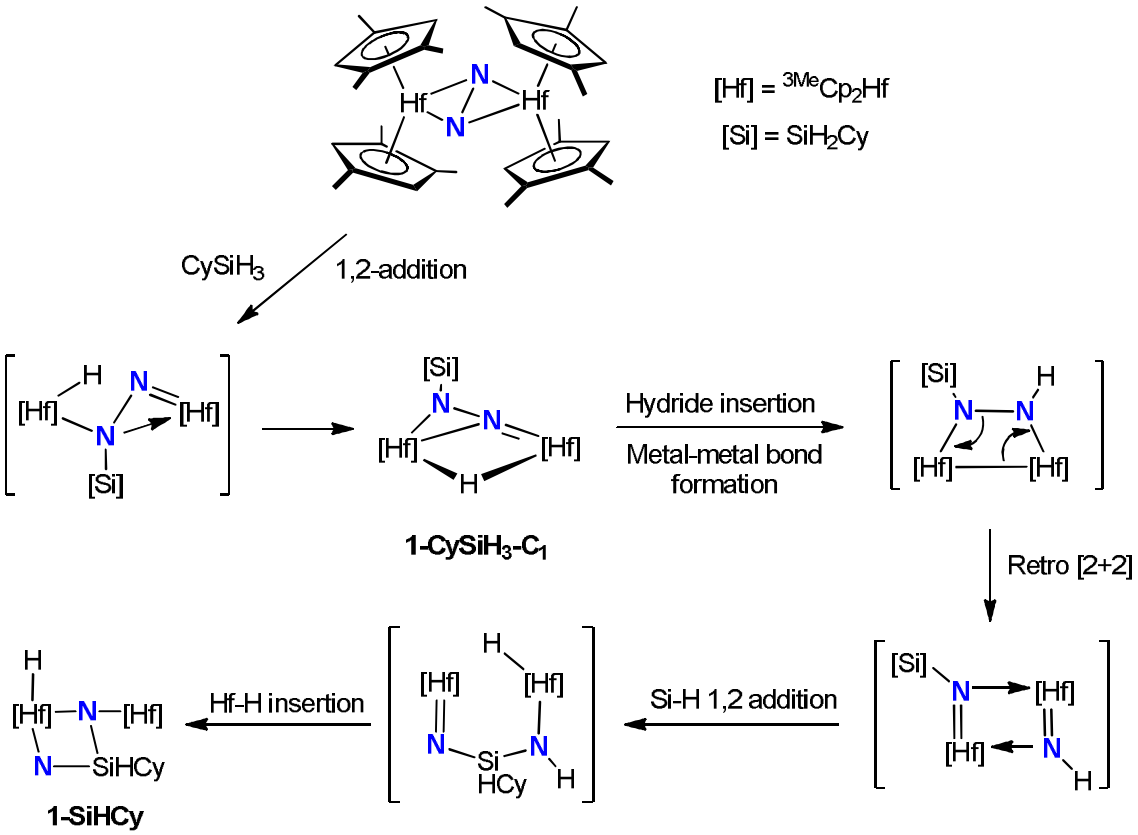

Figure 2.9. Proposed mechanism for the conversion of **1-N_2** to **1-SiHCy.**

The Hf(1)-N(1) and Hf(2)-N(2) bond lengths are quite short at 2.0415(18) and 2.053(2) Å respectively, comparable to hafnium imido complexes.[14] The Hf-N bonds in **1-N_2**, which possess significant imido character,[9] are 2.0590(12) Å, while the formally Hf-N

single bonds in **1-N_2H_4** are 2.165(3) and 2.272(3) Å.[15] A proposed mechanism for the conversion of **1-N_2** to **1-SiHCy** is presented in **Figure 2.9**. After formation of **1-$CySiH_3$-C_1** by 1,2-addition of a Si-H bond across a Hf-N bond of **1-N_2**, insertion of the resulting metal hydride into the Hf-N bond with imido character leads to N-H bond formation and can generate a metal-metal bonded species. Similar ditantalum species have been observed by Fryzuk to be able to provide the requisite two electrons necessary for N-N single bond scission.[7] A retro [2+2] cyclization provides the electrons needed to break the N-N bond, and generates a pair of hafnium-imido species which remain in close contact. Further Si-H 1,2-addition followed by another Hf-H 1,2-addition generates **1-SiHCy**. In general, 1,2-additions of C-H bonds across metal-imidos result in the formation of strong M-C and N-H bonds.. The reverse polarity of Si-H compared to C-H bonds allows 1,2-addition of silanes to produce N-Si bonds with the concomitant formation of metal hydrides. The cleavage and functionalization of dinitrogen was extended to other primary silanes; under the same conditions, *n*-hexylsilane generates analogous species to **1-$CySiH_3$-C_1** and **1-SiHCy**. To date, however, only 1,2,4-trimethylcyclopentadienyl metallocene complexes possess the unique ability to undergo this series of transformations. This likely lies in their reduced steric profile, enabling the formation of the putative hafnium-hafnium bonded species. In contrast, metallocene complexes of the more sterically demanding tetramethylcyclopentadienyl ligand have not shown similar reactivity with silanes. Compound **1-SiHCy** represents a rare instance of dinitrogen cleavage by silanes, the only other reported example being provided by a side-on/end-on dinitrogen ditantalum complex prepared by Fryzuk.[7] The intermediacy of a tantalum-tantalum bonded species in this transformation was also proposed and was investigated computationally.[7] Reductive elimination of dihydrogen from a ditantalum-dihydride provides the two electrons necessary to split the N-N bond. The electrons are stored in a tantalum-

tantalum bond, which undergoes electron transfer to the dinitrogen unit and generates bridging imido and nitride moieties. Detailed mechanistic and computational studies will be required to prove the formation of a hafnium-hafnium bonded species in the reaction of silanes with **1-N_2**.

Additional Functionalization of Cleaved Dinitrogen. The presence of hafnium-nitrogen multiple bond character in **1-SiHCy** suggested that additional functionalization of the dinitrogen fragment by 1,2-addition or cycloaddition was possible. To this end, four atmospheres of dihydrogen were added to a toluene solution of **1-SiHCy** and heated to 75 ^{o}C. Analysis of the reaction mixture by ^{1}H NMR spectroscopy revealed partial conversion to a new product after 18 h; the reaction was complete after 3 days at 75 ^{o}C. The product was of C_s symmetry and displayed the expected six Cp methyl and 4 Cp hydrogen resonances in the benzene-d_6 ^{1}H NMR spectrum. In addition, a broad signal integrating to two protons was observed at 4.04 ppm which split into a doublet of doublets upon labeling with $^{15}N_2$ ($^{1}J_{NH}$ = 56.1 Hz, $^{3}J_{HH}$ = 3.9 Hz). The large one-bond coupling constant led to the assignment of this peak as arising from protons directly bound to nitrogen. Analysis of the ^{1}H-^{1}H gCOSY spectrum revealed coupling of this signal to a triplet at 5.21 ppm, which ^{1}H-^{29}Si HSQC spectroscopy revealed to be a single Si-H proton. Lastly, a sharp singlet at 9.93 ppm integrating to two protons suggested the presence of equivalent terminal hafnium hydrides. Performing the hydrogenolysis with deuterium gas and analyzing the mixture by ^{2}H NMR spectroscopy revealed incorporation of deuterium at 4.04 (N-H) and 9.93(Hf-H) ppm. The increased symmetry of the molecule was further established by the observation of a triplet in the ^{29}Si NMR spectrum **(Figure 2.10**) and a singlet at 164.55 ppm in the ^{15}N NMR spectrum. On the basis of the NMR spectral data, the product was assigned as [(η^5-$C_5Me_3H_2$)$_2$Hf]$_2$(H)$_2$(μ-[NH-Si(H)(Cy)-NH]) **(1-H_2)**

(Figure 2.11). Rather than undergoing 1,2-addition across a Hf-N bond with imido character, addition of H_2 to **1-SiHCy** instead led to ring cleavage by hydrogenolysis of the Hf(2)-N(1) bond (*vide supra*). This result suggests that a catalytic cycle for the production of substituted silane diamines from atmospheric dinitrogen, dihydrogen and primary silanes may be possible, with the hafnium dihydride providing the means to re-access **1-N_2** via reduction elimination (**Figure 2.12**). The catalytic production of $HN(SiMe_3)_2$ and $N(SiMe_3)_3$ from N_2 and $ClSiMe_3$ was accomplished by Hidai using molybdenum and tungsten dinitrogen compounds,[16]

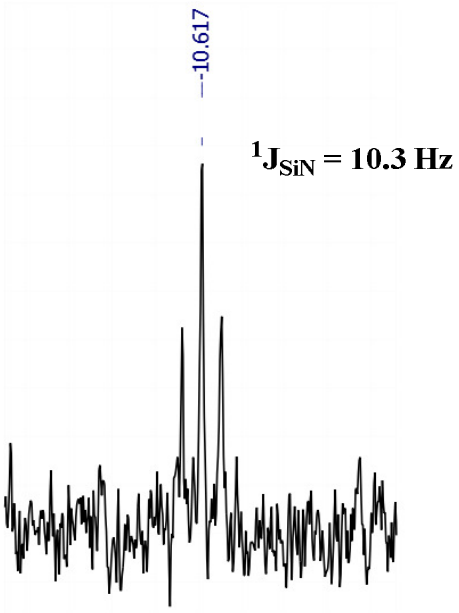

Figure 2.10 ^{29}Si NMR spectrum of **1-H_2** in benzene-d_6.

however, the reaction required the use of sodium as a reducing agent to regenerate the dinitrogen compound. Nevertheless, Hidai's work demonstrates that catalytic cycles which generate silylamines from N_2 and silane are synthetically accessible.

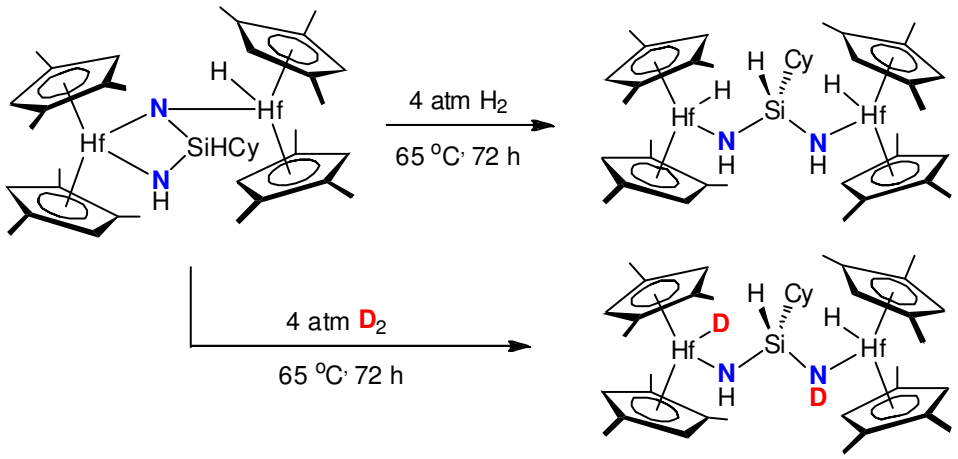

Figure 2.11 Hydrogenolysis of **1-SiHCy** at elevated temperature.

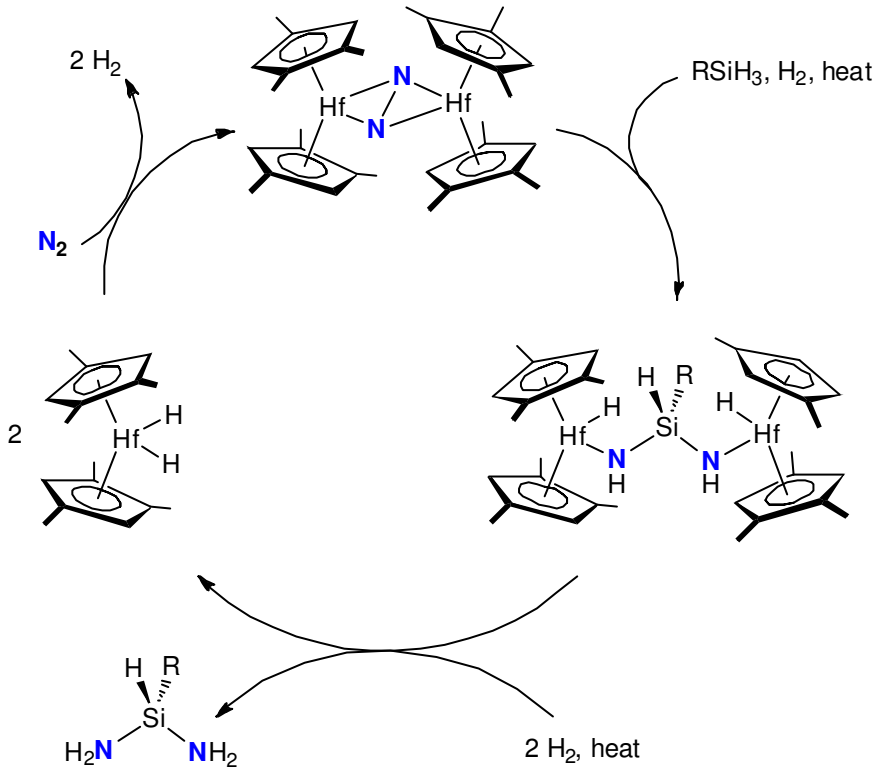

Figure 2.12 Possible catalytic cycle for the generation of silane diamines from N_2, H_2 and $RSiH_3$.

Insertion Reactions of 1-CySiH$_3$-*C$_1$*: Routes to New N-C bonds. The reaction of the hafnium μ-nitride **1-(N)(DMAP)(NCO)**[10] with CO gas demonstrated the ability of carbon monoxide to insert into hafnium-nitrogen multiple bonds. The hafnium-imido character in **1-CySiH$_3$-*C$_1$*** prompted us to investigate its reactivity with CO. Treatment of a freshly prepared sample of **1-CySiH$_3$-*C$_1$*** in benzene-d_6 with four atmospheres of CO gas resulted in an immediate color change from brown to dark red. The product, [(η^5-$C_5Me_3H_2$)$_2$Hf]$_2$(μ-[N-N(SiH_2Cy)-C(H)O]) **(1-CO)**, was identified by NMR spectroscopy, and arises from insertion of CO into the hafnium hydride, followed by formyl migration to nitrogen (**Figure 2.13**). NMR spectroscopic analysis showed a number of broadened peaks in the Cp methyl and Cp hydrogen regions, along with a sharp singlet at 9.22 ppm. A series of ^{1}H NMR spectra were recorded at various temperatures in toluene-d_8, and they show that the molecule undergoes a dynamic process on the NMR timescale (**Figure 2.14**).

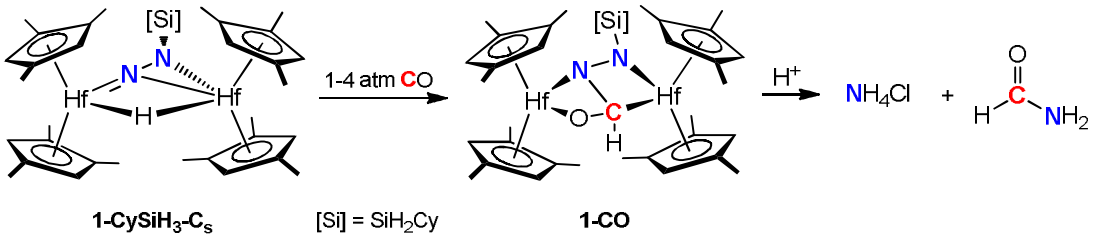

Figure 2.13 Carbon monoxide insertion into the hafnium hydride of **1-CySiH$_3$-C$_s$**.

At -50 °C, a new small singlet is observed at 9.44 ppm, while the larger downfield signal remains invariant. At 20 °C, there are four broad signals for the Cp hydrogens and two broad signals for the Cp methyl groups. At -50 °C, these signals have decoalesced into 12 Cp hydrogens and 12 broad Cp methyl groups. These correspond to a *C$_1$* and *C$_s$*/*C$_2$* symmetric product. The exact identity of the higher symmetry product remains unknown, but the equilibrium between **1-CySiH$_3$-*C$_1$*** and **1-CySiH$_3$-*C$_2$*** (*vide*

supra) suggested that the orientation of the cyclopentadienyl rings in this molecule may be giving rise to the two products at low temperature. If the central portion of the molecule is puckered, the dynamic process observed by ^{1}H NMR spectroscopy may be due to inversion of the core. The identity of the upfield signal at 9.22 ppm can be ascertained by using **1-$^{15}N_2$** and ^{13}CO gas, which caused the signal to split into a doublet of doublets with $^{1}J_{CH}$ = 186.5 Hz and $^{2}J_{NH}$ = 8.8 Hz.

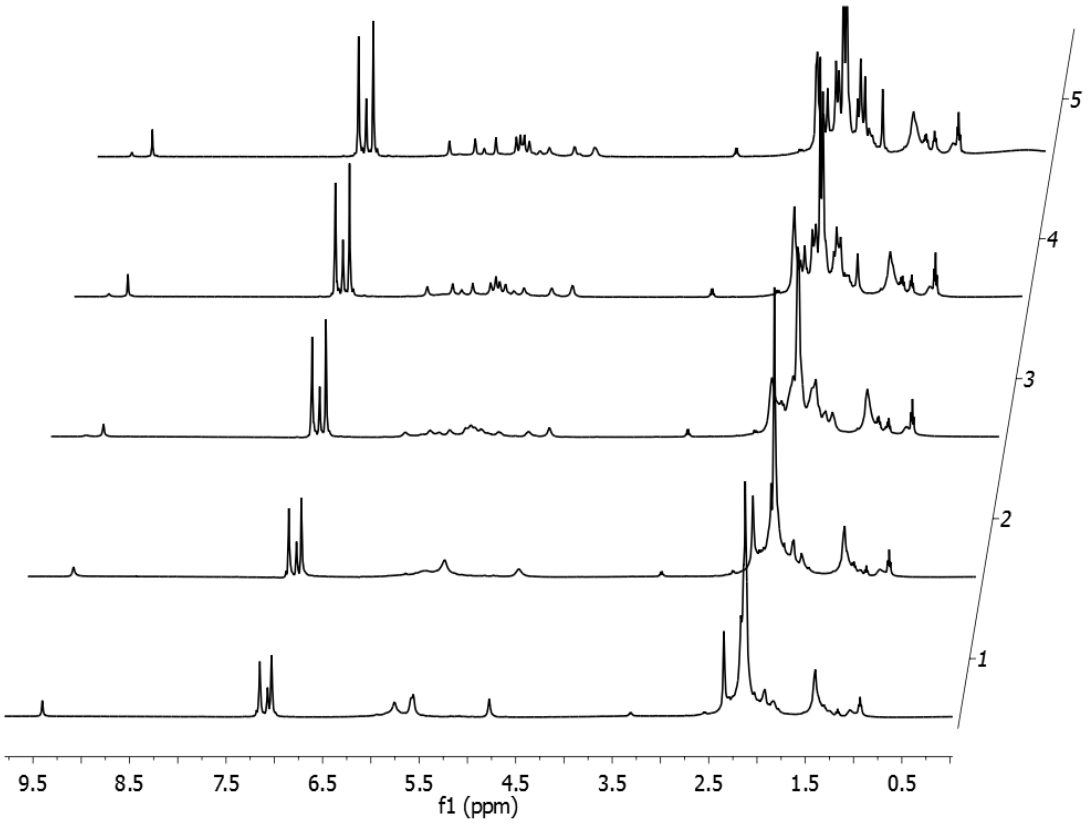

Figure 2.14 Variable temperature ^{1}H NMR spectra of **1-CO** in toluene-d_8 (1 = 20 °C, 2 = 0 °C, 3 = -30 °C, 4 = -40 °C, 5 = -50 °C)

This indicated insertion of carbon monoxide into the metal hydride to form a new C-H bond, followed by formyl transfer to the hafnium-imido nitrogen to generate a new N-C bond. Further evidence of N-C bond formation was found in the ^{13}C NMR spectrum of

the doubly labeled compound, which shows a doublet at 169.5 ppm with $^{1}J_{CN}$ = 8.5 Hz. Unfortunately, the dynamic process on the timescale of the NMR experiment led to the observation of only broad signals in the ^{15}N NMR spectrum, one located at 215.89 ppm and the other at 283.14 ppm. No signals were seen by ^{29}Si NMR spectroscopy, and the presence of a silyl group was only confirmed by observation of a correlation between a ^{1}H NMR singlet at 4.72 ppm and a signal at -37.28 ppm in a ^{1}H-^{29}Si HSQC experiment. In an effort to unambiguously confirm N-C bond formation, a sample of **1-CO** was treated with hydrochloric acid and the resulting mixture analyzed by ^{1}H NMR spectroscopy (**Figure 2.15**).

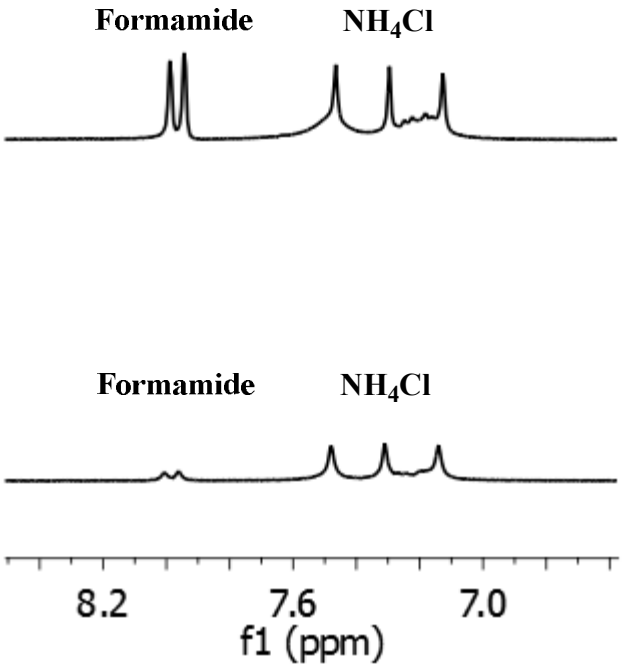

Figure 2.15 Dimethylsulfoxide-d_6 ^{1}H NMR spectra (normalized intensities) of protonated **1-CO** before (bottom) and after (top) addition of formamide

Observation of a triplet at 7.29 ppm indicated formation of NH_4Cl, likely from decomposition of the protonated silyl amine. The release of formamide from the

molecule was established by treatment of the protonated mixture with one microliter of authentic sample and observing the increased intensity of the peaks at 7.16, 7.21 and 7.94 ppm.

Solution IR spectroscopy of **1-CO** in benzene showed an intense carbonyl stretching band at 1557 cm^{-1} (which shifted to 1523 cm^{-1} upon labeling with ^{13}CO), indicating a weak C-O bond. Neutral late-metal formyls exhibit C-O stretching bands between 1560 and 1610 cm^{-1}. [17] A crystallographically characterized η^2-acetyl complex of zirconium prepared by Floriani exhibits a C-O stretching band at 1540 cm^{-1}, suggesting that the C-O bond is attenuated upon interaction with one of the Lewis acidic hafnium metal centers. Metal formyls are kinetically unstable in solution, and often undergo irreversible decomposition to carbonyl hydride species.[17] Migration of the formyl group from hafnium to nitrogen prevents decomposition via this pathway. One possible mechanism for this transformation is presented in **Figure 2.16**.

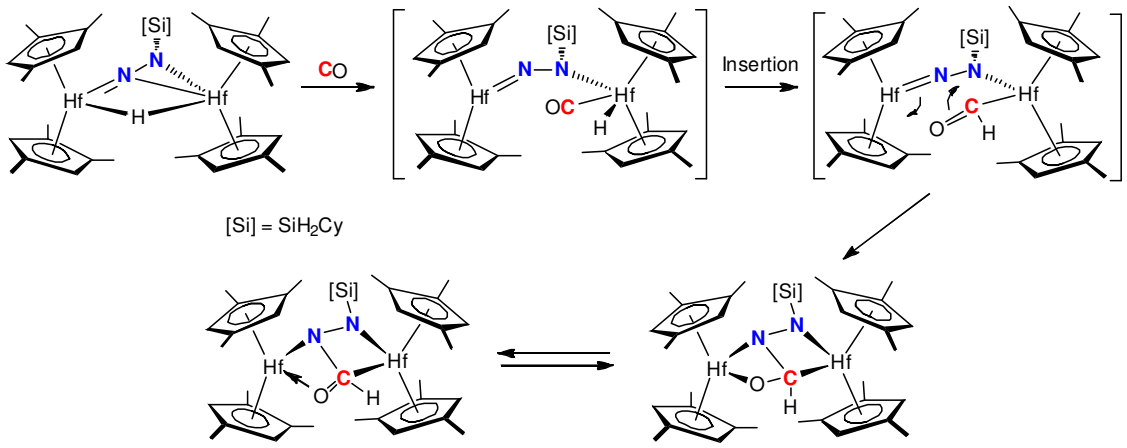

Figure 2.16 Postulated mechanism for formation of **1-CO**.

The formation of a new N-C bond by treatment of **1-N_2** with primary silanes and CO spurred our investigation into possible N-C bond forming reactions with other

organic fragments. In that vein, **1-CySiH$_3$-*C$_1$*** was treated with an excess of cyclohexylnitrile at room temperature.

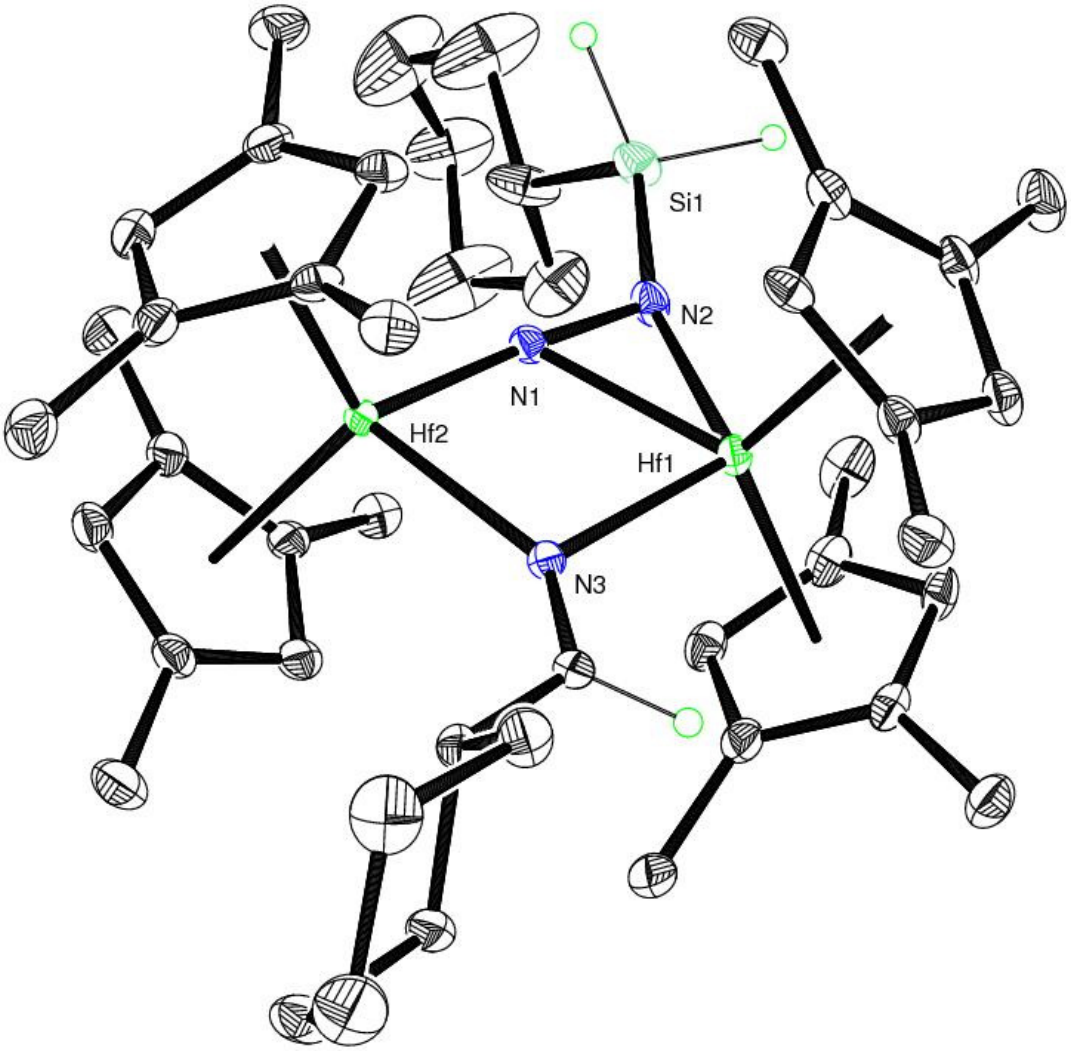

Figure 2.17 ORTEP plot of **1-CyCN** at 30% probability ellipsoids. Hydrogen atoms attached to cyclopentadienyl and cyclohexyl rings omitted for clarity.

A color change from dark brown to deep purple was observed over the course of five minutes, and concentrating and cooling the reaction mixture produced dark purple crystals of **1-CyCN** suitable for an X-ray diffraction study (**Figure 2.17**).
The solid state structure of **1-CyCN** consists of an aldimine unit bridging the two hafnium centers as well as a side-on/end-on silylated dinitrogen fragment. Selected metrical parameters are presented in **Table 2.2**.

Table 2.2. Selected Bond Distances (Å) and Angles (°) for **1-CyCN**

Hf(1)-N(2)	2.128(4)	Hf(2)-N(3)-Hf(1)	93.86(13)
Hf(1)-N(1)	2.167(3)	N(2)-N(1)-Hf(2)	176.0(3)
Hf(1)-N(3)	2.297(3)	Hf(2)-N(3)-Hf(1)	93.86(13)
Hf(2)-N(1)	1.921(4)	N(1)-Hf(1)-N(3)	75.88(13)
Hf(2)-N(3)	2.216(3)	N(1)-Hf(2)-N(3)	82.87(14)
N(1)-N(2)	1.412(5)	Hf(2)-N(1)-Hf(1)	107.38(15)
N(3)-C(39)	1.274(5)		

The N(1)-N(2) distance in the dinitrogen unit is contracted to 1.412(5) Å, shorter than the value of 1.457(5) Å found in **1-N_2**. The dinitrogen unit is functioning as an LX_3 type ligand; the short Hf(2)-N(1) bond suggests significant metal-imido character while the side-on coordination of the molecule to Hf(1) can be characterized as an LX type interaction, with Hf-N single bond distances of 2.128(4) and 2.167(3) Å. Based on this formalism, the bridging aldimine can be considered an X-type donor to Hf(2) and an L-type donor to Hf(1). The N(3)-C(39) bond length of 1.274(5) Å is shortened compared to a typical N-C double bond length of 1.35 Å.[19]

Multinuclear NMR spectroscopic data in benzene-d_6 are consistent with the solid-state structure being maintained in solution (**Figure 2.18**). ^{1}H NMR spectroscopy

reveals six Cp methyl and four Cp hydrogen resonances, consistent with the pseudo-C_s symmetry of the solid-state structure. The aldimine proton resonates at 8.46 ppm, and is split into a doublet by coupling with the cyclohexyl methine hydrogen. The silyl hydrogens appear as a singlet at 5.38 ppm, and are split by $^{2}J_{NH}$ = 5.9 Hz when labeled **1-$^{15}N_2$** is used in the preparation of **1-CyCN**. In addition to the expected cyclopentadienyl resonances, the ^{13}C NMR spectrum also displays a signal at 55.2 ppm, attributable to the cyclohexyl methine carbon connected to the aldimine, as well as a downfield resonance at 185.3 ppm, attributable to the aldimine carbon. As expected, the ^{29}Si NMR spectrum displays a singlet at -25.05 ppm which is split into a doublet of doublets ($^{1}J_{SiN}$ = 9.8, $^{2}J_{SiN}$ = 0.9) by coupling to ^{15}N nuclei.

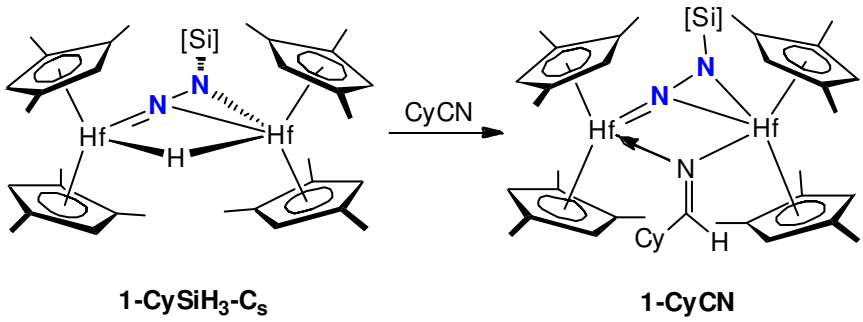

1-CySiH$_3$-C$_s$ **1-CyCN**

Figure 2.18 Reaction of **1-CySiH$_3$-*C$_s$*** with cyclohexylnitrile

The ^{15}N NMR spectrum of the fully labeled compounds displays two resonances, both split by $^{1}J_{NN}$ of 11.9 Hz; a signal at 71.80 ppm attributable to the silylated nitrogen, and a signal at 304.45 ppm corresponding to the nitrogen with more imido character. A strong band at 1702 cm^{-1} in the solution IR spectrum of **1-CyCN** was attributed to the aldimine C=N stretching mode.

While the expected insertion of the nitrile fragment into the hafnium hydride bond occurred, no N-C bond formation as in the reaction of **1-N$_2$** with carbon monoxide was observed. This may be attributed in part to the instability of metal formyl groups, or

the increased ability of the aldimine unit to bridge two metal centers. The prescense of substantial imido character in the Hf(2)-N(1) linkage suggests that additional functionalization of this fragment of **1-CyCN** may be possible be typical 1,2-addition routes. Reaction of **1-CySiH$_3$** with other reagents is currently being explored with an aim for further functionalization of the nitrogen fragment, coupled with eventual release from the metal center.

Concluding Remarks

The highly activated dinitrogen fragment of **1-N$_2$** has proven amenable to silylation at a single nitrogen, providing the first example of N_2 functionalization with silanes in Group 4 metallocene chemistry. The mono-silylated nitrogen compound displays a rich reaction chemistry, with complete N_2 cleavage occurring upon thermolysis. Hydrogenolysis of the cleaved product led to further nitrogen functionalization via ring opening of a four membered metallacycle. These reactions provide entry into a possible catalytic cycle for the production of silylated diamines from primary silanes, N_2 and H_2.

The mono-silylated product is also prone to undergo insertion into its bridging hafnium hydride. Reaction with carbon monoxide leads to N-C bond formation by transfer of a metal formyl unit to the unsilylated nitrogen atom of **1-CySiH$_3$**. Treatment of **1-CySiH$_3$** with cyclohexylnitrile also led to insertion into the bridging hydride, but the formation of an aldimine bridge between the two hafnium centers precluded N-C bond formation. As in Chapter One, the results presented here again display the subtle effect of cyclopentadienyl substitution on the reactivity of metallocene dinitrogen compounds, in this case furnishing the first example of silane induced N_2 cleavage supported by a Group 4 metal.

Experimental

General Considerations. All air- and moisture-sensitive manipulations were carried out using standard high vacuum line, Schlenk or cannula techniques or in an M. Braun inert atmosphere drybox containing an atmosphere of purified dinitrogen. The drybox was equipped with a cold well designed for freezing samples in liquid nitrogen. Solvents for air- and moisture-sensitive manipulations were dried and deoxygenated using literature procedures. Deuterated solvents for NMR spectroscopy were purchased from Cambridge Isotope Laboratories and were distilled from sodium metal under an atmosphere of argon and stored over 4 Å molecular sieves. Hydrogen and argon gas were purchased from Airgas Incorporated and passed through a column containing manganese oxide supported on vermiculite and 4 Å molecular sieves before admission to the high vacuum line. ^{1}H spectra were recorded on Bruker ARX 300, Varian Mercury 300, Inova 400 and 500 spectrometers operating at 299.763, 299.763, 399.780 and 500.62 MHz, respectively. ^{13}C NMR spectra were obtained on Bruker ARX 300 and Inova 500 spectrometers operating at 75.37 and 100.52 MHz, respectively. All chemical shifts are reported relative to $SiMe_4$ using ^{1}H (residual) chemical shifts of the solvent as a secondary standard. ^{2}H NMR spectra were recorded on a Varian Inova 500 spectrometer operating at 76.851 MHz and the spectra were referenced using an internal benzene-d_6 standard. ^{15}N NMR spectra were recorded on a Varian Inova 500 spectrometer operating at 50.663 MHz and chemical shifts were externally referenced to liquid ammonia. ^{29}Si NMR spectra were recorded on a Varian Inova 500 spectrometer operating at 99.288 MHz and chemical shifts were externally referenced to $SiMe_4$. Infrared spectroscopy was conducted on a Thermo-Nicolet Avatar FT-IR spectrometer calibrated with a polystyrene standard.

Single crystals suitable for X-ray diffraction were coated with polyisobutylene oil in a drybox and were quickly transferred to the goniometer head of a Siemens SMART CCD Area detector system or a Bruker X8 APEX2 system equipped with a molybdenum X-ray tube (λ = 0.71073 A). Preliminary data revealed the crystal system. A hemisphere routine was used for data collection and determination of lattice constants. The space group was identified and the data were processed using the Bruker SAINT program and corrected for absorption using SADABS. The structures were solved using direct methods (SHELXS) completed by subsequent Fourier synthesis and refined by full-matrix least-squares procedures. Elemental analyses were performed at Robertson Microlit Laboratories, Inc., in Madison, NJ.

$^{15}N_2$ gas was purchased from Cambridge Isotope Laboratories. All other chemicals were purchased from Aldrich or Acros and used as received.

Preparation of [(η^5-$C_5Me_3H_2$)$_2$Hf](μ-H)(η^2, η^2-N-NSiH_2Cy) (1-CySiH_3-*C_1* and 1-CySiH_3-*C_s*) A scintillation vial was charged with [(η^5-$C_5Me_3H_2$)$_2$Hf]$_2$(η^2, η^2-N_2) (40mg, 0.049 mmol) and diethyl ether (3 mL). Upon addition of cyclohexylsilane (7.7 μL, 0.054 mmol) via microsyringe, the solution immediately turned red. Multinuclear NMR spectroscopic analysis revealed the presence of two products in a 1:1 ratio. ^{1}H NMR (benzene- d_6, 23 ^{o}C) **1-CySiH_3-*C_1***: δ 1.03 (m, 1H, cyclohexyl C*H*), 1.39 (m overlapped, 2H, cyclohexyl C*H*$_2$), 1.72 (m overlapped, 2H, cyclohexyl C*H*$_2$), 1.81 (m overlapped, 2H, cyclohexyl C*H*$_2$), 1.85 (s, 3H, C_5*Me*$_3$$H_2$), 1.91 (s, 3H, C_5*Me*$_3$$H_2$), 1.95 (s, 3H, C_5*Me*$_3$$H_2$), 1.98 (s overlapped, 3H, C_5*Me*$_3$$H_2$), 1.99 (m overlapped, 2H, cyclohexyl C*H*$_2$), 2.07 (m overlapped, 2H, cyclohexyl C*H*$_2$), 2.12 (s, 3H, C_5*Me*$_3$$H_2$), 2.13 (s, 3H, C_5*Me*$_3$$H_2$), 2.14 (s, 3H, C_5*Me*$_3$$H_2$), 2.16 (s, 3H, C_5*Me*$_3$$H_2$), 2.23 (s, 3H, C_5*Me*$_3$$H_2$), 2.33 (s, 3H, C_5*Me*$_3$$H_2$), 2.41 (s overlapped, 3H, C_5*Me*$_3$$H_2$), 2.42 (s overlapped, 3H, C_5*Me*$_3$$H_2$), 4.64 (d, 1H, $^2J_{HH}$ = 10.5, Si*H*$_2$Cy), 4.97 (s, 1H, Hf-*H*), 5.11 (d, 1H, $^2J_{HH}$ =

10.5, SiH_2Cy), 5.24 (s, 1H, $C_5Me_3H_2$), 5.56 (s, 1H, $C_5Me_3H_2$), 5.83 (s, 1H, $C_5Me_3H_2$), 5.90 (s, 1H, $C_5Me_3H_2$), 6.09 (s, 1H, $C_5Me_3H_2$), 6.56 (s, 1H, $C_5Me_3H_2$), 6.70 (s overlapping, 1H, $C_5Me_3H_2$), 6.88 (s, 1H, $C_5Me_3H_2$). $\{^1H\}^{13}C$ NMR (benzene-d_6, 23 °C): δ 13.1, 13.3, 13.6, 13.8, 14.2, 14.3, 14.3, 14.4, 15.0, 15.0, 16.6, 16.6 ($C_5Me_3H_2$), 27.4 (cyclohexyl CH_2), 27.7 (cyclohexyl CH), 28.5, 28.9, 29.3, 30.3 (cyclohexyl CH_2), 104.4, 108.5, 109.8, 110.3, 111.6, 111.8, 112.8, 113.9, 114.2, 115.9, 116.2, 117.3, 117.9, 120.1, 120.5, 121.3, 122.8, 124.9, 125.3, 128.2 ($C_5Me_3H_2$). $\{^1H\}^{29}Si$ NMR (benzene-d_6, 23 °C): δ -28.67 (d, $^1J_{SiN}$ = 10.3, N-SiH_2Cy). $\{^1H\}^{15}N$ NMR (benzene-d_6, 23 °C): δ 183.23 (d, $^1J_{NN}$ = 13.3, *N*-SiH_2Cy), 320.97 (d, $^1J_{NN}$ = 13.3, Hf-*N*-Hf). **1-CySiH$_3$-C_s**: δ 1.03 (m, 1H, cyclohexyl C*H*), 1.39 (m overlapped, 2H, cyclohexyl CH_2), 1.72 (m overlapped, 2H, cyclohexyl CH_2), 1.81 (m overlapped, 2H, cyclohexyl CH_2), 1.98 (s, 6H, $C_5Me_3H_2$), 1.99 (m overlapped, 2H, cyclohexyl CH_2), 2.07 (m overlapped, 2H, cyclohexyl CH_2), 2.13 (s, 6H, $C_5Me_3H_2$), 2.19 (s, 6H, $C_5Me_3H_2$), 2.22 (s, 6H, $C_5Me_3H_2$), 2.27 (s, 6H, $C_5Me_3H_2$), 2.28 (s, 6H, $C_5Me_3H_2$), 4.78 (s, 1H, Hf-*H*), 4.85 (d, 2H, $^2J_{NH}$ = 6.5, N-SiH_2Cy), 5.43 (d, 2H, $^4J_{HH}$ = 2.6, $C_5Me_3H_2$), 5.47 (d, 2H, $^4J_{HH}$ = 2.6, $C_5Me_3H_2$), 6.48 (d, 2H, $^4J_{HH}$ = 2.6, $C_5Me_3H_2$), 6.68 (d overlapping, 2H, $^4J_{HH}$ = 2.6, $C_5Me_3H_2$). $\{^1H\}^{13}C$ NMR (benzene-d_6, 23 °C): δ 12.3, 13.5, 13.9, 14.2, 15.2, 15.7 ($C_5Me_3H_2$), 27.4 (cyclohexyl CH_2), 27.7 (cyclohexyl CH), 28.5, 28.9, 29.3, 30.2 (cyclohexyl CH_2), 107.6, 109.7, 112.5, 114.0, 115.2, 117.1, 118.8, 120.9, 121.6, 124.23 ($C_5Me_3H_2$). $\{^1H\}^{29}Si$ NMR (benzene-d_6, 23 °C): δ -28.1 (d, $^1J_{SiN}$ = 10.3, N-SiH_2Cy).$\{^1H\}^{15}N$ NMR (benzene-d_6, 23 °C): δ 183.98 (d, $^1J_{NN}$ = 12.9, *N*-SiH_2Cy), 317.05 (d, $^1J_{NN}$ = 12.9, Hf-*N*-Hf).

Preparation of [(η^5-$C_5Me_3H_2$)$_2$Hf]$_2$(H)(μ-[NH(SiHCy)N]) (1-SiHCy). A thick walled glass vessel was charged with [(η^5-$C_5Me_3H_2$)$_2$Hf]$_2$(η^2, η^2-N_2) (107 mg, 0.180 mmol) and toluene (5 mL). Upon addition of cyclohexylsilane (28.4 μL, 0.198 mmol) via

microsyringe, the solution immediately turned brown. The reaction mixture was heated at 65 °C for 24 h, whereupon it became light yellow. The volatiles were removed in vacuo and the oily yellow residue was re-dissolved in diethyl ether. Storage at -35 °C for 3 d induced deposition of $[(\eta^5\text{-}C_5Me_3H_2)_2Hf]_2(H)(\mu\text{-}[NH(SiHCy)N])$ as large yellow hexagonal crystals suitable for X-ray diffraction (60 mg, 49 % yield). Anal Calcd for $C_{38}H_{57}N_2SiHf_2$: C, 49.24; H, 6.20; N, 3.02. Found: C, 49.45; H, 6.43; N, 2.87.^{1}H NMR (benzene- d_6, 23 °C): δ 0.64 (br m, 1H, cyclohexyl C*H*), 1.2-1.41 (br m, 5H, cyclohexyl CH_2), 1.71 (s, 6H, (2 coincident environments), $C_5Me_3H_2$), 1.72-1.95 (br m, 5H, cyclohexyl CH_2) $C_5Me_3H_2$), 1.94 (s, 3H, $C_5Me_3H_2$), 2.04 (s, 3H, $C_5Me_3H_2$), 2.18 (s, 3H, $C_5Me_3H_2$), 2.19 (s, 3H, $C_5Me_3H_2$), 2.25 (s, 6H, (2 coincident environments), $C_5Me_3H_2$), 2.28 (m, 1H, N*H*), 2.36 (s, 3H, $C_5Me_3H_2$), 2.41 (s, 3H, $C_5Me_3H_2$), 2.58 (s, 3H, $C_5Me_3H_2$), 2.60 (s, 3H, $C_5Me_3H_2$), 4.74 (d, 1H, $^3J_{HH}$ = 3.1, Si-*H*), 5.27 (s, 1H, $C_5Me_3H_2$), 5.40 (d, 1H, $^4J_{HH}$ = 2.5, $C_5Me_3H_2$), 5.51 (d, 1H, $^4J_{HH}$ = 2.4, $C_5Me_3H_2$), 5.56 (d, 1H, $^4J_{HH}$ = 2.5, $C_5Me_3H_2$), 5.99 (d, 1H, $^4J_{HH}$ = 2.5, $C_5Me_3H_2$), 6.26 (s, 1H, $C_5Me_3H_2$), 6.28 (d, 1H, $^4J_{HH}$ = 2.5, $C_5Me_3H_2$), 6.53 (s, 1H, $C_5Me_3H_2$), 9.76 (s, 1H, Hf-*H*). $\{^1H\}^{13}C$ NMR (benzene-d_6, 23 °C): δ 13.3, 13.4, 13.8, 14.0, 14.4, 14.6, 14.8, 15.1, 15.3, 15.7, 15.9, 16.9 ($C_5Me_3H_2$), 27.9, 28.1, 28.4, 28.9, 29.0, 30.6 (cyclohexyl *C*), 110.5, 111.9, 112.0, 112.9, 113.9, 114.4, 114.9, 115.2, 116.0, 116.3, 116.6, 117.0, 117.1, 117.6, 118.5, 118.8, 119.1, 122.2, 125.2, 125.8 ($C_5Me_3H_2$). $\{^1H\}^{15}N$ NMR (benzene-d_6, 23 °C): δ 106.97 (br m., *N*-H), 281.40 (br m., Hf-*N*-Hf). $\{^1H\}^{29}Si$ NMR (benzene-d_6, 23 °C): δ -26.98 (dd, $^1J_{SiN}$ = 11.8, 2.2, *Si*CyH). IR (toluene): ν_{NH} = 3437 cm^{-1}.

Preparation of $[(\eta^5\text{-}C_5Me_3H_2)_2Hf]_2(H)(\mu\text{-}[NH(SiH^nHex)N])$ (1-SiH^{n}Hex). A thick walled glass vessel was charged with $[(\eta^5\text{-}C_5Me_3H_2)_2Hf]_2(\eta^2, \eta^2\text{-}N_2)$ (50 mg, 0.062 mmol) and toluene (5 mL). The vessel was moved to a high vacuum line, evacuated and

n-hexylsilane (0.074 mmol) was added via calibrated gas bulb (17.2 mL, 79.2 Torr). The reaction mixture immediately turned brown and was heated at 65 °C for 24 h, whereupon it became light yellow. The volatiles were removed in vacuo and the oily yellow residue was subjected to spectroscopic analysis. ^{1}H NMR (benzene- d_6, 23 °C): δ 0.95 (t, 3H, $^3J_{HH}$ = 7 Hz, hexyl *Me*), 1.11 (t, 2H, $^3J_{HH}$ = 7.0, hexyl C*H*$_2$), 1.24-1.48 (br m, 8H, hexyl C*H*$_2$), 1.69 (s, 3H, C$_5$*Me*$_3$H$_2$), 1.70 (s, 3H, C$_5$*Me*$_3$H$_2$), 1.95 (s, 3H, C$_5$*Me*$_3$H$_2$), 2.06 (s, 3H, C$_5$*Me*$_3$H$_2$), 2.10 (s, 3H, C$_5$*Me*$_3$H$_2$), 2.16 (s, 3H, C$_5$*Me*$_3$H$_2$), 2.30 (s, 3H, C$_5$*Me*$_3$H$_2$), 2.35 (s, 3H, C$_5$*Me*$_3$H$_2$), 2.43 (s, 6H, (2 coincident environments), C$_5$*Me*$_3$H$_2$), 2.44 (br m, 1H, N*H*), 2.48 (s, 3H, C$_5$*Me*$_3$H$_2$), 2.67 (s, 3H, C$_5$*Me*$_3$H$_2$), 5.02 (d, 1H, $^3J_{HH}$ = 3.9, Si-*H*), 5.11 (d, 1H, $^4J_{HH}$ = 2.4, C$_5$Me$_3$*H*$_2$), 5.26 (br s, 1H, C$_5$Me$_3$*H*$_2$), 5.53 (d, 1H, $^4J_{HH}$ = 2.4, C$_5$Me$_3$*H*$_2$), 5.57 (d, 1H, $^4J_{HH}$ = 2.4, C$_5$Me$_3$*H*$_2$), 5.86 (br s, 1H, C$_5$Me$_3$*H*$_2$), 6.23 (d, 1H, $^4J_{HH}$ = 2.4, C$_5$Me$_3$*H*$_2$), 6.26 (d, 1H, $^4J_{HH}$ = 2.4, C$_5$Me$_3$*H*$_2$), 6.28 (d, 1H, $^4J_{HH}$ = 2.4, C$_5$Me$_3$*H*$_2$), 10.3 (s, 1H, Hf-*H*). {^{1}H}^{13}C NMR (benzene-d_6, 23 °C): δ 7.7 (Si-*C*H$_2$), 13.3, 13.4, 14.4, 14.5, 14.7, 14.8, 14.8, 14.9, 14.9, 16.1, 16.1, 16.3, 16.8 (C$_5$*Me*$_3$H$_2$ and *n*-hexyl *Me*), 23.4, 24.8, 32.6, 34.1 (*n*-hexyl *C*H$_2$), 110.1, 111.6, 112.2, 112.2, 112.5, 113.1, 113.5, 113.7, 114.2, 114.6, 114.7, 115.4, 116.1, 117.0, 117.2, 118.2, 121.5, 122.7, 126.1, 126.2, 128.9. IR (toluene): ν_{NH} = 3436 cm^{-1}, ν_{ND} = 2548 cm^{-1}.

Preparation of [(η^5-C$_5$Me$_3$H$_2$)$_2$Hf]$_2$(H)$_2$(μ-[NH-Si(H)(Cy)-NH]) (1-H$_2$). In a glovebox, a thick walled glass vessel was charged with [(η^5-C$_5$Me$_3$H$_2$)$_2$Hf]$_2$(H)(μ-[NH(SiHCy)N]) (73 mg, 0.050 mmol) and toluene (5 mL). On a high vacuum line, the solution was frozen and degassed before H$_2$ gas (4 atm) was admitted. The solution was stirred at 80 °C for 4 d. The solvent was removed in vacuo and the brown residue was extracted with diethyl ether, evaporated to dryness, and subjected to spectroscopic analysis. ^{1}H NMR (benzene- d_6, 23 °C): δ 0.77 (tt, 1H, $^3J_{HH}$ = 13.1, 2.9, cyclohexyl CH),

1.24-1.36 (br m, 4H, cyclohexyl CH_2), 1.82 (m overlapped, 2H, cyclohexyl CH_2), 1.90 (m overlapped, 2H, cyclohexyl CH_2), 2.02 (m overlapped, 2H, cyclohexyl CH_2), 1.98 (s, 6H, $C_5Me_3H_2$), 2.01 (s, 6H, $C_5Me_3H_2$), 2.18 (s, 6H, $C_5Me_3H_2$), 2.19 (s, 6H, $C_5Me_3H_2$), 2.34 (s, 6H, $C_5Me_3H_2$), 2.45 (s, 6H, $C_5Me_3H_2$), 4.04 (dd, 2H, $^1J_{NH}$ = 56.1, $^3J_{HH}$ = 3.9, N*H*), 5.21 (t, 1H, $^3J_{HH}$ = 3.9, Si*H*Cy), 5.23 (d, 2H, $^4J_{HH}$ = 2.4, $C_5Me_3H_2$), 5.32 (d, 2H, $^4J_{HH}$ = 2.4, $C_5Me_3H_2$), 5.69 (d, 2H, $^4J_{HH}$ = 2.4, $C_5Me_3H_2$), 5.90 (d, 2H, $^4J_{HH}$ = 2.4, $C_5Me_3H_2$), 9.93 (s, 2H, Hf-*H*). $\{^1H\}^{13}C$ NMR (benzene-d_6, 23 °C): δ 14.1, 14.2, 14.9, 15.1, 15.4, 15.8 ($C_5Me_3H_2$), 28.4, 28.5, 29.3 (cyclohexyl *C*H_2), 31.4 (cyclohexyl *C*H), 108.9, 109.2, 111.2, 111.6, 114.3, 115.4, 117.5, 117.6, 120.3, 120.9 ($C_5Me_3H_2$). $\{^1H\}^{29}Si$ NMR (benzene-d_6, 23 °C): δ -10.62 (t, $^1J_{SiN}$ = 9.0). $\{^1H\}^{15}N$ NMR (benzene-d_6, 23 °C): δ 164.55 (s, *N*H).

Preparation of [(η^5-$C_5Me_3H_2$)$_2$Hf]$_2$(μ-[N-N(SiH$_2$Cy)-C(H)O]) (1-CO). A thick walled glass vessel was charged with [(η^5-$C_5Me_3H_2$)$_2$Hf]$_2$(η^2, η^2-N_2) (71 mg, 0.087 mmol) and toluene (5 mL). Upon addition of cyclohexylsilane (12.6 μL, 0.088 mmol) via microsyringe, the solution immediately turned brown. On a high vacuum line, the vessel was evacuated and CO gas (4 atm) was introduced. The solution immediately turned dark red and was stirred for 1 h. The volatiles were removed in vacuo and the oily red residue was re-dissolved in toluene and layered with pentane. Storage at -35 °C for 3 d induced deposition of [(η^5-$C_5Me_3H_2$)$_2$Hf]$_2$(η^2, η^2-SiH$_2$CyN-NC(H)=O) as an white powder (55 mg, 65 % yield). ^1H NMR (toluene-d_8, 23 °C): δ 0.99 (br m, 1H, cyclohexyl C*H*), 1.29-1.41 (br m, 10H, cyclohexyl CH_2), 2.06 (s, 6H, $C_5Me_3H_2$), 2.07 (s, 12H, (2 coincident environments), $C_5Me_3H_2$), 2.12 (s, 12H, (2 coincident environments), $C_5Me_3H_2$), 2.29 (s, 6H, $C_5Me_3H_2$), 4.72 (s, 2H, SiH_2Cy), 5.51 (br s, 2H, $C_5Me_3H_2$), 5.54 (br s, 2H, $C_5Me_3H_2$), 5.71 (br s, 4H, $C_5Me_3H_2$), 9.36 (dd, 1H, $^1J_{CH}$ = 186.5, $^2J_{NH}$ = 8.8, *H*-C(O)-N). ^1H NMR (toluene-d_8, -60 °C): δ 0.93 (br m, 1H,

cyclohexyl C*H*), 1.25-1.43 (br m, 10H, cyclohexyl CH_2), 1.64 (s, 3H, $C_5Me_3H_2$), 1.83 (s, 3H, $C_5Me_3H_2$), 1.88 (s, 3H, $C_5Me_3H_2$), 1.92 (s, 3H, $C_5Me_3H_2$), 2.03 (s, 3H, $C_5Me_3H_2$), 2.05 (s, 3H, $C_5Me_3H_2$), 2.07 (s, 3H, $C_5Me_3H_2$), 2.12 (s, 3H, $C_5Me_3H_2$), 2.14 (s, 3H, $C_5Me_3H_2$), 2.24 (s, 3H, $C_5Me_3H_2$), 2.34 (s, 3H, $C_5Me_3H_2$), 2.35 (s, 3H, $C_5Me_3H_2$), 4.65 (s, 2H, SiH_2Cy), 4.85 (s, 1H, $C_5Me_3H_2$), 5.32 (s, 1H, $C_5Me_3H_2$), 5.36 (s, 1H, $C_5Me_3H_2$), 5.40 (s, 1H, $C_5Me_3H_2$), 5.42 (s, 1H, $C_5Me_3H_2$), 5.67 (s, 1H, $C_5Me_3H_2$), 5.89 (s, 1H, $C_5Me_3H_2$), 6.16 (s, 1H, $C_5Me_3H_2$), 9.22 (s, 1H, *H*-C(O)-N). $\{^1H\}^{13}C$ NMR (toluene-d_8, -60 ^oC): δ 13.2, 13.7, 13.8, 14.0, 14.0, 14.3, 14.6, 14.8, 15.7, 15.9, 16.5, 17.3 (broad, $C_5Me_3H_2$), 106.4, 106.6, 106.7, 108.8, 109.2, 109.3, 113.9, 115.1, 115.3, 115.3, 115.5, 116.8, 116.9, 117.0, 117.3, 119.5, 119.8, 120.1, 120.7 (broad, $C_5Me_3H_2$). Formamide peak not observed at -60 ^oC and other carbon signals significantly broadened. $\{^1H\}^{13}C$ NMR (benzene-d_6, 23 ^oC): δ 14.3, 14.6, 15.6, 15.8, 16.0, 16.7 ($C_5Me_3H_2$), 21.7, 27.0, 27.7, 29.1, 30.6, 30.8 (cyclohexyl *C*), 104.6, 105.2, 108.3, 110.6, 113.2, 113.7, 116.7, 116.7, 117.7, 118.4 ($C_5Me_3H_2$), 169.5 (d, $^1J_{CN}$ = 8.5, H-*C*(O)-N).$\{^1H\}^{29}Si$ NMR (benzene-d_6, 23 ^oC): δ -37.28 $\{^1H\}^{15}N$ NMR (benzene-d_6, 23 ^oC): δ 215.89 (br s., *N*-SiH_2Cy), 283.14 (br m, H-*C*(O)-*N*). IR(C_6D_6): ν_{CO} = 1557 cm $^{-1}$, ν_{13CO} = 1523 cm $^{-1}$.

Preparation of[(η^5-$C_5Me_3H_2$)$_2$Hf]$_2$(μ-[N=C(H)(Cy)])(η^2, η^1-N-NSiH_2Cy) (1-CyCN). A thick walled glass vessel was charged with [(η^5-$C_5Me_3H_2$)$_2$Hf]$_2$(η^2, η^2-N_2) (80 mg, 0.099 mmol), a stirbar, and toluene (5 mL). Upon addition of cyclohexylsilane (15.6 μL, 0.109 mmol) via microsyringe, the solution immediately turned brown. Cyclohexyl nitrile (23.4 μL, 0.197 mmol) was added via microsyringe to the brown solution. The solution was stirred vigorously for 5 minutes whereupon a color change to dark bluish purple was observed. The volatiles were removed in vacuo and the residue was re-dissolved in toluene and layered with pentane. Storage at -35 ^oC for 1 d induced

deposition of [(η^5-$C_5Me_3H_2$)$_2$Hf]$_2$(μ-[N=C(H)(Cy)])(η^2, η^1-N-NSiH$_2$Cy) as purple prisms suitable for X-ray diffraction (43 mg, 42 %). ^{1}H NMR (benzene- d_6, 23 ^{o}C): δ 1.11-1.93 (m, 19H, Cy CH_2 and C*H*), 1.86 (overlapped, 1H, cyclohexyl C*H*-C=N), 2.02 (s, 12H, (2 coincident environments), $C_5Me_3H_2$), 2.08 (s, 6H, $C_5Me_3H_2$), 2.17 (s, 6H, $C_5Me_3H_2$), 2.28 (s, 6H, $C_5Me_3H_2$), 2.39 (s, 6H, $C_5Me_3H_2$), 5.20 (br s, 2H, $C_5Me_3H_2$), 5.22 (br s, 2H, $C_5Me_3H_2$), 5.38 (d, 2H, $^2J_{NH}$ = 5.9, SiH_2Cy), 5.47 (br s, 2H, $C_5Me_3H_2$), 5.60 (d, 2H, $^4J_{HH}$ = 2.3, $C_5Me_3H_2$), 8.46 (d, 1H, $^3J_{HH}$ = 7.8, *H*-C=N-Cy). {^{1}H}^{13}C NMR (benzene-d_6, 23 ^{o}C): δ 14.6, 14.7, 14.8, 14.8, 16.5, 16.6 ($C_5Me_3H_2$), 24.4, 25.6, 25.6, 26.4, 26.9, 27.8, 28.2, 29.1, 29.8, 30.6, 32.5 (cyclohexyl *C*H and *C*H$_2$), 55.2 (Cyclohexyl *C*H-C=N), 109.5, 110.0, 110.8, 115.5, 115.9, 116.5, 122.2, 126.0, 128.9, 129.7, ($C_5Me_3H_2$), 185.3 (H-N=*C*-Cy). {^{1}H}^{29}Si NMR (benzene-d_6, 23 ^{o}C): δ -25.05 (dd, $^1J_{SiN}$ = 9.8, $^2J_{SiN}$ = 0.9, N-N-*Si*H$_2$Cy). {^{1}H}^{15}N NMR (benzene-d_6, 23 ^{o}C): δ 71.80 (d, $^1J_{NN}$ = 11.9, N-*N*-SiH$_2$Cy), 304.45 (d, $^1J_{NN}$ = 11.9, *N*-N-SiH$_2$Cy). IR(C_6D_6): ν_{CN} = 1702 cm^{-1}.

Complete ^{1}H NMR Assignment of 1-CySiH$_3$-*C$_1$* and 1-CySiH$_3$-*C$_s$*

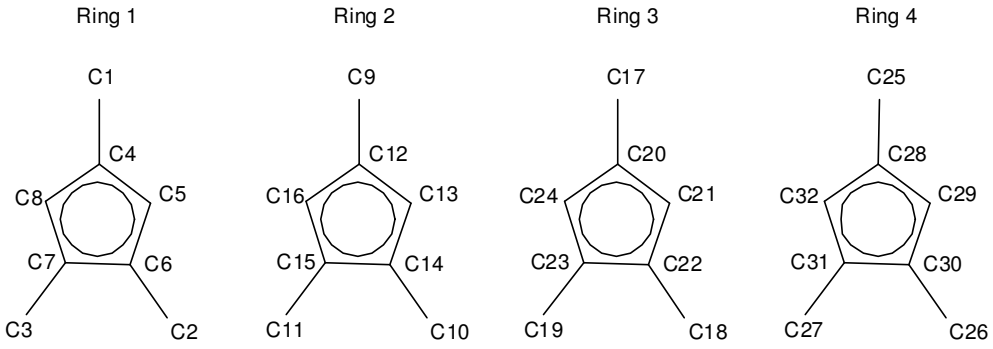

Figure 2.19: Ring Assignment of 1-CySiH$_3$-*C$_1$*

Table 2.3. NMR assignment for **1-CySiH$_3$-*C$_1$***

Atom Label	^{1}H Shift (δ)	^{13}C Shift (δ)	NOE correlation
C1	2.42	16.1	
C2	2.32	12.8	C29
C3	1.85	14.5	
C4	-		
C5	6.68	110.9	C16, C26, a-SiH$_2$, Hf-H
C6	-	119.4	
C7	-	124.0	
C8	5.90	117.1	C8
C9	1.94	13.3	b-SiH$_2$
C10	2.33	12.8	C21
C11	2.23	15.1	a-SiH$_2$
C12	-	113.1	
C13	6.55	109.1	C13, C17, a-SiH$_2$, Hf-H
C14	-	124.4	
C15	-	112.0	
C16	5.83	119.6	C5
C17	2.42	16.1	C13, b-SiH$_2$
C18	2.15	13.3	
C19	1.97	13.3	
C20	-	116.7	
C21	6.09	103.9	C10, C29, Hf-H
C22	-	127.2	
C23	-	112.8	
C24	5.24	113.3	C32

Table 2.3 (Continued)

C25	2.12	14.5	b-SiH_2
C26	2.14	13.0	C16
C27	1.98	11.8	
C28	-	107.3	
C29	6.88	109.6	C21, C2, Hf-H
C30	-	120.5	
C31	-	118.4	
C32	5.56	115.3	C24
Hf-H-Hf	4.97	-	C13, C29 (strong), C5, C21 (weak)
a-SiH_2	4.64	-	C5, C11,C13
b-SiH_2	5.11	-	C9, C17, C25

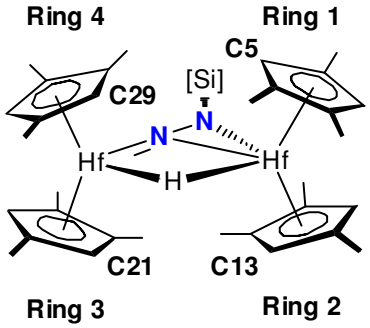

Figure 2.20 3-D Structure of **1-CySiH$_3$-*C$_1$***

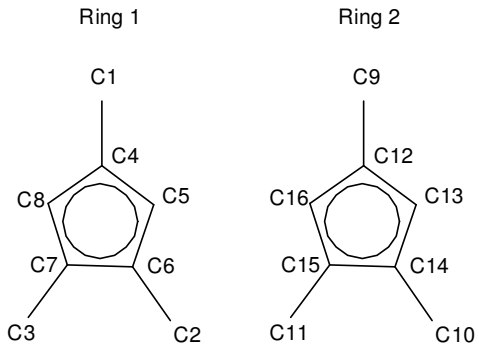

Figure 2.21 Ring Assignment of 1-CySiH$_3$-*C$_s$*

Table 2.4. NMR assignment for **1-CySiH$_3$-*C$_s$***

Atom Label	^{1}H Shift (δ)	^{13}C Shift (δ)	NOE Correlation
C1	2.22	14.7	Hf-H, C5
C2	2.28	13.4	
C3	2.19	13.0	Hf-H
C4	-	116.4	
C5	6.67	109.2	C1, C13
C6	-	120.1	
C7	-	118.0	
C8	5.46	121.1	
C9	2.27	15.2	C10
C10	2.13	13.7	C9, SiH_2
C11	1.98	12.6	SiH_2
C12	-	111.8	
C13	6.47	107.0	C5
C14	-	123.4	
C15	-	113.1	
C16	5.43	114.7	
Hf-H-Hf	4.78	-	C1, C3
SiH_2	4.85	-	C10, C11

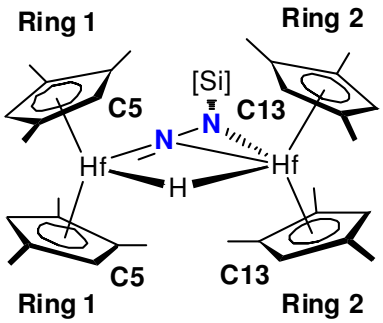

Figure 2.22 3-D Structure of **1-CySiH$_3$-*C$_s$***

The molecule is top-bottom equivalent, as seen by cross-ring NOE correlations.

REFERENCES

[1] Allen, A. D.; Senoff, C. V. *Chem. Commun.* **1965**, 621.

[2] MacKay, B.A.; Fryzuk, M.D. *Chem. Rev.* **2004**, *104*, 385.

[3] Fryzuk, M. D.; Johnson, S. A. *Coord. Chem. Rev*. **2000**, *200*, 379.

[4] (a) Fryzuk, M. D.; Love, J. B.; Rettig, S. J.; Young, V. G. *Science* **1997**, *275*, 1445. (b) Bernskoetter, W. H.; Lobkovsky, E.; Chirik, P. J. *J. Am. Chem. Soc.* **2005**, *127*, 14051. (c) Morello, L.; Love, J. B.; Patrick, B. O.; Fryzuk, M. D. *J. Am. Chem. Soc.* **2004**, *126*, 9480. (d) Bernskoetter, W. H.; Pool, J. A.; Lobkovsky, E.; Chirik, P. J. *J. Am. Chem. Soc.* **2005**, *127*, 7901.

[5] Morello, L.; Love, J. B.; Patrick, B. O.; Fryzuk, M. D. *J. Am. Chem. Soc.* **2004**, *126*, 9480.

[6] Bernskoetter, W. H.; Pool, J. A.; Lobkovsky, E.; Chirik, P. J. *J. Am. Chem. Soc.* **2005**, *127*, 7901.

[7] (a) Fryzuk, M.D.; Mackay, B.A.; Patrick, B.O. *J. Am. Chem. Soc.*, **2003**, *125*, 3234. (b) MacKay, B.A.; Munha, R.F.; Fryzuk, M.D. *J. Am. Chem. Soc.*, **2006**, *128*, 9472. (c) Fryzuk, M.D.; Love, J.B.; Rettig, S.J.; Young, V.G. *Science* **1997**, *276*, 1445. (d) Studt, F.; Mackay, B.A.; Fryzuk, M.D.; Tuczek, F. *Dalton Trans.* **2005**, 1137.

[8] (a) Hirotsu, M.; Fontaine, P.P.; Epshetyn, A.; Zavalij, P.Y.; Sita, L.R.; *J. Am. Chem. Soc.*, **2007**, *129*, 9284. (b) Hirotsu, M.; Fontaine, P.P.; Zavalij, P.Y.; Sita, L.R. *J. Am. Chem. Soc.* **2007**, *129*, 12690.

[9] Bernskoetter, W. H.; Olmos, A.V.; Lobkovsky, E.; Chirik, P.J. *Organometallics* **2006**, *25*, 1021.

[10] Chirik, P.J.; Henling, L.M.; Bercaw, J.E. *Organometallics* **2001**, *20*, 534.

[11] The signal at 183.23 ppm could be seen but did not have sufficient intensity in the directly detected ^{15}N NMR for assignment. Their assignment and location was confirmed by a ^{1}H-^{15}N HMBC experiment.

[12] In this case, intramolecular magnetization exchange occurs when the cyclopentadienyl resonances within the C_1 symmetric molecule exchange with one another. Intermolecular magnetization exchange occurs when the cyclopentadienyl resonances in the C_1 symmetric molecule exchange with cyclopentadienyl resonances in the C_2 symmetric molecule and vice versa.

[13] Analysis of the ROESY and assignment of all cyclopentadienyl resonances is presented in the experimental section

[14] Castillo, I.; Tilley, T. D. *J. Organomet. Chem.* **2002,** *643*, 431. Nugent, W. A; Haymore, B. L. *Coord. Chem. Rev.* **1980**, *31*, 123.

[15] See Chapter One, Table 1.1 of this thesis.

[16] Komori, K.; Oshita, H.; Mizobe, Y.; Hidai, M. *J. Am. Chem. Soc.* **1989,** *111*, 1940.

[17] Gladysz, J.A. *Adv. Organomet. Chem.* **1982**, *20*, 1.

[18] Fachinetti, G; Floriani, C; Marchetti, F; Merlino, S. *J. Chem. Soc. Chem. Comm.* **1976**, *13*, 522.

[19] Allen, F.H. *J. Chem. Soc. Perkin. Trans. II* **1997,** *S1-S19*.

APPENDIX A:

Crystal Structure Data

Table A.1. Compilation of X-ray data for compounds discussed in this manuscript.

Compound	Molecular Formula	CU X-ray ID
1-N_2	$C_{32}H_{44}Hf_2N_2$	sps2
1-N_2H_4	$C_{32}H_{48}Hf_2N_2$	sps4
1-SiHCy	$C_{38}H_{58}Hf_2N_2Si$	sps7
1-CyCN	$C_{45}H_{69}Hf_2N_3Si$	sps10

Table A.2. Crystal data and structure refinement of **1-N_2**

Identification code	**1-N_2**	
Empirical formula	C38 H49 F Hf2 N2	
Formula weight	909.77	
Temperature	173(2) K	
Wavelength	0.71073 Å	
Crystal system	Orthorhombic	
Space group	Pccn	
Unit cell dimensions	a = 13.4976(9) Å	□= 90°.
	b = 14.9955(11) Å	□= 90°.
	c = 17.1276(12) Å	□ = 90°.
Volume	3466.7(4) $Å^3$	
Z	4	
Density (calculated)	1.743 Mg/m^3	
Absorption coefficient	6.018 mm^{-1}	
F(000)	1776	
Crystal size	0.30 x 0.20 x 0.05 mm^3	
Theta range for data collection	2.03 to 28.28°.	
Index ranges	-17<=h<=12, -19<=k<=19, -22<=l<=21	
Reflections collected	16896	
Independent reflections	4258 [R(int) = 0.0248]	
Completeness to theta = 28.28°	99.0 %	
Absorption correction	Semi-empirical from equivalents	
Max. and min. transmission	0.7529 and 0.2654	
Refinement method	Full-matrix least-squares on F^2	
Data / restraints / parameters	4258 / 0 / 203	
Goodness-of-fit on F^2	1.031	
Final R indices [I>2sigma(I)]	R1 = 0.0199, wR2 = 0.0467	
R indices (all data)	R1 = 0.0279, wR2 = 0.0495	
Largest diff. peak and hole	1.298 and -0.723 $e.Å^{-3}$	

Table A.3. Atomic coordinates (x 10^4) and equivalent isotropic displacement parameters ($Å^2$x 10^3) for **1-N_2**. U(eq) is defined as one third of the trace of the orthogonalized U^{ij} tensor.

	x	y	z	U(eq)
F(1)	7500	-2500	2374(3)	94(2)
Hf(1)	8557(1)	1637(1)	2639(1)	17(1)
N(1)	7500	2500	3064(2)	18(1)
N(2)	7500	2500	2213(2)	20(1)
C(1)	8817(2)	348(2)	1689(2)	24(1)
C(2)	7834(2)	646(2)	1567(2)	24(1)
C(3)	7304(2)	479(2)	2261(2)	24(1)
C(4)	7932(2)	80(2)	2820(2)	23(1)
C(5)	8871(2)	-3(2)	2458(2)	25(1)
C(6)	10047(2)	1523(2)	3555(2)	28(1)
C(7)	9591(2)	2357(2)	3702(2)	26(1)
C(8)	9686(2)	2872(2)	3020(2)	24(1)
C(9)	10185(2)	2381(2)	2445(2)	25(1)
C(10)	10404(2)	1539(2)	2782(2)	27(1)
C(11)	9630(3)	298(2)	1089(2)	37(1)
C(12)	7414(3)	1038(2)	837(2)	36(1)
C(13)	7640(3)	-257(2)	3609(2)	35(1)
C(14)	10206(3)	788(2)	4146(2)	43(1)
C(15)	10486(3)	2697(3)	1648(2)	42(1)
C(1S)	7500	-2500	1576(3)	34(1)
C(2S)	7879(3)	-1775(2)	1195(3)	44(1)
C(3S)	7883(3)	-1783(3)	394(3)	52(1)
C(4S)	7500	-2500	-12(3)	52(2)
C(16)	9129(3)	2663(3)	4452(2)	41(1)

Table A.4. Crystal data and structure refinement of **1-N_2H_4**

Identification code	**1-N_2H_4**	
Empirical formula	C32 H48 Hf2 N2	
Formula weight	817.70	
Temperature	173(2) K	
Wavelength	0.71073 Å	
Crystal system	Monoclinic	
Space group	P2(1)/n	
Unit cell dimensions	a = 8.5125(8) Å	□= 90°.
	b = 21.1305(17) Å	□= 92.307(3)°.
	c = 16.5832(15) Å	□ = 90°.
Volume	2980.5(5) $Å^3$	
Z	4	
Density (calculated)	1.822 Mg/m^3	
Absorption coefficient	6.984 mm^{-1}	
F(000)	1592	
Crystal size	0.20 x 0.10 x 0.05 mm^3	
Theta range for data collection	1.56 to 28.70°.	
Index ranges	-11<=h<=11, -24<=k<=28, -22<=l<=20	
Reflections collected	29705	
Independent reflections	7722 [R(int) = 0.0384]	
Completeness to theta = 28.70°	100.0 %	
Absorption correction	Semi-empirical from equivalents	
Max. and min. transmission	0.7215 and 0.3356	
Refinement method	Full-matrix least-squares on F^2	
Data / restraints / parameters	7722 / 0 / 347	
Goodness-of-fit on F^2	1.035	
Final R indices [I>2sigma(I)]	R1 = 0.0242, wR2 = 0.0532	
R indices (all data)	R1 = 0.0340, wR2 = 0.0568	
Largest diff. peak and hole	0.893 and -1.061 e.$Å^{-3}$	

Table A.5. Atomic coordinates (x 10^4) and equivalent isotropic displacement parameters ($Å^2$x 10^3) for **1-N_2H_4**. U(eq) is defined as one third of the trace of the orthogonalized U^{ij} tensor.

	x	y	z	U(eq)
Hf(1)	9525(1)	1815(1)	5847(1)	16(1)
Hf(2)	7826(1)	3535(1)	6061(1)	15(1)
N(1)	7573(3)	2468(1)	5912(2)	19(1)
N(2)	8624(3)	2751(1)	5337(2)	20(1)
C(1)	11308(4)	1810(2)	7122(2)	26(1)
C(2)	10995(4)	1168(2)	6945(2)	24(1)
C(3)	9368(4)	1068(2)	7031(2)	24(1)
C(4)	8652(4)	1643(2)	7258(2)	22(1)
C(5)	9872(4)	2102(2)	7299(2)	22(1)
C(6)	9659(5)	1558(2)	4345(2)	33(1)
C(7)	10478(4)	1069(2)	4761(2)	26(1)
C(8)	9398(4)	740(2)	5236(2)	27(1)
C(9)	7884(4)	1016(2)	5109(3)	31(1)
C(10)	8082(5)	1514(2)	4552(3)	34(1)
C(11)	5428(4)	3454(2)	5069(2)	27(1)
C(12)	6180(4)	4038(2)	4944(2)	27(1)
C(13)	5986(4)	4407(2)	5652(2)	25(1)
C(14)	5164(4)	4049(2)	6214(2)	23(1)
C(15)	4851(4)	3461(2)	5852(2)	25(1)
C(16)	9322(4)	4471(2)	6682(2)	26(1)
C(17)	10065(4)	3932(2)	7016(2)	25(1)
C(18)	10731(4)	3590(2)	6384(2)	22(1)
C(19)	10457(4)	3929(2)	5653(2)	22(1)
C(20)	9571(4)	4468(2)	5843(2)	26(1)
C(21)	12921(5)	2094(2)	7211(3)	40(1)
C(22)	12211(5)	669(2)	6811(3)	38(1)
C(23)	6989(5)	1747(2)	7465(3)	32(1)
C(24)	12180(5)	912(2)	4663(3)	40(1)
C(25)	10358(7)	2017(2)	3772(3)	50(1)
C(26)	6376(5)	797(2)	5440(3)	45(1)
C(27)	5141(5)	2949(2)	4441(3)	43(1)
C(28)	6850(5)	4258(2)	4167(3)	46(1)
C(29)	4566(5)	4274(2)	7000(2)	34(1)
C(30)	8572(5)	4987(2)	7156(3)	37(1)
C(31)	10291(5)	3799(2)	7910(2)	38(1)
C(32)	11081(5)	3753(2)	4851(2)	31(1)

Table A.6. Crystal structure data for **1-SiHCy**

Identification code	**1-SiHCy**	
Empirical formula	C38 H58 Hf2 N2 Si	
Formula weight	927.93	
Temperature	293(2) K	
Wavelength	0.71073 Å	
Crystal system	Monoclinic	
Space group	P2(1)/n	
Unit cell dimensions	a = 9.2800(19) Å	□= 90°.
	b = 18.390(4) Å	□= 92.77(3)°.
	c = 23.140(5) Å	□ = 90°.
Volume	3944.4(14) $Å^3$	
Z	4	
Density (calculated)	1.563 Mg/m^3	
Absorption coefficient	5.316 mm^{-1}	
F(000)	1832	
Crystal size	0.40 x 0.30 x 0.20 mm^3	
Theta range for data collection	2.38 to 31.00°.	
Index ranges	-13<=h<=6, -26<=k<=26, -33<=l<=33	
Reflections collected	50852	
Independent reflections	12550 [R(int) = 0.0246]	
Completeness to theta = 31.00°	99.8 %	
Absorption correction	Semi-empirical from equivalents	
Max. and min. transmission	0.4161 and 0.2249	
Refinement method	Full-matrix least-squares on F^2	
Data / restraints / parameters	12550 / 1 / 411	
Goodness-of-fit on F^2	1.024	
Final R indices [I>2sigma(I)]	R1 = 0.0202, wR2 = 0.0472	
R indices (all data)	R1 = 0.0245, wR2 = 0.0489	
Largest diff. peak and hole	1.225 and -0.809 e.$Å^{-3}$	

Table A.7. Atomic coordinates (x 10^4) and equivalent isotropic displacement parameters ($Å^2$x 10^3) for **1-SiHCy.** U(eq) is defined as one third of the trace of the orthogonalized U^{ij} tensor.

	x	y	z	U(eq)
Hf(1)	4325(1)	7299(1)	2364(1)	18(1)
Hf(2)	5763(1)	8883(1)	1534(1)	17(1)
Si(1)	4048(1)	7893(1)	907(1)	20(1)
N(1)	4688(2)	7855(1)	1622(1)	18(1)
N(2)	4933(2)	8672(1)	712(1)	22(1)
C(1)	2314(3)	7908(1)	2914(1)	27(1)
C(2)	2430(3)	7196(1)	3149(1)	31(1)
C(3)	2027(3)	6701(1)	2707(1)	33(1)
C(4)	1667(3)	7090(1)	2194(1)	30(1)
C(5)	1840(2)	7840(1)	2326(1)	26(1)
C(6)	5055(3)	5973(1)	2331(1)	26(1)
C(7)	6200(2)	6346(1)	2073(1)	23(1)
C(8)	6895(3)	6780(1)	2504(1)	26(1)
C(9)	6239(3)	6662(1)	3037(1)	30(1)
C(10)	5124(3)	6160(1)	2928(1)	30(1)
C(11)	8111(2)	8527(1)	1053(1)	29(1)
C(12)	8212(2)	9283(1)	1170(1)	28(1)
C(13)	8322(2)	9369(1)	1777(1)	28(1)
C(14)	8243(2)	8680(1)	2044(1)	26(1)
C(15)	8090(2)	8163(1)	1588(1)	27(1)
C(16)	3492(3)	9731(1)	1493(1)	27(1)
C(17)	4644(3)	10184(1)	1336(1)	28(1)
C(18)	5612(3)	10244(1)	1819(1)	29(1)
C(19)	5126(3)	9816(1)	2273(1)	28(1)
C(20)	3804(3)	9496(1)	2065(1)	26(1)
C(21)	2448(3)	8583(1)	3278(1)	35(1)
C(22)	2803(4)	7030(2)	3777(1)	46(1)
C(23)	1013(3)	6773(2)	1645(1)	40(1)
C(24)	4141(3)	5379(1)	2058(1)	34(1)
C(25)	6679(3)	6242(1)	1470(1)	30(1)
C(26)	6763(4)	6959(2)	3615(1)	42(1)
C(27)	8123(3)	8182(2)	467(1)	41(1)
C(28)	8324(3)	9871(2)	724(1)	40(1)
C(29)	8424(3)	8529(2)	2684(1)	32(1)
C(30)	2149(3)	9581(2)	1128(1)	39(1)
C(31)	4733(3)	10561(2)	761(1)	41(1)
C(32)	5751(3)	9796(2)	2886(1)	39(1)
C(33)	4426(3)	7117(1)	403(1)	24(1)
C(34)	3518(3)	6439(1)	506(1)	33(1)

Table A.7 (Continued)

C(35)	3870(4)	5825(2)	90(2)	51(1)
C(36)	3666(4)	6069(2)	-538(2)	57(1)
C(37)	4540(4)	6751(2)	-647(1)	43(1)
C(38)	4191(3)	7360(1)	-227(1)	34(1)

Table A.8. Crystal structure data for **1-CyCN**

Identification code	**1-CyCN**	
Empirical formula	C45 H69 Hf2 N3 Si	
Formula weight	1037.10	
Temperature	173(2) K	
Wavelength	0.71073 Å	
Crystal system	Monoclinic	
Space group	P2(1)/c	
Unit cell dimensions	a = 11.4624(8) Å	□= 90°.
	b = 20.4735(14) Å	□= 92.510(4)°.
	c = 17.7603(14) Å	□ = 90°.
Volume	4163.9(5) $Å^3$	
Z	4	
Density (calculated)	1.654 Mg/m^3	
Absorption coefficient	5.046 mm^{-1}	
F(000)	2072	
Crystal size	0.20 x 0.10 x 0.03 mm^3	
Theta range for data collection	1.52 to 30.51°.	
Index ranges	-16<=h<=16, -26<=k<=28, -25<=l<=25	
Reflections collected	46668	
Independent reflections	12685 [R(int) = 0.0373]	
Completeness to theta = 30.51°	99.7 %	
Absorption correction	Semi-empirical from equivalents	
Max. and min. transmission	0.8842 and 0.4318	
Refinement method	Full-matrix least-squares on F^2	
Data / restraints / parameters	12685 / 16 / 482	
Goodness-of-fit on F^2	1.054	
Final R indices [I>2sigma(I)]	R1 = 0.0367, wR2 = 0.0824	
R indices (all data)	R1 = 0.0494, wR2 = 0.0878	
Largest diff. peak and hole	2.353 and -1.200 $e.Å^{-3}$	

Table A.9. Atomic coordinates (x 10^4) and equivalent isotropic displacement parameters ($Å^2$x 10^3) for **1-CyCN.** U(eq) is defined as one third of the trace of the orthogonalized U^{ij} tensor.

	x	y	z	U(eq)
Hf(1)	9543(1)	4822(1)	12615(1)	20(1)
Hf(2)	6691(1)	4727(1)	12767(1)	18(1)
Si(1)	8541(1)	6415(1)	11721(1)	31(1)
N(1)	7866(3)	5278(2)	12361(2)	21(1)
N(2)	8774(3)	5645(2)	12053(2)	26(1)
N(3)	8220(3)	4117(2)	13110(2)	19(1)
C(1)	10459(4)	4754(3)	11336(3)	33(1)
C(2)	9544(4)	4284(2)	11320(3)	30(1)
C(3)	9883(4)	3759(2)	11807(3)	29(1)
C(4)	10967(4)	3915(2)	12152(3)	29(1)
C(5)	11315(4)	4529(3)	11861(3)	31(1)
C(6)	10639(4)	4683(2)	13902(3)	26(1)
C(7)	11439(4)	4987(2)	13437(3)	31(1)
C(8)	11043(4)	5622(2)	13238(3)	30(1)
C(9)	9989(4)	5725(2)	13611(3)	28(1)
C(10)	9742(4)	5150(2)	14002(3)	26(1)
C(11)	5781(4)	5678(2)	13443(3)	29(1)
C(12)	4895(4)	5196(2)	13443(3)	31(1)
C(13)	5247(4)	4679(2)	13926(3)	28(1)
C(14)	6381(4)	4842(2)	14232(3)	26(1)
C(15)	6697(4)	5450(2)	13935(3)	28(1)
C(16)	5461(4)	3721(2)	12180(3)	28(1)
C(17)	6363(4)	3892(2)	11689(3)	28(1)
C(18)	6110(4)	4509(2)	11368(3)	25(1)
C(19)	5098(4)	4746(2)	11699(3)	29(1)
C(20)	4693(4)	4243(2)	12177(3)	31(1)
C(21)	10581(5)	5347(3)	10847(4)	48(2)
C(22)	9301(4)	3103(2)	11847(3)	36(1)
C(23)	11732(4)	3454(3)	12609(3)	36(1)
C(24)	10856(4)	4072(2)	14348(3)	33(1)
C(25)	11703(5)	6113(3)	12801(4)	43(1)
C(26)	9338(5)	6361(2)	13623(3)	36(1)
C(27)	5684(5)	6338(2)	13076(4)	41(1)
C(28)	4534(5)	4101(3)	14149(3)	38(1)
C(29)	6990(4)	4492(2)	14875(3)	32(1)
C(30)	5253(5)	3062(2)	12523(4)	40(1)
C(31)	6738(4)	4843(2)	10752(3)	31(1)
C(32)	4437(5)	5356(3)	11468(3)	37(1)

Table A.9 (Continued)

C(33)	7599(6)	6544(2)	10839(3)	49(2)
C(34)	7129(11)	7220(5)	10796(5)	122(5)
C(35)	6334(10)	7366(6)	10111(5)	126(5)
C(36)	6832(9)	7186(4)	9404(4)	83(3)
C(37)	7083(11)	6458(5)	9461(5)	121(5)
C(38)	7956(7)	6307(4)	10110(4)	72(2)
C(39)	8516(4)	3588(2)	13445(3)	22(1)
C(40)	7769(4)	3117(2)	13855(3)	23(1)
C(41)	7728(4)	2448(2)	13469(3)	31(1)
C(42)	6951(5)	1968(2)	13878(4)	43(1)
C(43)	7324(6)	1895(3)	14697(4)	55(2)
C(44)	7419(6)	2556(3)	15096(3)	47(2)
C(45)	8246(4)	3005(2)	14674(3)	34(1)